CHALMERS
UNIVERSITY OF TECHNOLOGY

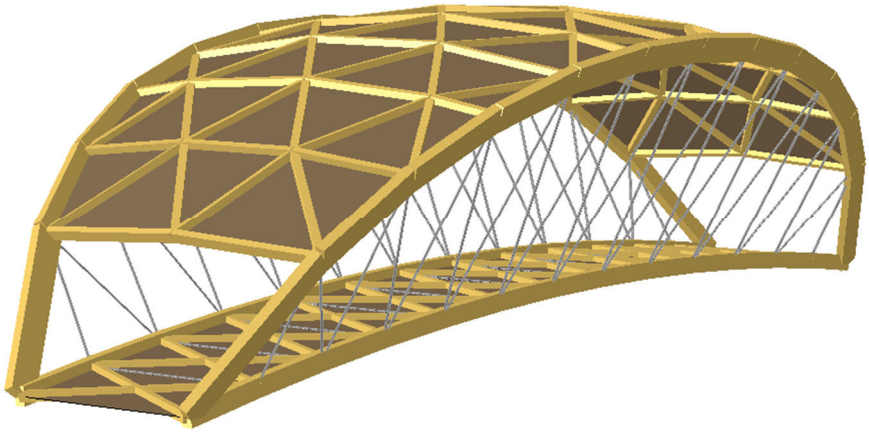

Covered Timber Pedestrian Bridges

3D-modelling and analysis of connections

Master's Thesis in the Master's Programme Structural Engineering and Building Technology

ANITA OSHALIM
MALIN STJERNEMAN

Department of Civil and Environmental Engineering
Division of Structural Engineering
Steel and Timber Structures
CHALMERS UNIVERSITY OF TECHNOLOGY
Gothenburg, Sweden 2015
Master's Thesis 2015:150

MASTER'S THESIS 2015:150

Covered Timber Pedestrian Bridges

3D-modelling and analysis of connections

Master's Thesis in the Master's Programme Structural Engineering and Building Technology

ANITA OSHALIM

MALIN STJERNEMAN

Department of Civil and Environmental Engineering
Division of Structural Engineering
Steel and Timber Structures
CHALMERS UNIVERSITY OF TECHNOLOGY
Göteborg, Sweden 2015

Covered Timber Pedestrian Bridges
3D-modelling and analysis of connections

Master's Thesis in the Master's Programme Structural Engineering and Building Technology

ANITA OSHALIM

MALIN STJERNEMAN

Examensarbete 2015:150/ Institutionen för bygg- och miljöteknik,
Chalmers tekniska högskola 2015

Department of Civil and Environmental Engineering
Division of Structural Engineering
Steel and Timber Structures
Chalmers University of Technology
SE-412 96 Göteborg
Sweden
Telephone: + 46 (0)31-772 1000

Cover:
3D-model of the *Leaf bridge*.

Chalmers Reproservice
Göteborg, Sweden, 2015

Covered Timber Pedestrian Bridges

3D-modelling and analysis of connections

Master's thesis in the Master's Programme Structural Engineering and Building Technology

ANITA OSHALIM
MALIN STJERNEMAN
Department of Civil and Environmental Engineering
Division of Structural Engineering
Steel and Timber Structures
Chalmers University of Technology

ABSTRACT

The addition of a cover in form of a roof or a shell can aid to improve the durability and to increase the lifetime of a bridge. Although many timber bridges have been built recently, only one single old covered bridge, the Vaholms bridge, exists in Sweden today. To make timber more competitive, compared to steel and concrete, in the choice of structural material for bridges, the design of the connections is very important since it greatly influences the performance of the structure. Connections are commonly modelled as either pinned or fixed, but in reality they have an intermediate degree of fixation. Neglecting the consideration of degree of fixation in design leads to over-dimensioning of either the structural elements or the connections themselves. By taking the degree of fixation into account, unnecessary over-dimensioning can be reduced.

This Master's Thesis project comprises a 30 meter long covered pedestrian and bicycle timber bridge. The architectural and conceptual design of this bridge was made by Flårback (2015). The aim of this thesis was to suggest a design of one type of connection in the roof of the bridge. Furthermore, the project aimed to investigate the influence of rotational stiffness of the semi-rigid connection on the structural behaviour of the bridge. To be able to achieve the aims, 3D-modelling of the bridge was performed in the finite element modelling (FEM) program *Abaqus* (Dassault Systèmes) and the performance of the bridge was structurally analysed in both serviceability limit state (SLS) and ultimate limit state (ULS).

A bolted connection with slotted-in plates was suggested, but its design is not completely realistic, since the amount of fasteners required to satisfy Eurocode requirements is excessive with regard to the space available. Preferably, another more efficient type of design should be chosen for this type of connection. The rotational stiffness of the designed connection was calculated and its influence on the structural behaviour of the bridge was investigated. The investigation showed that the deflection of the bridge increased with decreasing rotational stiffness. It also showed that the designed connection has a degree of fixation in the semi-rigid range.

Key words: Covered timber bridge, Timber engineering, Connection design, Rotational stiffness, Structural analysis, Abaqus.

Gångbroar av trä med tak
3D-modellering och analys av förband

Examensarbete inom masterprogrammet Structural Engineering and Building Technology

ANITA OSHALIM
MALIN STJERNEMAN
Institutionen för bygg- och miljöteknik
Avdelningen för Konstruktionsteknik
Stål- och Träbyggnad
Chalmers tekniska högskola

SAMMANFATTNING

Att förse en bro med ett tak eller ett klimatskal kan förbättra dess beständighet och förlänga dess livstid. Trots att det byggts många träbroar på senare tid finns det idag endast en täckt gammal träbro i Sverige, nämligen Vaholmsbron. För att göra trä mer konkurrenskraftigt, jämfört med stål och betong, i valet av strukturellt material i broar är det viktigt att ta hänsyn till effekten av förbandens utformning, vilka i hög grad påverkar brons verkningssätt. Förband modelleras vanligtvis antingen ledade eller fast inspända, men i verkligheten har de en viss grad av inspändhet. Att försumma graden av inspändhet resulterar i överdimensionering av antingen strukturelementen eller förbanden. Genom att ta hänsyn till graden av inspändhet kan onödig överdimensionering undvikas.

Den här masteruppsatsen behandlar en 30 meter lång, täckt gång- och cykelbro av trä. Den arkitektoniska och konceptuella designen är gjord av Flårback (2015). Syftet med uppsatsen var att föreslå en typ av utformning av ett förband i takkonstruktionen i bron. Dessutom syftade uppsatsen till att undersöka hur rotationsstyvheten hos de delvis inspända förbanden påverkar brons verkningssätt. För att uppnå målen gjordes en 3D-modellering av bron i det finita elementmodelleringsprogrammet (FEM) *Abaqus* (Dassault Systèmes) där bron verkningssätt analyserades strukturellt i både bruksgränstillstånd (SLS) och brottgränstillstånd (ULS).

Ett förslag på ett bultförband med inslitsade plåtar tog fram, men dess utformning är inte helt realistisk eftersom mängden erfordrade bultar är överdrivet stor i förhållande till tillgänglig plats. Företrädesvis bör en annan mer effektiv utformning väljas för den här typen av förband. Rotationsstyvheten hos det utformade förbandet beräknades och dess påverkan på bron verkningssätt undersöktes. Undersökningen visade att brons nedböjning ökar med minskande rotationsstyvhet och att det utformade förbandets rotationsstyvhet ligger i det delvis inspända intervallet.

Nyckelord: Täckt träbro, Träkonstruktioner, Utformning av förband, Rotationsstyvhet, Strukturanalys, Abaqus.

Contents

Preface

This thesis is a part of a Master's Thesis project of 30 HP (Swedish: Högskolepoäng) per student within the Master's Programme Structural Engineering and Building Technology at the Chalmers University of Technology, Sweden.

The project was carried out between January and June 2015 at the Department of Civil and Environmental Engineering, Division of Structural engineering - Steel and Timber structures.

We would like to thank our supervisor and examiner Professor Robert Kliger for his enthusiasm and commitment in this project. We also appreciate all the help and support received from associate Professor Mohammad Al-Emrani and associate Professor Reza Haghani Dogaheh during this project.

Göteborg October 2015

Anita Oshalim

Malin Stjerneman

1 Introduction

1.1 Background

Timber is an old traditional building material in Sweden and in other regions with natural access to it, which has been used throughout time to serve as all kinds of components in different structures, e.g. in bridges. The earliest type of bridges was simply fallen trees, fallen in favourable places or placed strategically to overcome obstacles. Many different types of timber arch and truss bridge, and also covered ones, were developed already from medieval times up to the 19th century in Europe, Asia and America (Svenskt trä, 2015).

As technology and the requirements of traffic developed during the industrialization in the 19th and 20th centuries, timber slowly began losing its share of the market and began being replaced first by iron and steel and later by concrete. Since the use of timber decreased over time, much of the knowledge and experience of building timber bridges, and especially covered ones, has gone missing. Some countries were keener than others to keep the tradition of building timber bridges and preserving the already existing ones, and Sweden was not one of them.

Nowadays, timber is considered to be a more environmentally-friendly material compared to steel and concrete, which is one contributing factor to why the desire to use timber in greater extent is growing. Efforts to start increasing the use of timber began in the 1990's and in 1994 the Swedish Road Administration, Vägverket (now Trafikverket), published specified requirements for timber bridges (Svenskt trä, 2015). Even though it is nowadays allowed to use timber in bridge structures, the more well-known materials steel and concrete are still often chosen in favour of timber.

With good architecture and engineering work, a bridge can be built of timber and still achieve an attractive appearance, desirable functions and also competitive costs for both construction and maintenance. The addition of a cover in form of a roof or a shell can aid to improve the durability and to increase the lifetime of the bridge. The cover will protect the bridge from weather, especially from precipitation which reduces the durability of timber significantly. Although many timber bridges have been built lately, only one single covered one, the Vaholms bridge, exists in Sweden today.

To make timber more competitive, compared to steel and concrete, in the choice of structural material for bridges and other structures, the design of the connections is very important. The joints in a structure can be considered as weak points, both structurally and economically and the configuration of them can highly influence the performance of the structure (Engström, 1994; Engström, 1997). Connections are commonly modelled as either perfectly pinned or perfectly fixed, but in reality it is difficult to achieve a mode of any of these extremes. Instead, the connections will have an intermediate degree of fixation. By considering the degree of fixation of the connections, unnecessary over-dimensioning can be reduced (Engström, 1995).

1.2 Aim

The aim of this Master's Thesis project was to improve the *Leaf bridge* concept, which is a 30 meter long covered pedestrian and bicycle timber bridge, developed by Flårback in his Master's Thesis *Covered Timber Bridges* (2015), by structurally analysing the bridge in SLS (serviceability limit state) and ULS (ultimate limit state) and design its connections. In addition, the rotational stiffnesses of the connections was calculated and the bridge performance of a model using fixed connections and a model using semi-rigid connections were compared.

1.3 Limitations

This Master's Thesis project focused on the static analysis in SLS and ULS and the design of one connection. No dynamic analysis of the bridge was performed. The analysis in SLS was limited to the deflections in the deck. Neither environmental nor long-term effects, such as temperature, moisture content and creep, were considered in this project. Only the bridge itself was analysed and not its foundations or anchorages. The design of connections was limited to the connections in the roof truss systems.

1.4 Method

Initially, a literature study of timber truss and arch bridges, both covered and uncovered ones, was performed to increase knowledge of their mechanical behaviour and also their history. Also a study of timber connections was carried out in order to investigate different possible solutions for the design of the connections. In addition, tutorials of the finite element software *Abaqus* (Dassault Systèmes) were studied in order to gain more knowledge about modelling and the different analyses that can be performed in this software. The structural behaviour of the bridge in both SLS and ULS was analysed numerically using *Abaqus* and compared to the requirements specified in Eurocode. Thereafter connections were designed based on the results obtained from the numerical analyses. Finally, the influence of rotational spring stiffness on the deflection was investigated.

2 Arch and Truss Timber Bridges

Using bridges to cross obstacles spans human history. From the beginning, it could be naturally fallen trees that made it possible to cross rivers or ravines. Eventually logs were used more systematically to be able to pass obstacles in the terrain. The character of bridges changed from pure use items to construction object when the method of building bridges became more sophisticated. Different aspects were considered now when building bridges, such as technical, craftsmanship and artistic aspects. The timber as a construction material became more important since it was a versatile material and was available almost everywhere (Svenskt Trä, 2003).

From the middle ages until the 1800s, many timber bridges were built, which in turn resulted in development of several types of arch and truss. From the 1700s, covered timber bridges were built both in the US and in Europe and under the 1800s a large number of wooden bridges with large truss structures were built, which later on became very common. In the pace of the technology and transport development in the late 1800's and during the 1900's, the importance of timber as construction material in bridges decreased and was eventually replaced by steel and concrete. However, there are some countries that still use timber as a construction material in bridges. In central Europe and especially in Switzerland, there are more than 200 timber bridges, many of them from medieval time. The reason why so many old timber bridges still exist is because they are covered (Svenskt Trä, 2003).

The development process that timber bridges have undergone through the passing years has resulted in increasing awareness of their advantages in comparison with other types of bridge. Timber bridges compared to bridges made of steel and concrete have the same performance and technical lifespan, both in terms of pedestrian and bicycle bridges and overpasses adapted to heavy vehicular traffic. The development of wood materials and construction methods has made it possible for timber bridges to meet the requirements of modern bridges. Development of glulam during 1990's meant that larger beams could be produced, which resulted in longer spans of the girder bridges. Additionally, the time consumed on assembling a timber bridge is usually much shorter compared to other type of bridges and the material itself is very environmentally friendly (Martinsons, 2015).

For covered timber bridges, the most common structures used are heavy timber truss and arch structures since they provide rigidity and enable longer spans. The different kind of trusses and arches are discussed in the coming section.

2.1 Different types of truss

The most common trusses that are used in covered timber bridges are presented and described in this section. Other types of truss have been used in covered timber bridges with only some technical differences but the behaviour of the structure are basically the same. The following trusses are arranged in the range of span length.

2.1.1 Kingpost

The most heavy, but yet very simple in structural design, timber truss in the range of short span lengths is the kingpost truss, see Figure 2.1. It consists of single member components, which are two inclined elements serving as main diagonals and upper

chord in pure compression, a vertical central element, called the kingpost, and a bottom chord, both working in tension. The kingpost member has two main tasks which are uniting the two diagonals and supporting the floor load. The connections between the diagonals and the bottom chord are critical and should be taken into consideration (Federal Highway Administration, 2005).

The span limit is quite short, in general around 7 – 9 m but can be further increased to approximately 10 – 12 m when applying sub-diagonals from the centre of the main diagonals to the bottom chord. As seen in Figure 2.2, a smaller truss is then created within the main truss in which steel rods can be added to enable the inclusion of floor beams. The floor beams are usually placed at the ends of the bridge or next to the central vertical member. Since the point load arising from the floor beams do not coincide with the symmetry line of the truss, bending stresses at the bottom chord will occur, which can vary in magnitude depending on how the floor beams are arranged in terms of distance to the joints (Federal Highway Administration, 2005). The heel connection of the main diagonal of the truss is critical due to some weaknesses.

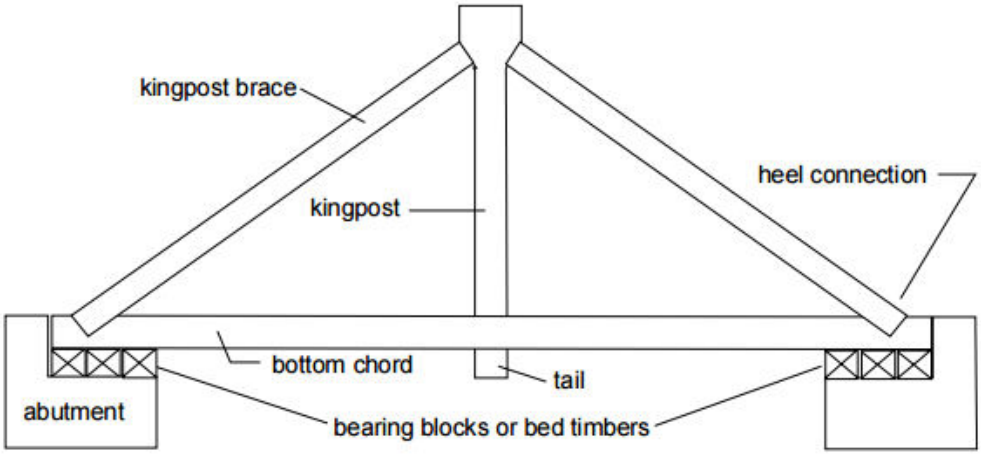

Figure 2.1 Kingpost truss.

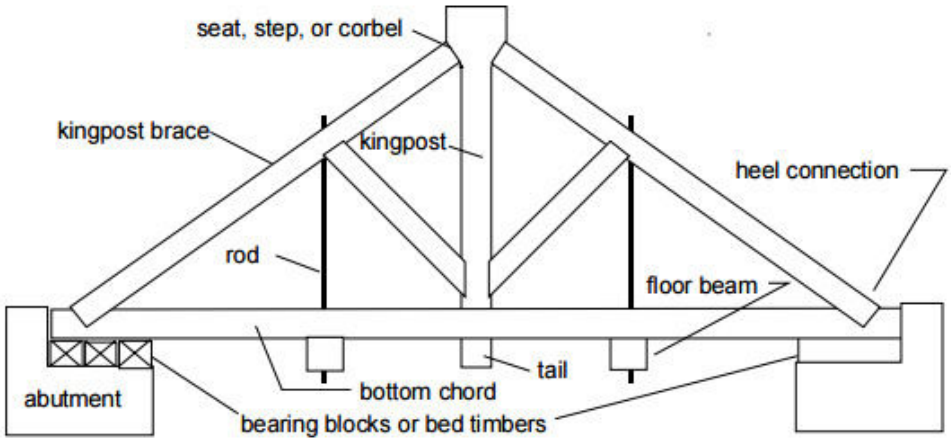

Figure 2.2 Kingpost truss with vertical steel rods.

2.1.2 Queenpost

This type of truss has a very similar structure to Kingpost truss but with the difference that it is constructed with an additional central panel consisting of diagonals, vertical members and chords working in compression and tension. The vertical members are referred to as queenposts, see Figure 2.3. Despite the minor differences in structure, the queenpost truss has a number of similarities with the kingpost truss, such as the critical section (the heel connection), components consisting of single members and similar methods are used when aiming for longer spans (Federal Highway Administration, 2005).

As for the span limits, the most common is between 12 – 18 m but as mentioned earlier longer spans can be obtained. With increased span length the bottom chord elements increase which further increases the tensile stresses and this in turn implies that the connection between the chords is a critical point and should be taken into consideration (Federal Highway Administration, 2005).

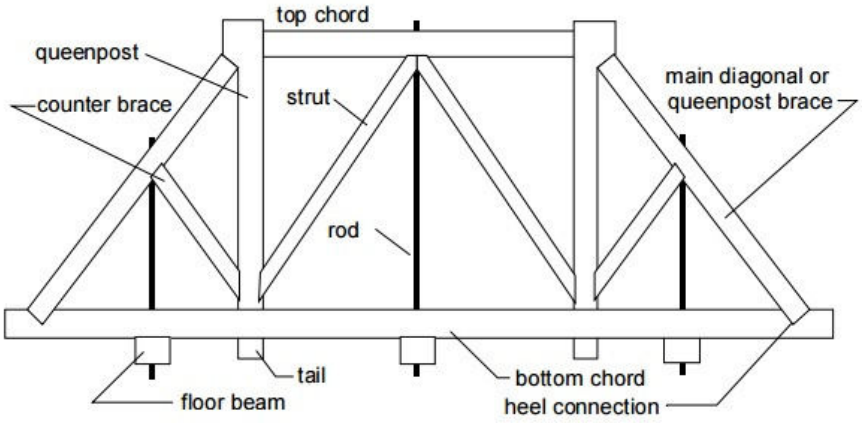

Figure 2.3 Queenpost truss.

2.1.3 Multiple kingpost

The capacity of enabling larger spans is increased in this type of truss since panels are being added to the basic kingpost truss and thus providing a more rigid structure, see Figure 2.4. By adding an even number of panels, the load is distributed in such a way that compression is taken by the diagonals and tension by the vertical components under condition of normal loading. Most of the multiple kingpost trusses used in covered timber bridges have a structure of even number of panels but there are some few with odd number of panels (Federal Highway Administration, 2005).

Since short panels are used in this type of truss, transverse floor beams can be placed so that they rest against the vertical members in the truss. This will lead to reduced eccentricity and thereby the bending stresses in the bottom chord. Moreover, the forces in the diagonals are smaller in comparison with the trusses mentioned earlier. The areas of interest in this structure are the tail in the bottom chord (the lower parts of the posts) and the connection between the diagonal and the top chord since shear failure is likely to happen in these parts due to high stress range in the plane of the grains.

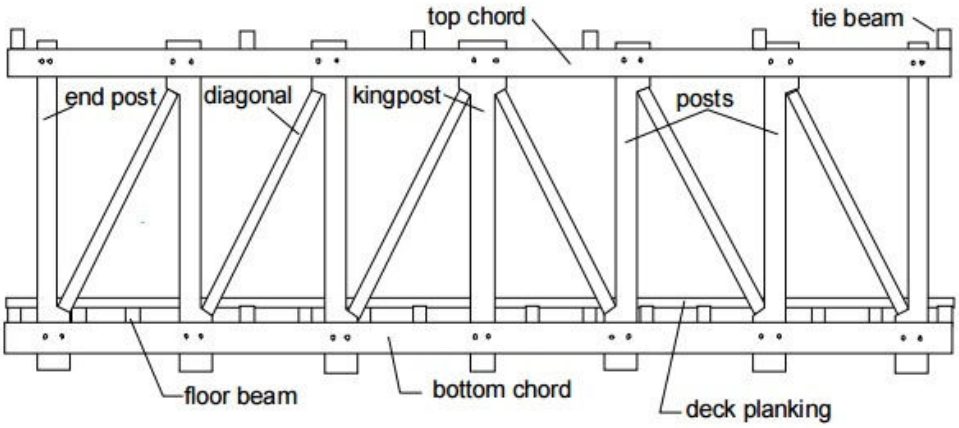

Figure 2.4 Multiple kingpost truss.

2.1.4 Burr Arch

In the early 1800s, Theodore Burr introduced a truss configuration consisting of two structural members, multiple kingpost truss and an arch, which immediately became the most popular one among bridge builders. The intention of including an arch was to allow higher load carrying capacity of the truss and enabling longer spans. Furthermore, the arch in this truss can be seen as the main structural element while the truss provides buckling resistance and helps transferring the load into and along the arch. Most covered timber bridges are composed of this particular type of truss, with spans of up to almost 68 m (Federal Highway Administration, 2005).

The connection between these two load bearing elements is arranged so that the arch is attached to the kingpost truss at the lateral support and to the vertical members by single bolts, see Figure 2.5. In order for the vertical loads to be transferred, the bolts must be stiff enough to be able to take the resultant shear force. Additionally, the stiffness of the bolts determines how the load is distributed between the truss and the arch. Beside the previously mentioned areas of interest in the kingpost truss, which also applies for this type of truss, the ends of the arch and the connection between the arch and the vertical members should be taken into account (Federal Highway Administration, 2005).

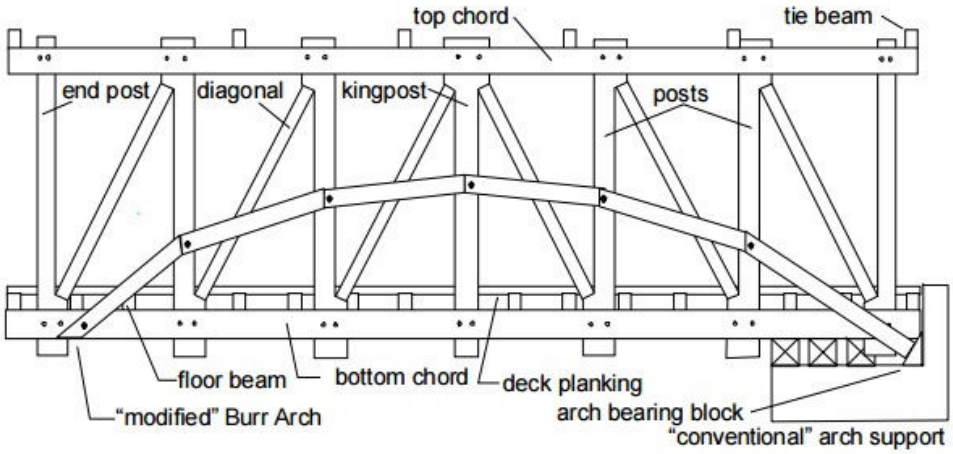

Figure 2.5 Burr arch truss.

2.1.5 Town Lattice

It was the architect Ithiel Lattis who developed this form of truss that consists of large number of inclined elements arranged in close distance to each other and in turn forming a shape of a lattice. This lattice shaped web is further connected to two bottom chords, of which the lower one carries the floor beams, and either a single or double top chords (Federal Highway Administration, 2005). This configuration enabled larger spans, 7- 49 m, and streamlined the complex and time consuming connection details, such as mortice and tenon joint into slotting and wedging of treenails (Roth, 1981)

As for the load distribution in this truss model, it is very efficient since the load is being distributed equally without any use of vertical members as it is in the Burr design. The load is distributed so that the diagonals carry compression forces and the chords take tension forces. Furthermore, the design of the connection, at which they are fastened at each intersection point, prevents each triangle from moving independently which further implies that the load is borne equally by all triangles (Connecticut history, 2015).

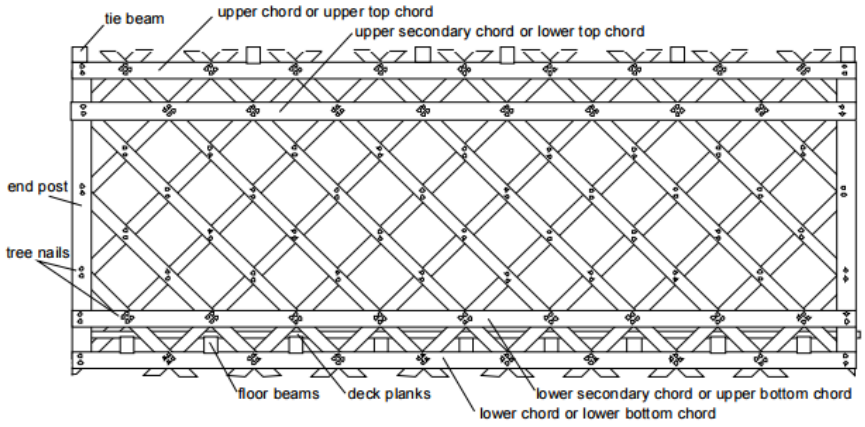

Figure 2.6 Town lattice truss.

2.1.6 Long truss

Colonel Stephen H. Long configured a truss type in 1830 that was made of heavy timber parallel chords and diagonals, see Figure 2.7. Regarding span length, it extends from 15 to 51 m. The connection of different parts of the truss was made of timber wedges which enabled adjustment of the shape of the panels and also the adjustment of initial camber. The use of the wedge is also very good considering the load distribution since the load is being distributed from the chord over a larger area of the vertical through the wedge (Federal Highway Administration, 2005). The strength of the connection between the horizontal component of the load in the inclined element and the chord is increased when introducing the wedge.

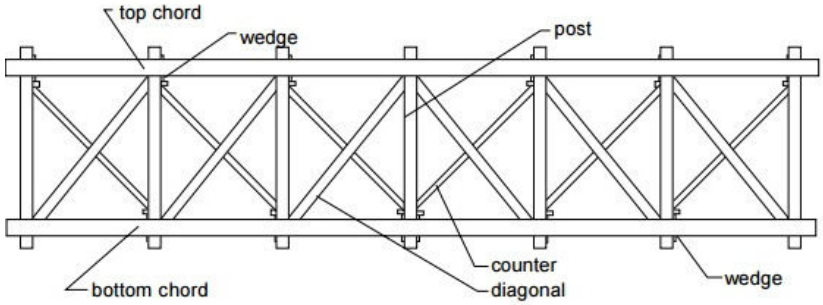

Figure 2.7 Long truss.

2.1.7 Howe Truss

William Howe presented his first truss model in 1840 and later on the same year he introduced an improved version which consisted of diagonals of timber and rods of steel as vertical member, see Figure 2.8. The span range extends from 6 to 61 m and the longest bridges supported by the Howe truss is only 10% shorter than the longest Burr arch bridge. Even though Burr arch truss is the dominant truss among covered timber bridges, the Howe truss quickly became very popular due to its simple structure and ease of assembly. The prefabricated parts were put together by a threaded connection at the end of each rod, of which the rods were welded to the chords (Federal Highway Administration, 2005).

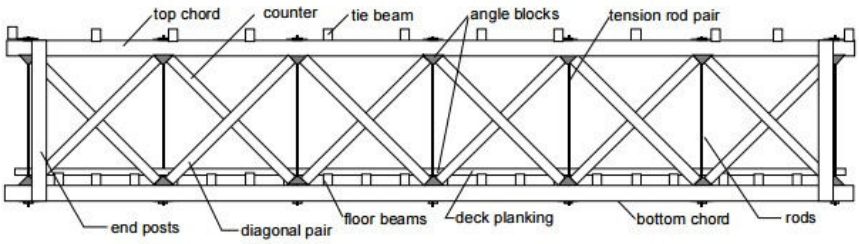

Figure 2.8 Howe truss.

2.1.8 Bowstring (tied-arch)

The tied arch bridge consists of an arch, working as an upper chord, and a longitudinally element between the arch to resist the large horizontal thrusts. The upper chord can be made of small straight elements connected to each other forming a curvature or as a whole single curved element. Regarding spans, it extends between 30-40 m but can be increased when dividing the arch in smaller elements, which in turn means that rigid connections must be designed and constructed which are seldom aesthetically pleasing and require more workmanship and are hence more expensive.

Implementing this kind of structure in a bridge gives several ways to classify an arch bridge. The placement of the deck in relation to the superstructure and the connection at the support and midpoint of the arch are factors that describe the type of arch bridge. As seen in Figure 2.9, three different types are presented in which the first one, type A, is the basic arch bridge where the bow is supported to the foundation directly and is subjected to bending, shear and axial force. The second and the third one are typical

tied arches, in where the thrust is resisted by tying the ends of the arch. The structural behaviour of type B is very similar to the first mentioned, while in type C the bow is mainly in compression and the stiffening girder takes both bending moments and axial forces.

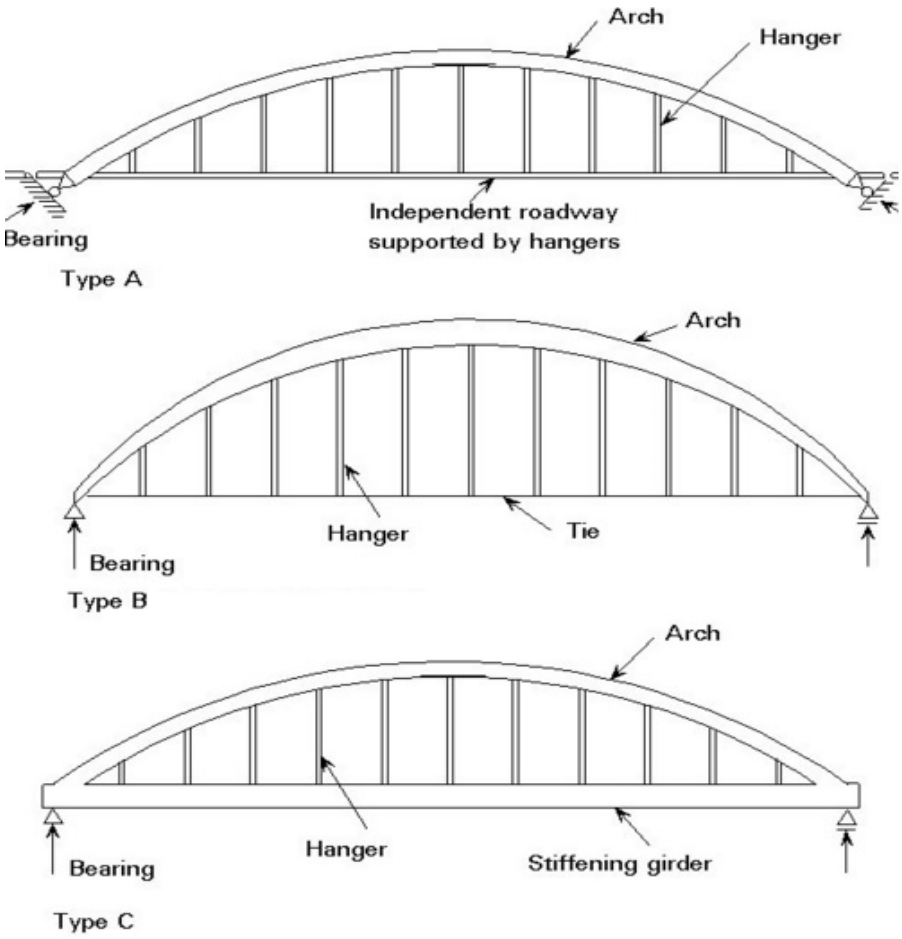

Figure 2.9 Bowstring truss (tied arch).

3 Connections in Timber Structures

There are multiple ways of connecting timber elements depending on the type of structure, the direction of the connecting elements and the loads which are to be transferred. One way of categorizing connections is to group them according to which type of fastener is used to attach the elements to one another. The very first method of connecting elements of any kind was to use rope-like materials and tie the elements together, carrying the loads by bearing and friction (Madsen, 1998). Later on, the traditional timber joinery was developed, which resembles a puzzle with various types of notch, wedge, slot and finger fitting together, with or without fasteners. Initially only timber fasteners were used. Subsequently, connections involving steel fasteners, which increase the load carrying capacity of the joints, and steel plates or adhesives, which also increase the stiffness of the joints, were developed. Lately there has been a revival of traditional timber joinery due to the efficiency and precision of modern CNC (computer numerical control) machinery (Al-Emrani et al., 2011).

Another way of categorizing connections is to divide them into three groups depending on the direction in which the elements are to be assembled; lengthening (end to end), widening (edge to edge) or framing (change in direction). Further grouping can be made with regard to the design and shape of the connecting pieces. Due to the large amount of different designs, many connections are rather similar and can have attributes belonging to multiple categories.

In the following sections some traditional and some new innovative fasteners and a few different types of connection used for lengthening and framing are described. Connections for widening are omitted.

3.1 Types of fastener

There are multiple types of fastener used in connections of timber elements to secure the members in place and to strengthen the connection. Two main types of fastener are mechanical fasteners and adhesives. Mechanical fasteners can be further divided into dowel-type fasteners, e.g. nails, dowels, screws and bolts, and plates, such as nail plates, punched metal plates, shear plates and split rings. In the past, when steel was very expensive, mostly timber fasteners were used, but nowadays steel fasteners are the most commonly used.

3.1.1 Mechanical fasteners: dowel types

Dowel-type fasteners are the most common type of fasteners used in timber structures today. They should preferably be placed transverse to the direction of the load (Federal Highway Administration, 2005). Depending on if two or three elements are connected, the fasteners will act in either single or double shear and the fasteners can end either inside the member, like nailed or screwed connections or be through, like bolted connections. The fasteners can also be inserted either from one side only or from both sides of the connection. All of these options are illustrated in Figure 3.1.

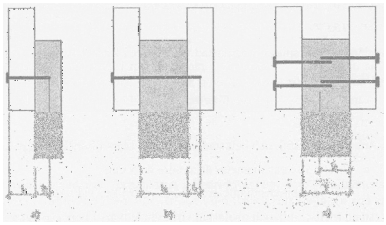

Figure 3.1 Nails acting in single shear (a and c) and double shear (b) (Al-Emrani et al., 2011).

A connection can include one single fastener or a group of fasteners, placed in a row or in a grid pattern, depending on the direction of the members which are to be connected and what types of load that are to be transferred. Since the capacity of a single nail is rather low, due to its small diameter, a nailed connection most often contains a group of nails. The larger diameter of bolts, compared to nails, results in a higher capacity, and hence a bolted connection can consist of only one single bolt, but in order to prevent rotation of the connection it should consist of at least two fasteners. A single bolt which is tightened hard may prevent rotation to some extension due to friction (Connections in timber structures, 2006).

The loads which are to be transferred are mainly carried by bearing of the timber and by shearing of the fasteners. Some shear can also be carried by friction between timber members if such exists, and friction between the fastener and the timber which can arise in case the fastener has been excessively deformed. Depending on the loads acting on the connection, fasteners can also be subjected to withdrawal forces. The withdrawal capacity of nails is low since it relies only on the friction between the nail and timber surfaces. A higher resistance is provided by screws, due to the threads, and by bolts with nuts and washers.

Since the bolted connections generally contain fewer fasteners than nailed connections, its assembly can be considered cheaper, but due to the oversized holes for bolts, consideration must be made with regard to reversal of loads, since the connections act in bearing. This type of connection is unsuitable in statically indeterminate systems. If desired from an aesthetic point of view, the fasteners can be sunk into the elements and covered with timber plugs (Madsen, 1998).

3.1.2 Mechanical fasteners: plates

The capacity of connections can be increased by the addition of steel plates, either on the surface or on the inside of the elements, so called slotted-in plates, if the element thickness is sufficient, see Figure 3.2. The slotted-in plates are inserted into a slot cut in the timber and just like the surface plates fastened transversely with dowel-type fasteners. The loads in connections including steel plates are transferred by shearing of the fasteners and compression in the steel plates.

Figure 3.2 External steel plates and internal steel plate (slotted-in).

Common types of surface plate are nail plate, which are plates with pre-drilled holes fastened to the surface of the elements by nails, and punched metal plates, which are plates with nails punched out from the surface, fastened to the element surface by applying a pressure. These types of plate are shown in Figure 3.3 and they are commonly used in timber roof trusses or other trusses with smaller spans (Svenskt trä, 2015). The ability to punch out nails in the punched metal plates limits the plate thickness, which in turn limits the capacity of the nails themselves and the connection as whole, making this type of connection rather weak. Besides being used as a connector, punched metal plates can also be used as reinforcement in parts of timber elements that are subjected to a high risk of splitting (Svenskt trä, 2015).

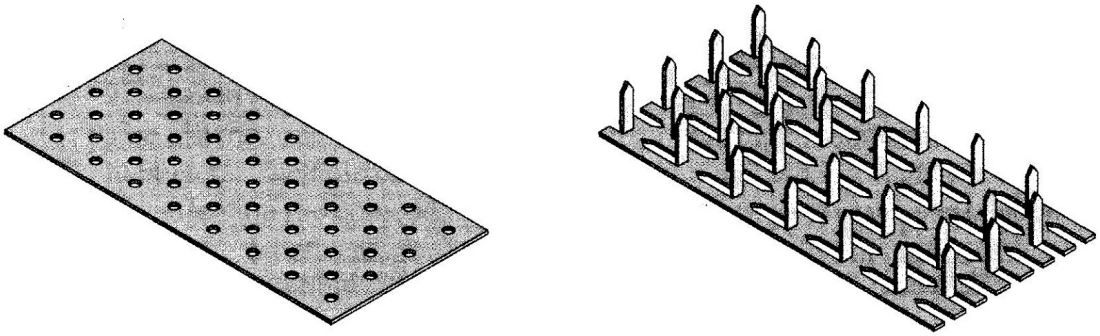

Figure 3.3 Nail plate and punched metal plate (Crocetti et al, 2011).

Another type of plate-like connector is beam shoes, which have shown to be efficient with regard to bearing, stiffness and costs. A beam shoe is placed on the outside of the timber element and fastened with dowel-type fasteners. There are two different types of beam shoe consisting of either one single U-shaped part or two L-shaped parts, see Figure 3.4. Using two L-shaped parts instead of one U-shaped part makes the connector independent of the dimension of the elements which are to be connected (Engström, 1994).

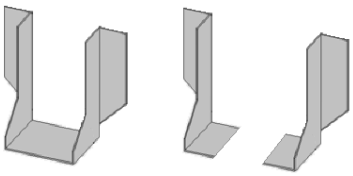

Figure 3.4 U-shaped beam shoe and L-shaped beam shoe.

Connectors similar to the slotted-in plates are split rings and shear plates, which are inserted into grooves between the timber elements. The split rings can have either a flat edge or be toothed, as the tooth plate, see Figure 3.5. They do not rely on additional fasteners but the shear force is transferred over the circumference of the ring. As for the shear plates, the shear force is transferred from the circumference of the ring to a centrically placed bolt. Split rings were developed as proprietary and hence it is difficult to find data for capacity (Madsen, 1998).

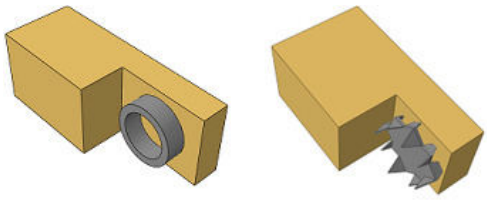

Figure 3.5 Split ring and tooth plate.

3.1.3 Adhesives

Adhesives can be used for assembling both structural joints, such as scarf and finger joints, and laminar and board products, such as plywood, OSB (oriented strand boards), glulam, LVL (laminated veneer lumber), I-joists and stressed skin panels. They are non-corrosive and stiffer than dowel-type fasteners and they are considered brittle despite their high capacity (Wood Information Sheet, 2003). Adding an adhesive to a connection with dowel-type fasteners increases the stiffness of the connection but also makes it more brittle (Svenskt trä, 2015). Adhesives are often chosen due to aesthetic reasons and if possible, choosing an adhesive connection over a connection with mechanical fasteners can influence the appearance of a connection, making it look more "clean". There are both brown and transparent adhesives to choose from (Wood Information Sheet, 2003).

Some of the most commonly used adhesives in load-bearing applications are resorcinol formaldehyde, phenol-resorcinol formaldehyde, polyurethanes, urea formaldehyde and melamine urea formaldehyde based resins and epoxies. The latter two are mostly used when repairing parts of elements. All of the above mentioned adhesives are thermosetting and do not easily dissolve or soften and perform well in fire. Phenolic resins, such as resorcinol formaldehyde and phenol-resorcinol formaldehyde are resistant to moisture and suitable for conditions with moisture content up to 25% (Wood Information Sheet, 2003).

It is not recommended to use adhesives in connections where a change in angle of the grain exists or in environments with fluctuating moisture content and temperature conditions. Fluctuating moisture content can lead to dimensional changes in the elements, which in turn can result in a decrease in strength of the resin. Using adhesives requires extensive quality control at manufacturing and on-site gluing is not recommended unless a high level of control can be assured (Wood Information Sheet, 2003), (Crocetti et al, 2011).

Both axial forces and moments can be transferred in a glued connection (Engström, 1997). Combining a glued connection with nails can increase the strength of the connection perpendicular to the grain, but the resin will take most of the axial loads (Wood Information Sheet, 2003). The strength of a glued lap joint is non-uniform, similar to the group effect of dowels. Therefor a maximum length of overlap exists beyond which no further increase in strength occurs. Today there is a lack of precise design rules regarding adhesive connections, aggravating the design procedure and increasing the need to rely on empirical studies (Crocetti et al, 2011).

3.2 Types of timber connection

3.2.1 Lengthening connections

Connecting elements lengthwise, i.e. end to end, is called scarfing or splicing and can be done in numerous ways. The scarf joint, also known as lap joint, can connect both tension and compression members longitudinally. The design of this type of joints is based on various shapes of notches, where the depth of parts of the elements is reduced, enabling the elements to overlap without changing the cross section of the assembly compared to the original cross sections of the elements. For the different types of connection described below see Figure 3.6.

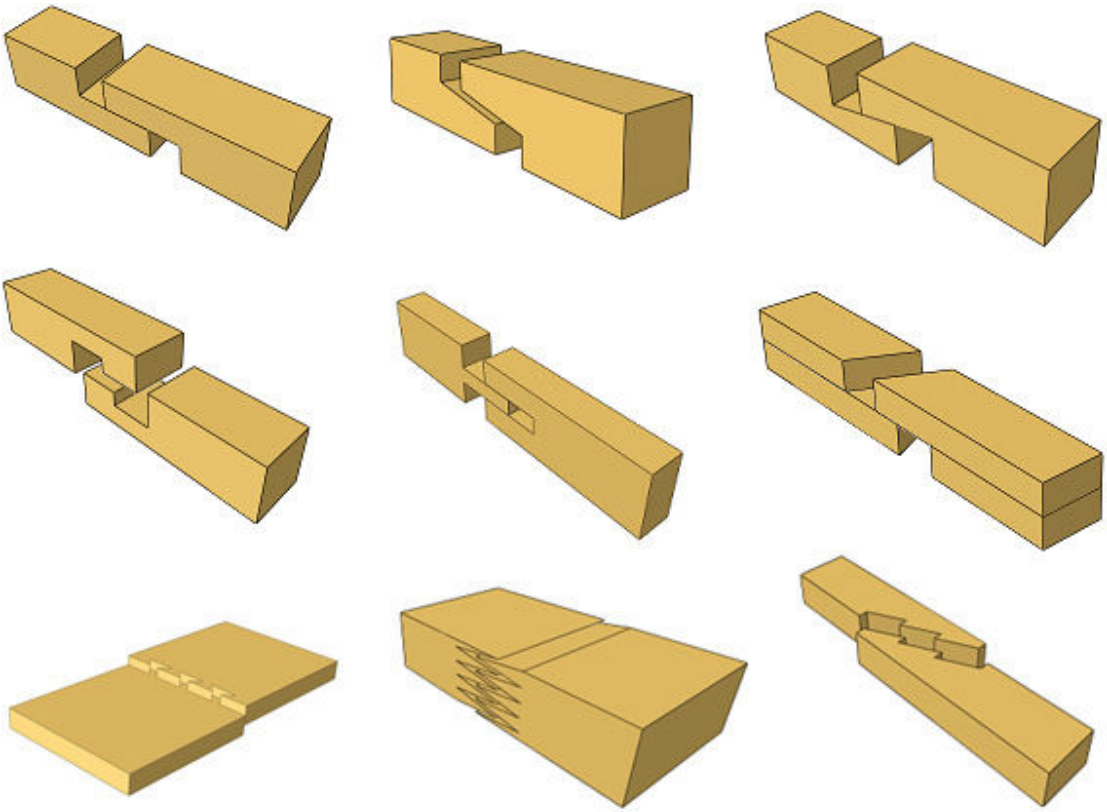

Figure 3.6 *Upper row from left: half lap joint, regular scarf joint, dovetailed scarf joint. Middle row from left: tabled scarf joint, double lap joint, half lap joint with tapered shoulders. Lower row from left: scarfed finger joint with dovetail fingers (fingers along width), Scarfed finger joint with tapered fingers (fingers along height), bolt-of-lightning joint.*

The scarf joints is one of the simplest joints and it can be designed in a vast number of ways, depending on which type of load is to be transferred. For example, the overlapping surfaces can be either plane, as in the half lap joint, or inclined, as in the regular scarf joint. Furthermore, the joint can have an interlocking, as the dovetail scarf joint and the tabled scarf joint, consist of a single lap or a double lap, and the bearing faces, which are also called shoulders, can be either straight or tapered. To increase the tensile capacity, the connection can be provided with transverse fasteners.

A scarfed finger joint with tapered fingers is a special type of lap joint in which a zigzag pattern is cut from the ends of the elements, creating fingers and slots which are glued together. The zigzag cut can be made either along the width or along the height of the elements and its purpose is to increase the glue area which contributes to the increased strength compared to members with plane ends.

Elements can also be spliced end-to-end by attaching different types of steel plate, with transverse fasteners, to the sides or inside the elements, in order to enable the elements to retain their original cross section. The different types of plate suitable for this purpose were discussed previously in Section 3.1.2. One of the most efficient longitudinal tension lap splices is the bolt-of-lightning splice, which relies on both interlocking bearing faces and transverse fasteners but requires a high level of craftsmanship (Woodworker Series, 2003).

Forces along the elements are transferred from one member to the other by bearing of the timber or by transverse or in-plane connectors acting in shear. In-plane connectors lie in the shear plane and shear such that the fibres of the connectors are rolled by one another.

For both tensile and compressive forces, it can be difficult to make all bearing faces carry load evenly and uniformly. The eccentricity of the load path, due to the halved members, can cause splitting along the plane of the lap. To increase the resistance against splitting, the elements can be reinforced by winded straps placed close to the notch. Furthermore, the reduction in cross sectional area of the individual elements in the overlapping region, by halving and due to potential transverse fasteners, affects the tensile strength of the connection, which is less than half of the tensile strength of the original members. However, in double laps the connectors act in double shear, which doubles the capacity of the connectors in comparison to the same connectors working in single shear, and also increases the stiffness of the joint (Federal Highway Administration, 2005).

3.2.2 Framing connections

Connecting elements at an angle to one another, e.g. at corners or at crossings, is called framing, and can be performed in many different ways. Elements can be connected end-to-end, end-to-face or face-to-face, perpendicularly or obliquely, creating shapes similar to the letters T, L, X or other shapes (Woodworker Series, 2003). Different types of connection are described in Figure 3.7.

Similarly to the lengthening connections described previously, simple lap joints of different shapes, e.g. single, double or dovetailed half laps and notched joints, can be used in framing connections. The bearing faces, also called shoulders, can be either straight, as in the tabled joint, or inclined, as in the dovetail connections. The inclination of the shoulders in the dovetail connection creates an interlocking, locking yet another direction of motion (the axial direction of the protruding element) beyond the ones locked by the straight shoulders (the transverse direction of the protruding element). Elements without axial interlocking can be secured with additional wedges, transverse fasteners or adhesives.

For corners also finger joints can be used, but unlike finger joints in lengthening connections, the fingers in framing connections are box or dovetail shaped. Just as for the lengthening finger joint, the strength of the connection is increased by the increased glue area, compared to an element with a straight end, but also by the interlocking.

Another type of framing connection is the mortise-and-tenon connection, which is very pleasing aesthetically but requires a high level of craftsmanship. It consists of a protrusion (the tenon) on the end of the first element and a cavity (the mortise) on the end or on the face of the second element. The connection can be made through, with an open mortise which lets the tenon pass all the way through, or blind, where the tenon ends inside a closed mortise. Through connections can end in level with the mortise element, being secured by wedges or dowels, or protrude additionally to allow being secured by a key.

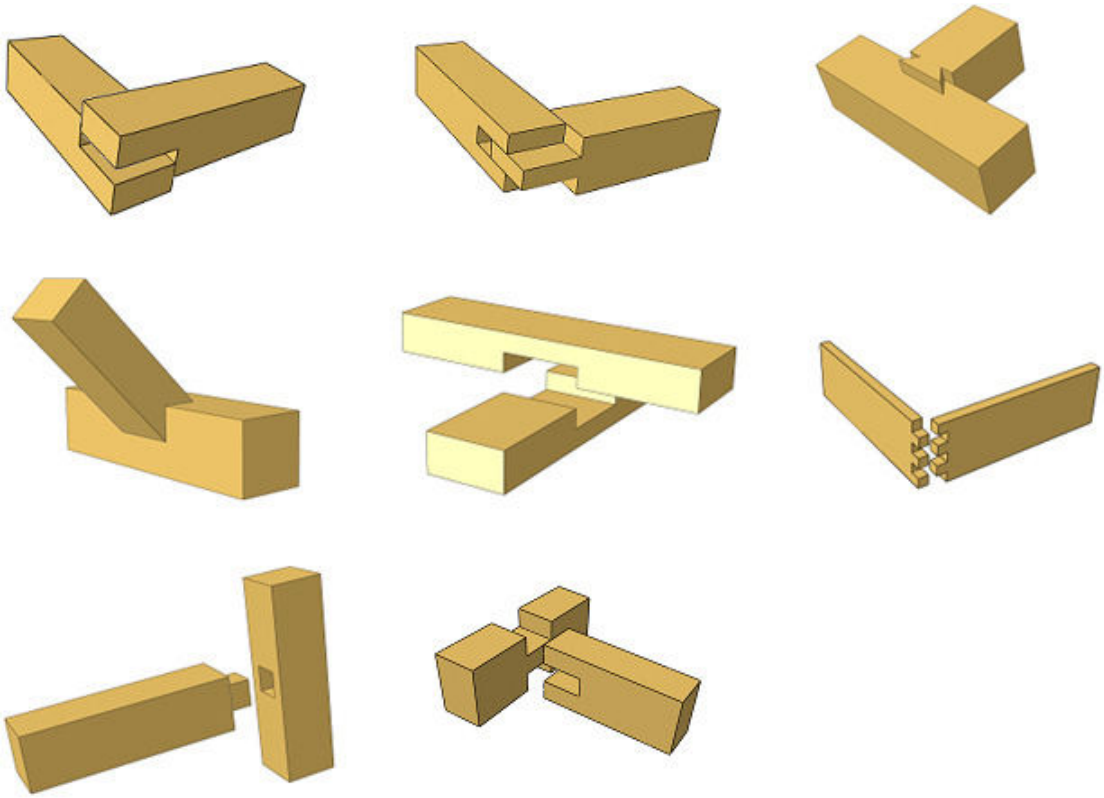

Figure 3.7 *Upper row from left: frame corner lap joint, frame corner double lap joint, dovetailed frame joint. Middle row from left: notched joint, tabled frame joint, box fingered frame joint. Lower row from left: blind mortise-and-tenon joint, bridle joint.*

Variants of the mortise-and-tenon connection can be achieved by choosing the number of shoulders on the tenon element. An element with one shoulder has a tenon with half the thickness of the element, whereas an element with two shoulders generally has a tenon with a thickness equal to one third of the element thickness. The increase in thickness of the tenon is restricted by the requirement for tensile strength in the mortise element, i.e. enough wood must remain. Another version is the inverse of the mortise-and-tenon, which is called a bridle joint. It looks similar to a lengthening double lap joint but with the exception that the elements are connected at an angle to one another instead of lengthwise (Woodworker Series, 2003).

For stability, especially for shear loaded connections, the mortise can consist of two levels, firstly the so called housing, which has the same area as the tenon element, and secondly the ordinary mortise with the same width as the tenon (Teike, 2013). Even though double tenons are stronger than single, an alternative that should be avoided is to design a connection with multiple mortises and tenons, because of the difficulty of avoiding unevenly loaded tenons (Tredgold, T., Hurst, J. T., 1871).

Also for framing connections, by using different types of steel plate or beam shoe in addition with transverse fasteners, the members can be joined without reducing the cross section. Similarly to the lengthening connections, forces are carried by bearing of the timber or by friction from wedges, filling gaps in mortises, and shearing of the additional mechanical fasteners or adhesives.

3.2.3 Engineered timber connections in glulam structures

Traditionally, the connections in timber structures have consisted of the previously mentioned types of connection, but lately some modern, innovative engineered timber connections have been developed, which provide more reliable methods of evaluation. Two contemporary types of connection for glulam are e.g. the glulam rivet system and the glued-in rods (Madsen, 1998).

The glulam rivet system works similarly to a nail plate. It consists of a steel plate with pre-drilled holes, which is placed over the splice between the two glulam elements, and fastened with glulam rivets with tapered heads. The tapered heads cause ring tension in the steel plates, which further fixes the rivets in place. The innovative thing about the glulam rivets is that they have an oval shape instead of a circular, which increases their capacity due to the increased sectional modulus. They are inserted such that the long diameter is parallel to the grains in the glulam member, regardless of the direction of the applied loads. One benefit of the oval shape, besides the increase in capacity, is the increased friction due to the larger surface area of the rivets and due to the compaction of the timber in the glulam member when the rivets are inserted. Because of this the rivets are difficult to remove. Yet another benefit of the oval shape is that the smaller width of the rivet, compared to a circular rivet, causes less damage to the fibres in the glulam member when the rivets are inserted (Madsen, 1998). As for the regular nail plates the bending stresses in the beams are transferred by tension and compression in the steel plates and by shear in the fasteners (Engström, 1994).

The glued-in rod system consists of a steel rod which is glued into an oversized pre-drilled hole in the end grain of a glulam member, see Figure 3.8. It is a suitable method for creating knee joints, beam to column joints or column to foundation joints (Madsen, 1998). In members subjected to axial forces, the rods should be threaded to provide interlocking with the resin (Wood Information Sheet, 2003). In the column to foundation joints, the bending moment resistance is increased by placing the rods as close to the glulam face as possible. The pre-drilled holes can either be parallel to the grain or have an angle to the grain. Having an angle of 30 ° to the grain provides shear reinforcement to the glulam member. The rods can also be combined with steel plates, to which the rods are welded. The plate is placed in a recess such that it is flush with the end of the glulam member and the holes are filled with glue in such an amount that also the underside of the plate is glued to the recess. The assembly of two members is then performed by bolting another steel plate over the splice of the individual glulam members, see Figure 3.8. This method was developed to provide an easy assembly on site and to avoid on-site gluing and welding. During the design process, it is important to choose a plate large enough to handle the compression that arises perpendicular to the grain if the rod is placed at an angle to the grain. So far, the placement of this type of joint is limited to the end grain of the glulam member (Madsen, 1998).

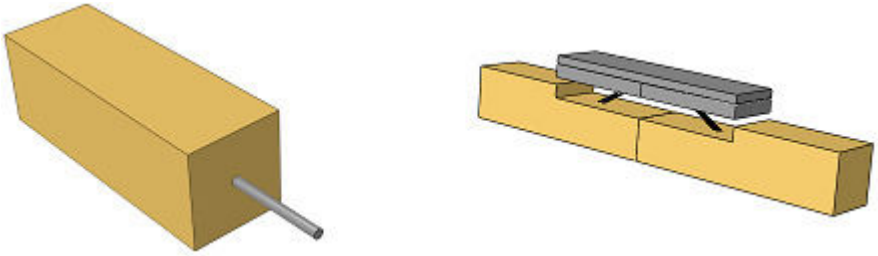

Figure 3.8 Glued in rod and glued in rod with steel plate.

3.3 Properties of fasteners and connections

The purpose of connections is to transfer forces between different components in a structure in an efficient way. The structural efficiency of the connections is dependent on the properties of the timber itself, the fastener itself and the assembly of the connection, and can be evaluated as the ratio of transferred load to required area of the connection (Connections in timber structures, 2006). The capacity and stiffness of a straight piece of wood is always greater than any mechanical connection and in order to design efficient connections many different aspects have to be considered (Federal Highway Administration, 2005). In the following sections failure mode, strength and stiffness aspects are discussed.

3.3.1 Failure mode

A connection can fail in different types of failure mode. The failure modes that the fasteners can experience are e.g. bending, pull-out and pull through. Axially loaded fasteners are particularly subjected to pull-out failure and should be avoided if possible. Instead through bolts can be used which carry the force by compression on the opposite side of the timber. Bending failure can occur in different ways depending on the number of shear planes through which the fasteners pass. The failure modes that the structural members can experience are e.g. embedding failure (transversally loaded fastener crushing the timber), splitting and row, block and plug shear failures. Figure 3.9 illustrate a few failure modes of the fasteners and structural members.

By design choices, it is possible to control the failure mode of the connection, which should preferably be ductile and not brittle. Ductile failures are more predictable compared to brittle ones, which are considered more severe as they often give no prior indication of the failure or the collapse (Farreyre, A., Journot, J., 2005). In design it is therefore preferable to aim at yielding of the connection before failure in the structural elements, since the former is considered more ductile than the latter (Engström, 1995). This aim can be achieved by designing the connection such that it is weaker than the structural elements. It should be considered that a high number of fasteners in the connection increases the risk for brittle failure, since the strength of the connection increases in relation to the structural elements (Engström, 1997).

Failure in a steel plate is ductile and rather predictable whereas the addition of glue to a connection increases its brittleness and makes the failure less predictable. In connections using glued-in rods, failure in the steel plate can be assured by providing enough embedment length for the rods. Here it must also be assured that the timber can handle the compression induced by the steel plate (Madsen, 1998). From economic aspects the design should also aim at reducing the size of the connection to avoid the need for over-dimensioning of the structural elements, but at the same time care should be taken to the placement of the fasteners, since too closely placed fasteners can cause splitting. Small and strong connections can be achieved by aiming at embedding failure of the timber (Engström, 1994).

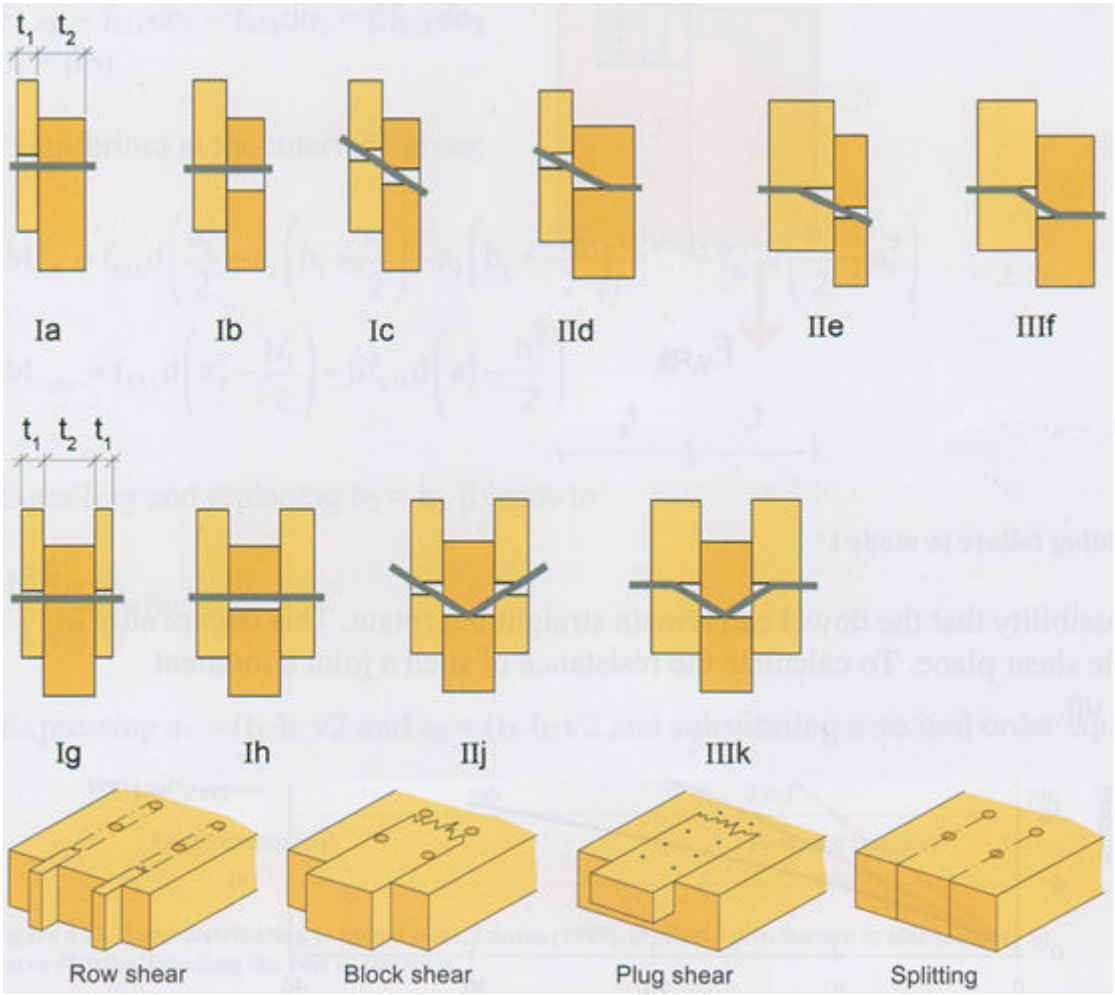

Figure 3.9 Different types of failure mode.

3.3.2 Strength

Timber is an anisotropic material, which means that it has different properties in different directions. This is an important aspect to consider when designing connections. Carrying loads through compression is more efficient than through tension (Connections in timber structures, 2006) (Madsen, 1998). The magnitude of the tension perpendicular to the grain should be minimized, since this is the weakest direction of the timber, and the compression perpendicular to the grain should be distributed over a sufficiently large area in order to avoid local crushing of the timber (American Institute of Timber Construction, 2012). Another weak property of timber is its longitudinal shear strength. Hence it is preferable to avoid eccentrically loaded elements and to reduce stress concentrations in areas with high amount of shear stress, i.e. close to supports (Connections in timber structures, 2006). Holes and drilling in primary members should be avoided if possible, in order to avoid large stress concentrations, which arise due to the deviated load path as the load path has to go around the hole, see Figure 3.10. Furthermore, the reduction of the cross-section in order to make room for fasteners should be limited to 25%.

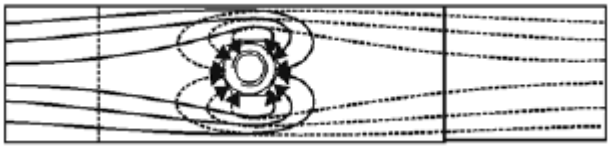

Figure 3.10 Stress concentration due to hole (Connections in timber structures, 2006).

The strength of a connection is dependent on the strength of the fasteners, the structural members and the assembly of these components. A connection in which all forces go through a common point can be considered to experience only pure tensile and compressive forces, but if the forces do not go through a common point, bending will arise. Many considerations must be made with regard to the strength of the structural members when using fasteners, and factors such as shrinkage and creep deformations should be considered. If shrinkage is prevented by fasteners, splitting may occur close to the fasteners due to the developed tension perpendicular to the grain as the timber tries to shrink (Connections in timber structures, 2006). The addition of adhesives can reduces the effect of creep (Engström, 1994; Engström, 1997).

Also the placement and quantity of fasteners is of importance. One effect that must be considered when designing connections is the group effect of fasteners. The strength of the connection does not increase linearly with increased number of fasteners and hence the total capacity of the fasteners is not equal to the sum of the capacities of each individual fastener. The fasteners closest to the loaded edge are more efficient than the fasteners placed furthest away.

3.3.3 Stiffness

The extent to which a member resists deformation under applied load is called stiffness and there are both translational and rotational stiffness. The translational stiffness is defined as applied force divided by deflection whereas the rotational stiffness is defined as applied moment divided by rotation. The stiffness of the fasteners, the structural members and the assembled joint all affect the brittleness of the failure, where a higher stiffness causes a more brittle failure. The joint stiffness also affects the overall stiffness of the entire structure. Therefore it is important to consider the joint stiffness, especially in slender structures which are less stiff and more prone to large deflections (Engström, 1994). Also the number of shear planes through which fasteners pass affect the stiffness. For example transverse connectors in double shear are stiffer than in single shear (Federal Highway Administration, 2005). Mechanical fasteners provide mostly bearing whereas glue provides mostly stiffness. These can be combined to achieve the desired properties in a connection (Engström, 1994).

3.4 Improving and developing connections

In order to be able to increase the competitiveness of timber structures, it is important to aim at development of joints in order to make them more efficient, more economical and increase the usability (Engström, 1993; Engström, 1994). The joints in a structure can be considered as weak points, both structurally, with regard to strength and stiffness, and economically, with regard to labour costs of the man-hours required for the assembly (Engström, 1994; Engström, 1997). Mechanical connections including e.g. nails, nail plates, bolts or dowels can often be bulky and consist of many parts. This

might result in a need for larger dimensions of the structural components than what would have been necessary with regard to the strength requirements. It might also lead to the assembly being time consuming. Both of these aspects result in the connections being economically inefficient (Engström, 1993).

Engström defines the aim of developing the design of simple connections as "Connection design for buildability", where the term "buildability" stands for ease of assembly and low costs while still guaranteeing structural safety and function. To achieve these objectives, the connections should consist of as few parts as possible, need no special equipment or education to perform the assembly, have a minimum need for accuracy and preferably have a high degree of prefabrication (Engström, 1997).

3.5 Modelling connections

Performing very accurate structural analyses of a jointed timber structure can be difficult owing to the inhomogeneous properties of timber and non-linear load-deformation behaviour in connections due to e.g. gaps in predrilled holes and plasticity (Engström, 1994). Generally, as a simplification, the joints are modelled as either perfectly pinned or perfectly fixed. Connections which are assumed to be perfectly hinged allow for rotations, but do not transmit moments, resulting in an efficient use of material, since the elements act in pure tension or compression and not in bending, but the moment peaks in the elements are large. Connections which are assumed to be perfectly fixed allow for no rotations and moments are transmitted by the connection, causing elements to act in bending, which is less efficient than action in pure tension and compression, but resulting in a more even moment distribution, see Figure 3.11.

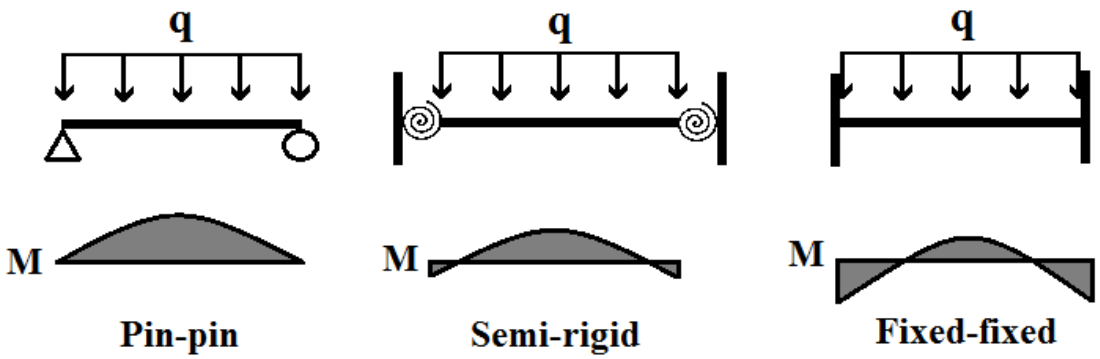

Figure 3.11 Moment distribution for a beam with different support connections, cf. (McGuire, 1995)

In reality it is very difficult to achieve a connection which is perfectly hinged or perfectly fixed. The connections will experience an intermediate degree of fixation as connections which are considered to be perfectly hinged do take small amounts of moment (e.g. by friction) and connections which are considered to be perfectly fixed do experience small deformations. By a more accurate design, modelling the connections with a degree of semi-rigidity instead of perfectly hinged or perfectly fixed, over-dimensioning can be reduced (Engström, 1994). Also the minimum natural frequency is affected by the degree of fixation of the connections (McGuire, 1995). In contrary to Eurocode 3, which specifies requirements on steel structures and connections, this matter is not addressed in Eurocode 5, according to which timber connections should be designed (Engström, 1995). In order to increase the

competitiveness of timber connections, it would be favourable if requirements and guidelines, on which the engineer could rely, were specified for this matter.

The connections can be modelled as semi-rigid using linear rotational springs. Not the stiffness of the spring itself, but the joint stiffness determines the behaviour of the connection. The joint stiffness is defined in Equation (3.1).

$$s = \frac{k \cdot L}{E \cdot I} \tag{3.1}$$

where:

k = *spring stiffness*

$\frac{E \cdot I}{L}$ = *flexural stiffness of the member*

The joint stiffness is unitless and for a constant spring stiffness, the rigidity of the connection decreases with increasing stiffness of the attached member, see Figure 3.12.

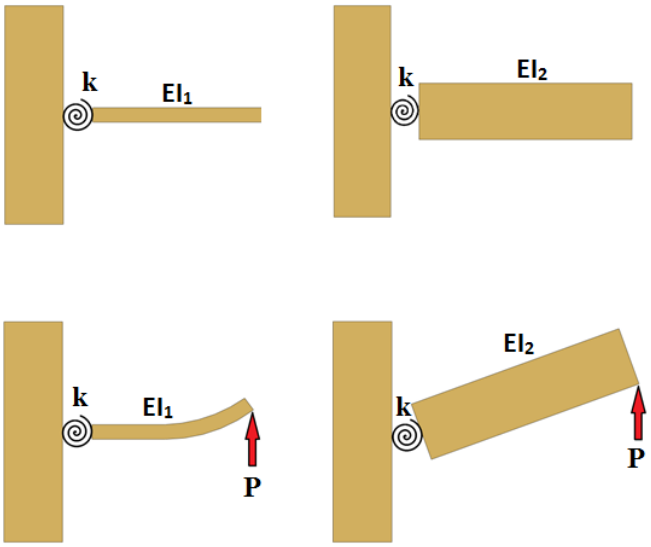

Figure 3.12 *Comparison of joint stiffness for members with different flexural stiffness. The joint stiffness is lower for a connection with stiffer members, cf. (McGuire,1995).*

According to an analysis performed by NASA Goddard Space Flight Centre, a beam which ends are connected to two rotational springs can be considered as pinned-pinned if the joint stiffness is less than 1 and considered as fixed-fixed if the joint stiffness is greater than 100 (McGuire, 1995), see Figure 3.13.

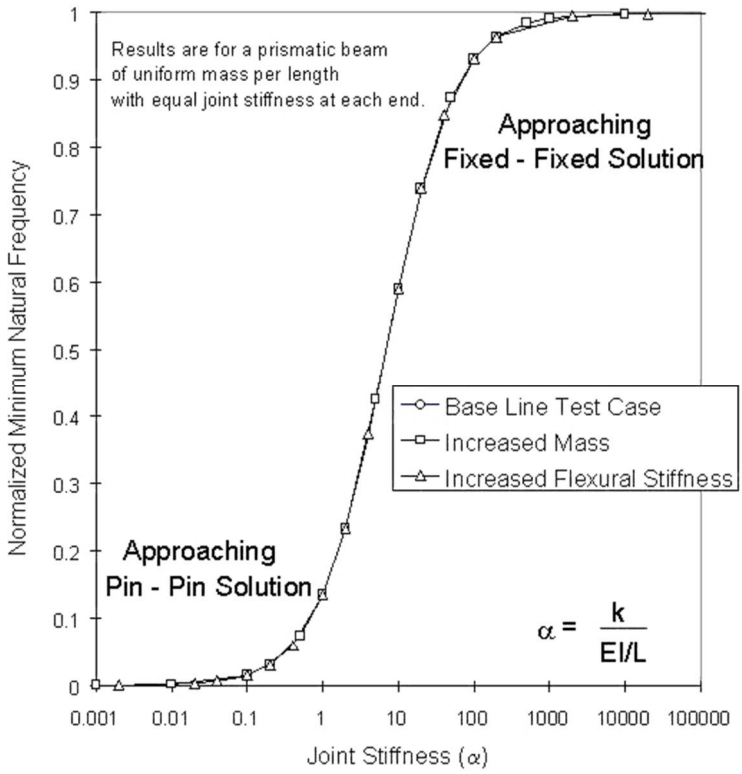

Figure 3.13 Graph of joint stiffness vs. normalized minimum natural frequency (McGuire, 1995).

4 The *Leaf Bridge* Concept

The bridge design which will be analysed in this Master's Thesis project is based on the *Leaf bridge*, a tied-arch bridge developed conceptually by Flårback (2015) in his Master's Thesis Covered Timber Bridges. Figure 4.1 shows a day and a night view of the bridge. Since the bridge design is only conceptual, the bridge does not have a specific geographical location.

Figure 4.1 View of the Leaf bridge by day and by night (Flårback, 2015).

4.1 Bridge geometry and elements

An accurate description the Leaf bridge concept can be found in Flårback (2015). In this Master's Thesis project, some modifications were made to the design proposed by Flårback. The modifications will be discussed at the end of this section. A model of the modified geometry of the bridge and its constituting elements are shown in Figure 4.2. Note that the bridge is modelled with centre lines, which is why the deck and the roof boards do not lie on top of the structure but in the centre, and all elements are connected to the centres of the adjacent elements.

Figure 4.2 3D model of the Leaf bridge and its constituting elements.

The bridge spans 30 meters and consists of glulam beams and steel cables. There are two inclined 3-pinned arches, i.e. they are pinned at the mid-span, which are approximately 6 meters high and continuously curved. From the arch the 4 meter wide bridge deck is suspended by inclined cables. It is also connected to the ends of the arches. The deck consists of a horizontal truss which is put together by two longitudinal curved edge beams, stabilizing diagonals forming crosses and transverse cables. At the mid-span, the deck has an initial distance of 994 mm to the horizontal level of the supports. The arches are transversally stabilized by curved beams and a truss system. Both the deck and the roof are covered with boards, but their contribution the structural behaviour, such as the board action, is not considered. Only the weight of the boards are considered.

Materials and dimensions of the individual structural components are specified in Table 4.1.

Table 4.1 List of all components in the Leaf bridge. The colours in brackets refer to Figure 4.2 above.

Component	Material	Dimensions
Arches (red)	Glulam GL30c	405 x 215 mm
Roof curved beams (yellow)	Glulam GL30c	245 x 140 mm
Roof truss beams (blue)	Glulam GL30c	225 x 140 mm
Edge beams (green)	Glulam GL30c	180 x 90 mm
Deck truss beams (purple)	Glulam GL30c	180 x 90 mm
Cables (grey)	Steel S460	Ø 19mm

4.1.1 Modification of the *Leaf bridge* concept

Some modifications were made to Flårback's design. The pre-stressed cables were replaced by edge-beams since no good method of modelling the connections between vertical cables, main cables and deck truss members was found. The desired type of connection would have been a slot connection, where the secondary cables would be pinned to the deck truss and the main cable would run through this connection, allowing the pinned connection to slide along the main cable. The pinned connection should not clamp the pre-stressed cable, since this would create different stresses along the main cable, which is not desirable. Another modification made was that the connections were considered to be semi-rigid instead of completely fixed, as they were considered in Flårback's design. After numerically analysing the geometrically modified bridge, the dimensions of some of the elements were altered, compared to the dimensions in Flårback's design, in order to meet SLS and ULS requirements.

4.2 Structural behaviour

The structural behaviour of the bridge, subjected to only vertical loads, is presented below. The bridge has two competing load carrying systems; the main arches and the truss system. The force pattern of axial sectional forces of the roof and the deck are shown in Figure 4.3 and Figure 4.4, respectively. Figure 4.5 shows the force pattern of axial sectional forces of the entire bridge except for the cables. The figures are taken from the *Abaqus* model and the cables are not included since their axial sectional force could not be plotted in *Abaqus*. In order to see the forces in the cables, the axial stress (S11) had to be plotted. The axial stress indicated that the cables were all in tension except for the outermost ones.

The arches and the inclined steel cables carry the weight of the entire structure which puts the arch in compression and the cables in tension. Due to the inclination of the arches, the transverse curved beams act in tension and the truss system between these beams takes mostly compressive forces. Some truss members close to the entrances of the bridge take tensile forces. The longitudinal glulam beams are prevented from transverse translations by the diagonal truss elements and the cables in the deck. Most of the elements in the deck act in tension (red elements), but some act in compression (blue elements).

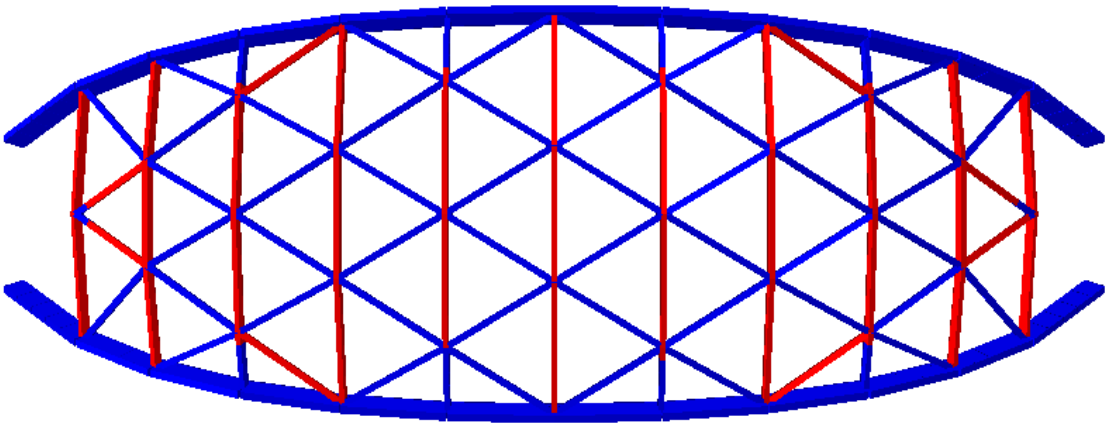

Figure 4.3 Force pattern in the roof structure. Blue = compression, red = tension.

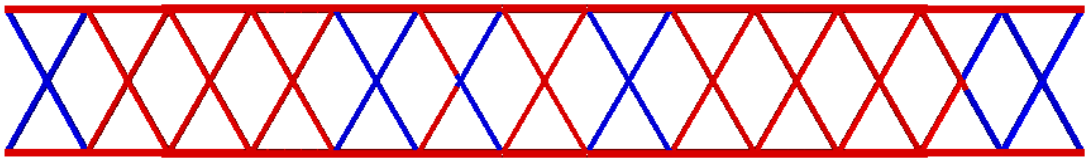

Figure 4.4 Force pattern in the floor structure. Blue = compression, red = tension.

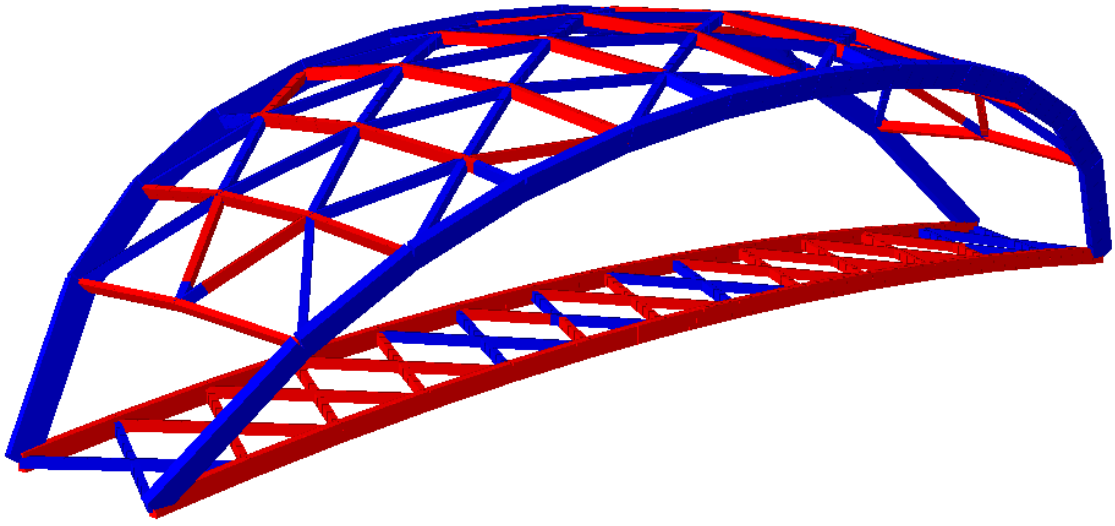

Figure 4.5 Force pattern in the entire bridge. Blue = compression, red = tension.

5 Requirements for Pedestrian and Bicycle Bridges

There are several requirements that have to be fulfilled when designing a structure, both regarding safety and comfort. Safety requirements mean that the capacities are large enough to withstand the applied loads for the designed life length and hence failure of elements is avoided. Comfort requirements refer to the deflections and frequencies, which should be kept within a limit in order to avoid discomfort for the users. By designing the structure according to the ultimate limit state (ULS) where safety requirements are taken into account and the serviceability limit state (SLS) in which deflection and frequencies are included, the requirements can be checked and further fulfilled. In the following section some requirements which have been taken into account for this pedestrian and bicycle timber bridge, the *Leaf bridge*, are explained.

5.1 Loads and service classes

Timber bridges should be designed for loads according to Eurocode, SS-EN1990-1. The loads for which a bridge is designed for can be categorized in two different types, static and dynamic. (VVFS 2004:31 2.2.1). In this project, only the static loads have been considered, such as permanent and variable loads, which are described further in this section. Regarding rigidity and load carrying capacity of a timber structure, it is mostly dependent on the duration of the acting load. Therefore, it is of importance to distinguish different type of load duration of the loads, such as between the permanent loads and variable loads, see Table 5.1 for different type of load duration.

Further, different safety classes are assigned to enable the consideration of different type of failure in the structure. By different type of failure means that the damage or injuries cause by a failure in a structural element can be different depending on the type of the structure, their use and their function. Other factors that are taken into account are the size of the timber element, moisture content in the material and the surrounding relative humidity. In Table 5.2, three different durability classes, which are dependent on the relative humidity and moisture content are presented.

Table 5.1 Different type of load duration.

Type of load	Duration	Example
Permanent load	>10 years	Dead weight
Long term	6 months – 10 years	Live load
Medium term	1 week – 6 months	Live load
Short term	<1 week	Wind load, snow load
Instantaneous		Accidental loads

Table 5.2 Service classes.

Service classes	Relative humidity	Moisture content
1	≤ 65	≤ 12
2	≤ 85	≤ 18
3	> 85	> 18

To be able to find the dimensioning load that is acting on the structure, it should be checked for different combinations of the different types of load. The load combination consider each load as a leading action and in turn reduces all the other loads with a combination factor, ψ. Equation (5.1) is used in the ultimate limit state (ULS), while Equations (5.2) and (5.3) are used in the service limit state (SLS). In SS-EN 1991-1 the factors γ_i and ψ_i are given for different loads acting on the bridge, see Table 5.3.

$$\sum\left(\gamma_{g,j} \cdot g_{k,j}\right) + \gamma_p \cdot p + \gamma_{q,1} \cdot q_{k,1} + \sum\left(\gamma_{q,i} \cdot q_{k,i} \cdot \psi_{0,i}\right) \tag{5.1}$$

$$\sum\left(g_{k,j}\right) + q_{k,1} + \sum\left(q_{k,i} \cdot \psi_{0,i}\right) \tag{5.2}$$

$$\sum\left(g_{k,j}\right) + \sum\left(q_{k,i} \cdot \psi_{2,i}\right) \tag{5.3}$$

Table 5.3 The factors γ_i and ψ_i for different type of unfavourable loads.

Type of load	γ_i	ψ_i
Gravity	1,35	N/A
Live load	1,5	0,4
Snow load	1,5	0,8
Wind load down	1,5	0,3
Wind load transversal	1,5	0,3
Wind load longitudinal	1,5	0,3
Service vehicle (vertical)	1,5	0,4
Service vehicle (horizontal)	1,5	0,4

5.1.1 Permanent loads

Under the permanent load, the dead weight, based on the density of the wood according to SS-EN 1990-1-1:2002, of various components in a bridge is considered. Beside the dead weight, other loads are also taken into account, such as earth pressure, shrinkage, support displacements and tension force (Svenskt trä, 2015). In this project, only the dead weight of the different materials was included.

5.1.2 Variable loads

Variable load includes snow, wind, traffic, live load and other specific loads such as joints and attachment of the railing, of which their duration can vary from short, medium to long term.

Considering snow load, it should be taken into account especially when the bridge is covered since there might be a risk of snow drift depending on the design and the angle

of the roof. It is recommended that the angle of the roof should be between 3 and 45 degree, even though a larger angle would minimize the risk of snow drift, it could on the contrary increase the surface that is affected by the wind load (Pousette, 2008).

The calculations of the wind load for bridges that spans less than 40 m can be based on the conditions of static analysis if the load does not cause any significant deformations or induces risk for fluctuations or fatigue. The magnitude of the load is determined by the loading area, the density and velocity of the air and also on a wind load safety factor (Pousette, 2008). Moreover, depending on the design of the bridge, its stiffness and the damping factor, the wind load can have a dynamic impact on the structure and therefore the dynamic analysis should be included. The dynamic effects caused by the wind load should be taken into account when designing and analysing suspension bridges, arch bridges and cable stayed bridges, since these are not considered to be static structures (Trafikverket, 2004). For this project, the dynamic effects cause by the wind load was not considered.

Considering the impact from the traffic load, it is included in calculations to be acting in both vertical and horizontal direction of the bridge deck. A pedestrian and bicycle bridge should be designed for a surface load of 4 kN/m^2 and if the bridge is connected to a pedestrian and bicycle road in coplanar, the impact of the sanitation and emergency vehicles should be included. The load of a sanitation vehicle, in which the dynamic effects are included, is divided into two axle weight of 40 and 80 kN with an axle distance of 3 m, whereof they are further divided into two point loads of 20 and 40 kN respectively and a centre distance of 1.6 m, see Figures 5.1, 5.2 and 5.3. (Trafikverket, 2004).

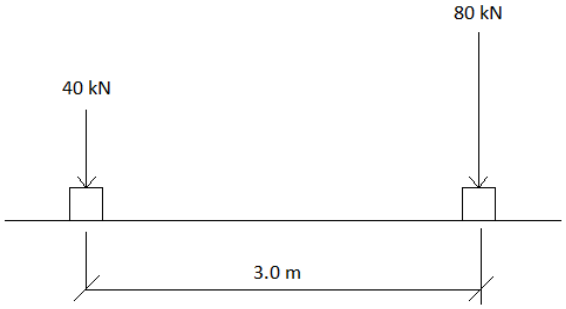

Figure 5.1 The load of the sanitation vehicle in the longitudinal direction.

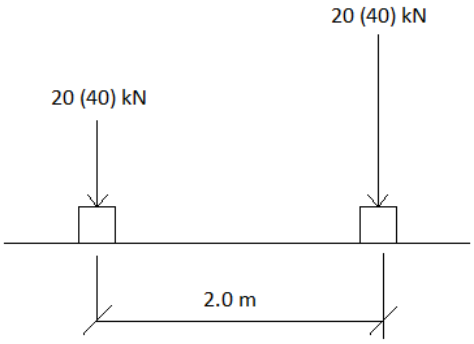

Figure 5.2 The load of the sanitation vehicle, divided in two sub-loads in the traversal direction.

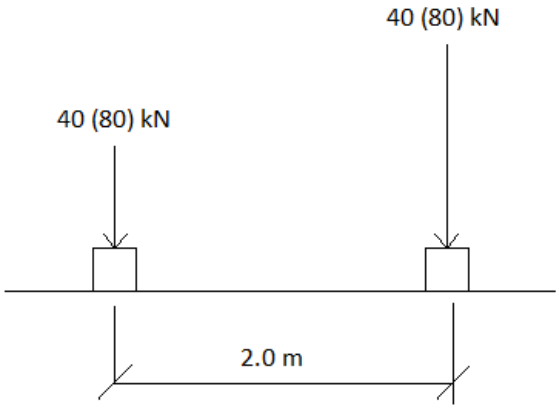

Figure 5.3 *The load of the sanitation vehicle, divided in two sub-loads in the traversal direction.*

As for the emergence vehicle, it consists of four axle weights of 80 kN and an axle distance of 3.8 m, 1.3 m and 1.3 m. Further, each axle weight is divided into two point loads of 40 kN and a centre distance of 2 m, see Figures 5.4 and 5.5 (Trafikverket, 2004).

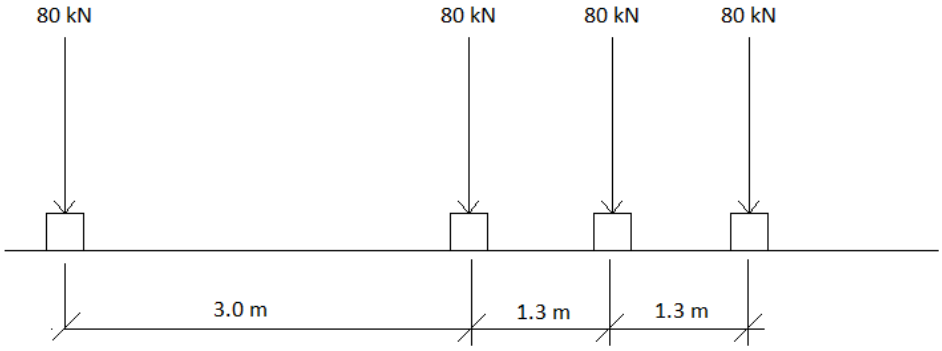

Figure 5.4 *The load of the emergence vehicle in the longitudinal direction.*

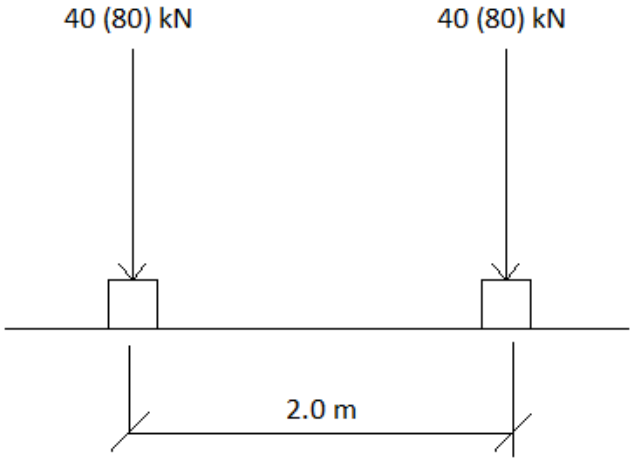

Figure 5.5 *The load of the emergence vehicle, divided in two sub-loads in the traversal direction.*

5.2 Deflection

Standing or moving along a bridge which experiences large deflections can be uncomfortable for the user. As a result, the structure must be designed in such way that the deflection are kept below the limit value. According to TRVK Bro 11 the maximum vertical deflection (for variable loads) for a pedestrian and bicycle bridge must be less than 1/400 of the theoretical span length of the bridge. Not only the deflection caused instantly by applied loads, but also the long-term deflections due to e.g. creep should be considered. Also the vertical displacement of deck ends caused by traffic loads and the horizontal settlement difference between supports should be limited. Due to the inability to define different boundary conditions for positive and negative movements in one single degree of freedom in the finite element modelling and that the substructure of the bridge is not part of this thesis, none of these two latter displacements are considered. Also the long-term deflections were omitted in the modelling.

The *Leaf bridge* is 30 meters long, and the maximum deflection allowed is calculated according to Equation (5.4).

$$\delta_{\max} = \frac{30\ m}{400} = 75\ mm \tag{5.4}$$

5.3 Frequency

The natural frequency, also called eigenfrequency, is a frequency at which the amplitude increases without increasing load and its unit is rad/sec. It decreases with increasing mass of the structure, but increases with increasing flexural stiffness. The contents of a dynamic analysis are stated in TRVK Bro 11 A.3.5.4 (Trafikverket, 2011) and the analysis itself should be carried out according to SS-EN 1991-2 6.4. According to SS-EN 1990:2004, the acceleration should be checked to ensure comfort if the natural frequency is less than 5 Hz for vertical movements. If the frequency is above 5 Hz no further investigation is required (Svenskt trä, 2014).

Due to the manual assignment of pinned connections between nodes in the finite element model, problems with the degrees of freedom arose and the program was unable to run the frequency analysis. Therefore these requirements were omitted.

5.4 Connections

The design of connections should aim at efficient, durable connections with sufficient performance with regard to strength and stiffness. Strength, stiffness and efficiency properties of connections were discussed earlier in Section 3.3. The durability aspect mostly regards protection against moisture and fire. It is also important that the connections are designed in such a way that they are easily accessible for maintenance.

With regard to moisture, joints should be designed such that moisture is not trapped within the connection. Attention should be paid to exposed areas such as end-grain and special consideration should be made when using steel connectors, since moisture can condense on the steel surface and steel plates can act as moisture barriers. It is desirable

to keep the moisture content below 20% since an increasing moisture content increases the risk of fungal decay (Connections in timber structures, 2006).

With regard to fire, it is more preferable to avoid through fasteners which, when heated up by fire, transfer heat to the interior of the timber member more efficiently than fasteners that are not through. Structural members can also be knowingly over-dimensioned to provide the members with additional volume of material, so called sacrificial over-dimensioning. The additional sacrificial volume increases the time it takes to reduce the volume of the member to such an extent that it fails (Connections in timber structures, 2006). By over-dimensioning members, also time dependent effects like creep, which affects the strength and stiffness by reducing the failure load and increasing the deformations, can be taken into consideration (Engström, 1994).

6 Numerical Analysis of the *Leaf Bridge*

To investigate the difference in performance of the bridge between perfectly and partially fixed connections, numerical linear analyses were performed using the finite element software *Abaqus/CAE* (Dassault Systèmes). An analysis can be assumed to be linear of the strain is kept below 5%. Since the capacity of timber is much lower than its Young's modulus, it can be assumed that the analysis will always be linear. A short summary of the procedure of the analysis is presented below in this section and a more detailed description of the procedure is presented in Chapter 6.2 Finite element modelling.

The bridge structure was initially modelled with perfectly pinned and fixed connections. The goal of the numerical analysis was to first perform an SLS analysis, checking the maximum deflections and changing the dimensions of the elements if the SLS limits of deflections were not fulfilled, and then perform a ULS analysis, extracting stresses in the elements and checking the utilization ratios. No attempts were made to additionally improve the structure to fulfil the ULS limits. The element stresses from the ULS analysis were then used as input values for the design of the connections, which were designed to fulfil ULS requirements. After the connections were designed, the rotational stiffness of the connections was calculated and inserted into the SLS model in Abaqus and new analyses were run. The deflections and the stresses in the elements from the new analyses were checked and compared to the ones from the initial analyses. Additionally, the impact on deflection due to the degree of fixation between 0% and 100%, was investigated.

Before starting the modelling, and also during the modelling, of the bridge structure in *Abaqus*, verifications were made in order to check differences of modelling choices and alternatives. A verification of the behaviour of connections in a single part model compared to a multiple part model is described in the following section.

6.1 Verification of connection behaviour in single and multiple part models

When a model in *Abaqus* contains only one part consisting of both beam and truss elements, these elements are perfectly fixed and perfectly pinned, respectively, to one another by default. If a model instead contains multiple parts, the degree of fixation can be chosen manually by modelling connectors between the elements and then applying spring-like behaviours to these connectors.

A verification was made to ensure that there is no difference in the structural behaviour between a model containing one single part and a model containing multiple parts. The verification was performed by comparing the deflections and the reaction forces from two truss structures, one consisting of one single part and the other one consisting of multiple parts connected manually by wire sections with connections of type basic having a rigid spring-like behaviour. The connection type basic was chosen over *MPC* connections since the *MPC* connections cannot be assigned behaviours. The truss structure chosen is part of a task given in Strukturmekanik (Dahlbom and Olsson, 2010) and its geometry is presented in Figure 6.1.

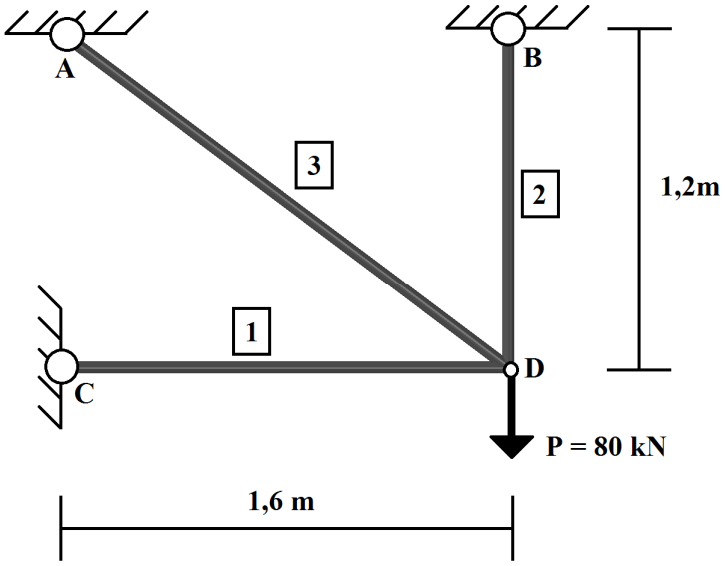

Figure 6.1 Geometry of the elements, nodes and loads.

The truss consists of three bars which are pinned to the supports and pinned to each other. A point load of 80 kN is applied to the node where the elements meet. All elements have a Young's modulus of 200 GPa. The lengths and cross sectional areas of the individual element are presented in Table 6.1. The deflected shape of the structure due to the load is shown in Figure 6.2.

Table 6.1 List of length and cross sectional area of the elements.

	Element 1	Element 2	Element 3
Length [m]	1,6	1,2	2,0
Cross sectional area [m2]	$6{,}0 \cdot 10^{-4}$	$3{,}0 \cdot 10^{-4}$	$10{,}0 \cdot 10^{-4}$

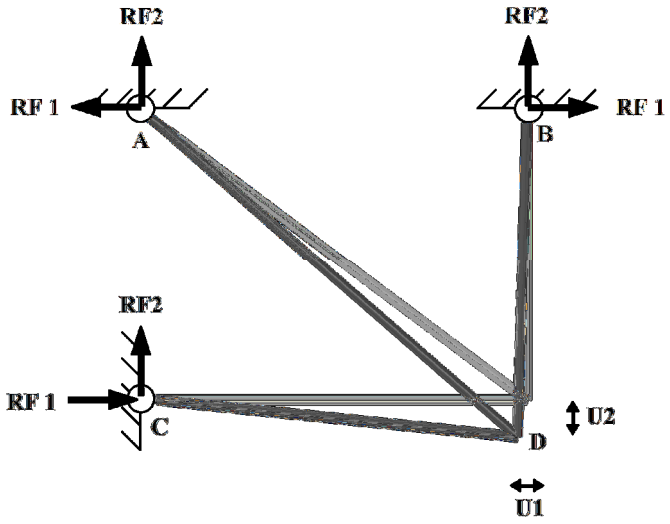

Figure 6.2 Reaction forces and direction of displacements.

Six different cases were investigated, according to Table 6.3, for different combinations of element types (truss or beam, both with circular cross sections), connection types of the common node (pinned or fixed) and assembly types (one part (OP) or multiple parts (MP) in Table 6.2). The elements are always pinned to the supports. Unlike the OP model, which has only one node at node D, the MP model has three nodes overlapping.

Because of this, the load in the MP model must be applied by clicking the node once and not by dragging the marker across the area of the node. If the marker is dragged across the area of the node, the three nodes will be assigned one load each, which is not correct. It is not of importance which of the three nodes is selected for the application of the load, as long as only one of them is selected.

Table 6.2 List of all cases and their model type, element type and connection type. OP = one part, MP = multiple parts.

Case	Model	Element type	Connection type
1	Task in book	Unknown	Pinned
2	OP	Truss	Pinned
3	OP	Beam	Fixed
4	MP	Truss	Pinned
5	MP	Truss	Fixed
6	MP	Beam	Pinned
7	MP	Beam	Fixed

The resulting deflections from all cases are presented in Table 6.3 and Table 6.4 and the resulting reaction forces from all cases are presented in Table 6.5 and Table 6.6.

Table 6.3 Displacements U1 and U2 [mm] at node D for case 1-3.

	Node	Case 1	Case 2	Case 3
U1	D	-0,40	-0,40	-0,10
U2	D	-1,15	-1,15	-0,29

Table 6.4 Displacements U1 and U2 [mm] at node D for case 4-7.

	Node	Case 4	Case 5	Case 6	Case 7
U1	D	-0,40	N/A	-0,10	-0,10
U2	D	-1,15	N/A	-0,29	-0,29

Table 6.5 Reaction forces RF1 and RF2 [N] at the supporting nodes A, B and C for case 1-3.

	Node	Case 1	Case 2	Case 3
RF1	A	-29840	-29845	-29843
	B	0	0	-3
	C	29840	29845	29846
Sum		0	0	0
RF2	A	22380	22383	22380
	B	57620	57617	57616
	C	0	0	4
Sum		80000	80000	80000

Table 6.6 Reaction forces RF1 and RF2 [N] at the supporting nodes A, B and C for case 4-7.

	Node	Case 4	Case 5	Case 6	Case 7
RF1	A	-29845	N/A	-29845	-29843
	B	0	N/A	0	-3
	C	29845	N/A	29845	29846
Sum		0	N/A	0	0
RF2	A	22383	N/A	22383	22380
	B	57617	N/A	57617	57616
	C	0	N/A	0	4
Sum		80000	N/A	80000	80000

The first thing that can be observed is that the results from the *MP-truss-fixed* model are not reliable since the connections between the elements would not function as desired. The elements parted from each other, and thus the resulting deflections and reaction forces from this model are not considered. Changing the connection from a connection of type *basic* to a connection of type *MPC tie* resulted in a functional model, but the resulting deflections and reaction forces showed to be equal to the ones from both the *OP-truss-pinned* and the *MP-truss-pinned* models. Also a connection of type *MPC beam* was tested, but the element parted also in this model. This indicates that truss members cannot be fixed. Even if tied connections are applied to the structure, they will behave like pinned connections.

Another observation made is that the balance of the system is verified by the sum of the reaction forces RF1, which is zero, and by the sum of the reaction forces RF2, which is equal to the total load applied.

It can also be seen that the deflections obtained from the *OP-truss-pinned* model and the *MP-truss-pinned* model are equal. Also the deflections obtained from the *OP-beam-fixed* model and the *MP-beam-fixed* model are equal. This observation verifies that there is no difference between using a model containing one part and using a model containing multiple parts which are connected manually.

A strange observation is that the deflections from the *MP-beam-pinned* model are almost equal to those from both the *OP-beam-fixed* model and the *MP-beam-fixed* model, which is not what was expected. To investigate this problem, the rigid behaviour of the connections in the *MP-beam-fix* model was replaced by a rotational stiffness of 1 N/mm, to simulate pinned connections. The results were equal to those from the *MP-beam-pinned* model. This observation is of concern since the *Leaf bridge* will have connections with spring-like behaviour between beam elements. No solution to this problem was found, but as will be shown in Section 0, the spring-like behaviour of the connections in the *Leaf bridge* seem to function in a satisfactory manner anyway.

What might also appear strange is that there are small reaction forces in point B for RF1 and in point C for RF2 for the fixed beam cases. These forces occur due to the fixed connection where the elements meet, which causes the elements to bend when trying to maintain the angles between them.

6.2 Finite element modelling

In the following sections the procedure of modelling the bridge structure in *Abaqus* is described. The modelling consists of different parts which are divided into different modules in the program. Each module is discussed separately, but the order is not completely chronological since both the initial modelling and the changes made after the initial analysis are discussed in the respective modules.

6.2.1 Preparing the geometry

Since the geometry of the bridge was preliminarily designed by Flårback in his Master's Thesis Covered Timber Bridges (2015), a DWG-file (.dwg) (Drawing) with the geometry was provided in order to be able to import it into *Abaqus*, and thus creating the geometry anew was avoided. *Abaqus* allows for a number of different file types to be imported as parts, but DWG is not one of the supported ones. Using *AutoCAD* (Autodesk Inc.), the geometry was exported to SAT- (.sat) (Standard ACIS Test) and IGS-files (.igs) (Initial Graphics Exchange Specification), some of which in turn were converted into STEP-files (.step) (Standard for the Exchange of Product Data) by a software named *gCAD3D* (CADCAM-Services Franz Reiter).

The reason for using different types of file was that, when importing the IGS-files into *Abaqus*, it creates one single part of all the separate lines in *AutoCAD*, whereas the STEP-file creates separate parts for each of the lines. The problem with having only one single part in *Abaqus* is that the program automatically assumes that beam elements are connected with perfectly fixed connections and truss elements are connected with perfectly hinged connections. For the initial analysis, assuming perfectly fixed or hinged connections, using one IGS-file would be sufficient. However, to apply a degree of fixation to the connections later on would not be possible using only one single part.

Hence, multiple IGS-files were imported for each type of member separately, such as the arches, the curved roof beams and the deck edge beams. In *AutoCAD*, these curved members consist of multiple lines but in reality they are continuous. Because of this they were joined by the JOIN function in *AutoCAD* to create continuous lines. Additionally, the geometry was to rotate in *AutoCAD*, such that it was positioned in the XZ-plane and had its height in the Y-direction, since this is the default orientation in *Abaqus*. The arches and the deck edge beams were chosen to be designed as three-hinged and hence pinned connections were needed at the mid-spans. Since these elements were to be modelled with beam elements, they had to be divided and imported in separate halves, otherwise *Abaqus* would have assigned these members perfectly fixed connections, see Figure 6.3. The secondary cables could also be imported as an IGS-file, since the cables were assumed to always be perfectly hinged to the structure. They are shown in Figure 6.3.

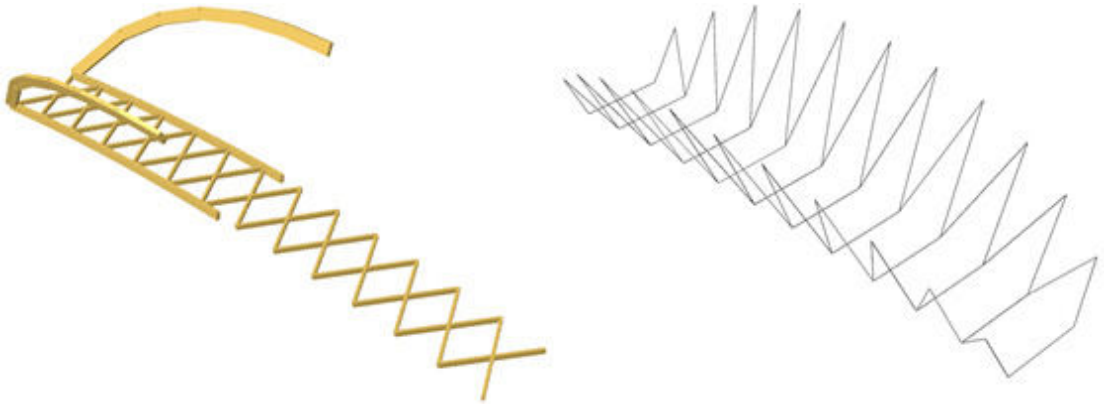

Figure 6.3 *Arches and deck edge beams divided into halves (to the left) and the cables as one part (to the right).*

Also the deck crossings were imported as IGS-files, even though they were to be assigned partially fixed connections. This was enabled by importing the deck as two IGS-files, i.e. as two parts, each containing the deck crosses with the same orientation, which are not connected to each other, see Figure 6.4. The curved roof beams, shown in Figure 6.5, were imported one IGS-file, whereas the roof truss elements, shown in Figure 6.5, were the only parts which required to be imported as a STEP-file. It would also be possible to import some roof truss elements which are not connected to each other, as IGS-files, similar to the case with the deck crosses, but this was considered more cumbersome than importing them simultaneously but separately with a STEP-file.

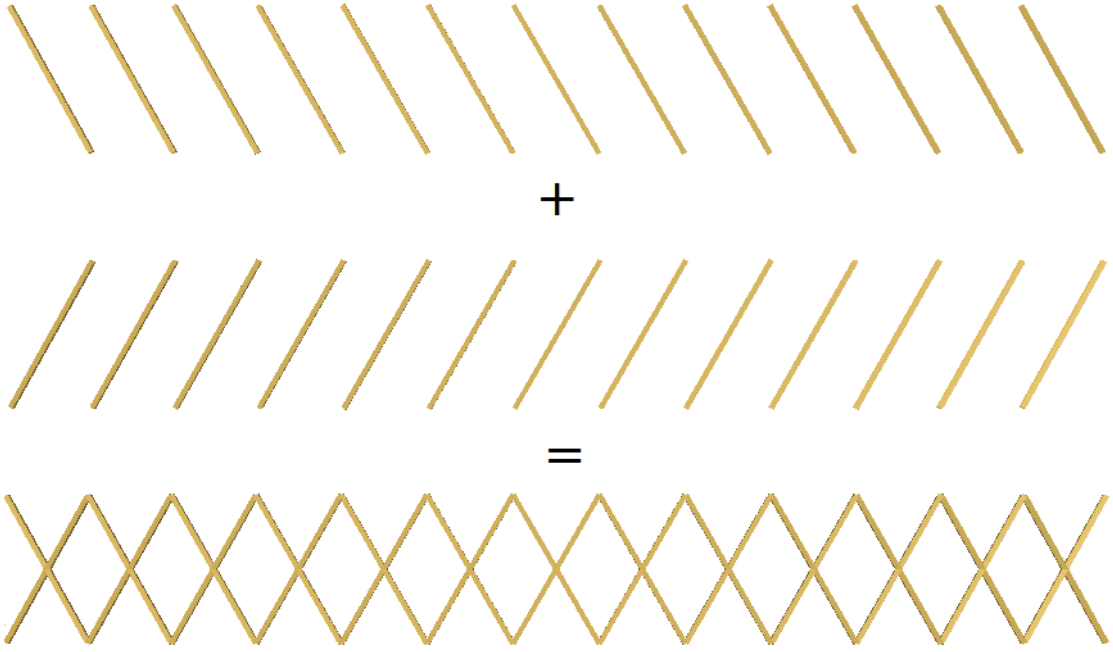

Figure 6.4 *Deck crossings imported as two separate parts.*

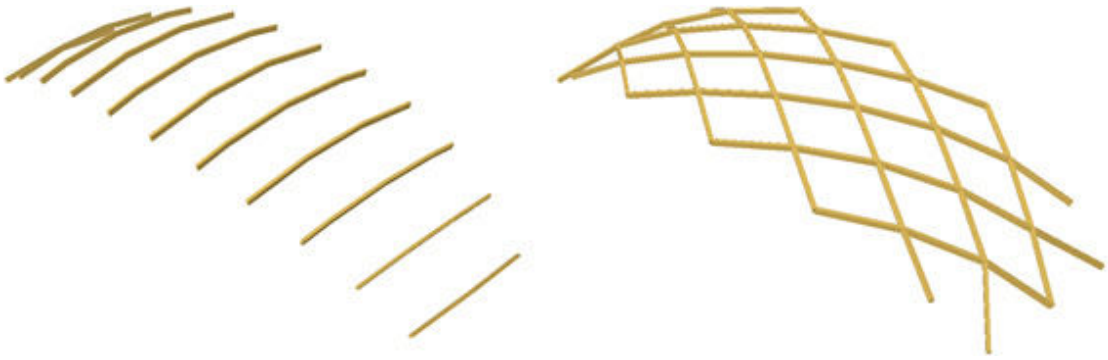

Figure 6.5 Curved roof beams (to the left) and roof truss elements (to the right).

Finally, surfaces representing the roof and deck surfaces were created in *AutoCAD* using the LOFT function. For the roof structure, the option "guide" was used to fit the surface to the roof trusses. These surfaces were exported as SAT-files (.sat) which were imported as parts in *Abaqus*, the deck surface as one single part and the roof surfaces as multiple strips. When importing parts as SAT-files, *Abaqus* creates separate parts for each of the multiple surfaces. The deck and roof surfaces could also have been created as two single surfaces, since no consideration was taken to the stiffness of these parts, which was the initial intention. If the stiffness would have been taken into consideration, having these surfaces modelled as single parts would overestimate their stiffness. It was considered not likely to have one single surface covering the entire roof due to the curvature, and therefore the roof surfaces were imported as multiple parts spanning between the curved roof beams. The deck surface was still imported as one single part, since it was considered more likely that such a cover could be continuous over the deck, since the curvature of the deck is small. In reality probably planks would be placed transversely on the deck, and the stiffness of these would still be rather low.

For a case where both boundary conditions and loads are symmetrical, the use of symmetry boundary conditions enables modelling of only half or a quarter of the whole structure. However, in order to be able to assign horizontal wind loads in both the axial and the transverse direction of the bridge, the use of symmetry boundary conditions is not possible, and the whole bridge structure needed to be modelled.

6.2.2 Part module

All parts were created by importing the files exported from the DWG-file previously. They were all imported as three dimensional deformable wire parts. Having conveniently named the SAT-, IGS- and STEP-files, the parts were easily identified in the model tree. The model contained a total number of 75 parts. Notable was that no changes to the geometry of the parts could be made in *Abaqus*. If changes would be required, these would have to be done in *AutoCAD* and the parts would have to be imported anew.

6.2.3 Property module

The materials used in the bridge were created in the property module. As a simplification, the glulam was assumed to be homogeneous and isotropic. Eurocode specifies different Young's moduli for glulam depending on if capacity analyses (ULS) or deformation analyses (SLS) are performed. Hence, two different materials for glulam

were created for the different types of analysis. The materials used in capacity and deformation were assigned a Young's modulus of 10800 MPa and 13000 MPa, respectively. The Poisson's ratio was set to zero and the mass density to 430 kg/m^3 for both materials.

The steel material for the cables was created and assigned a Young's modulus of 150 GPa (EN 1993-1-11:2006(E) Table. 3.1) and a Poisson's ratio of 0.3. The density of a spiral strand rope is 83 kg/m^3 and the fill factor, taking the void space into account, is 0.75 (EN 1993-1-11:2006(E) Table. 2.2). The density in kg/m^3, which is the unit for density in *Abaqus*, is calculated according to Equation (6.1).

$$\frac{\rho_{steel} \cdot f}{g} = 6348 \, \frac{kg}{m^3} \tag{6.1}$$

where:

ρ_{steel} = *density of the spiral strand rope*

f = *fill factor and g is the standard gravity*

However, a density of 6628 kg/m^3 was entered by mistake in *Abaqus*. This was discovered after all analyses and results were extracted. Since the density entered in *Abaqus* was higher than the theoretically correct one, it is assumed to be on the safe side and due to limited time this issue was not corrected. Since all steel members were cables, the "no compression" alternative was chosen, disabling these elements from carrying any compressive forces. In reality the cables would become slack and bend under compressive forces, but this is not possible for elements of truss types in *Abaqus*.

Next, cross section profiles were created for the beam elements. It was important to stick to the definition of measurements for rectangular cross sections stated by *Abaqus*, which said that the larger dimensions were to be assigned in the local 1-direction, and the smaller dimension in the local 2-direction, since the corresponding sectional forces and sectional moments were to be extracted. The directions are illustrated in Figure 6.6. Subsequently, beam and truss sections were created with the different cross section profiles and materials and were then assigned to the parts. All beams were modelled with beam sections and all cables were modelled with truss sections. For the SLS analysis, the glulam members were assigned the glulam deformation material, and for the ULS analysis they were assigned the glulam capacity material.

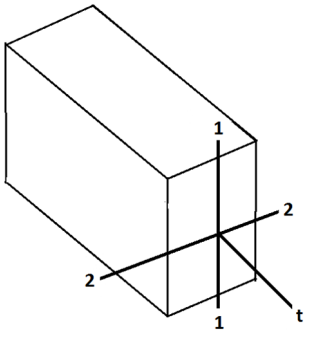

Figure 6.6 The local cross sectional directions in Abaqus.

Finally, beam tangent and beam section orientations were assigned to all beam elements. For the arches an approximate n1-vector in the global x-direction (1,0,0) was chosen, which is in the horizontal direction of the longitudinal direction of the arches. This allowed the cross-section to be rotated along the arches, resulting in a flat but inclined arch. If a vector in the global y-direction (0,1,0) would have been chosen, the cross-section would not be rotated and the arch would become strangely twisted along its length. The difference is shown in Figure 6.7, where the roof has been removed to improve the visibility.

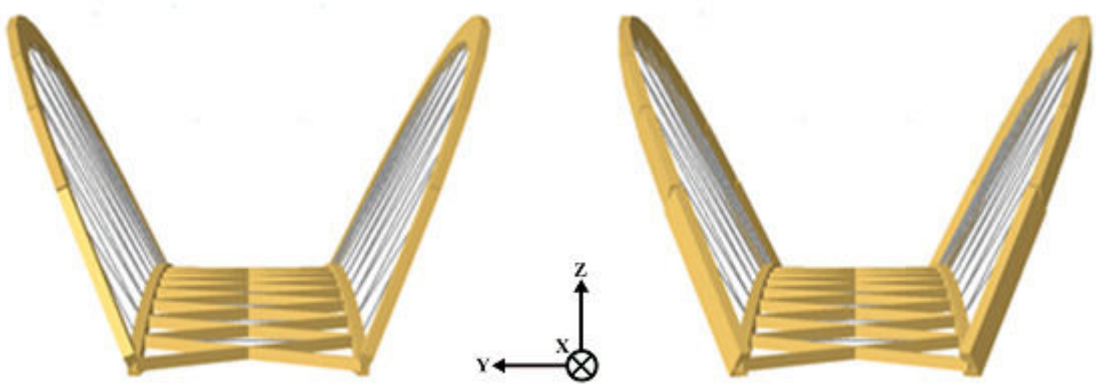

Figure 6.7 *The difference between the choices of n1-vector. The figure to the left shows the desired rotation of the cross-section.*

As the curved roof beams were included in one single part, they could be assigned beam section orientation simultaneously. They were given an approximate n1-vector in the negative z-direction, which was the horizontal direction of the longitudinal axis of the curved beams. This allowed for the cross-section of the individual curved beams to rotate along the path of the arch, from the outermost curved beam to the middle one, see Figure 6.8. If instead the approximate n1-direction for all beams would be given in the global y-direction the beams would not rotate along the path, and their position would look strange, see Figure 6.8. Five of the curved beams, which were located exactly in the global z-direction, could not be assigned this n1-vector since they coincide. For these beams an approximate n1-vector was selected in the global xy-plane close to the global y-direction, such that their cross-sections were reasonably visually aligned with the connecting elements. This was not the exact n1-vector of these elements, but rather close.

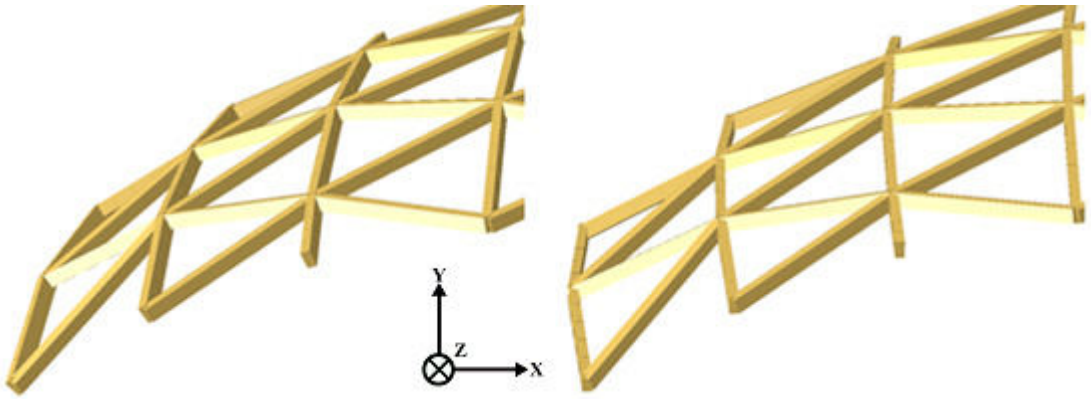

Figure 6.8 *The difference in the choices of n1-vector. The figure to the left shows the desired rotation of the roof beams.*

Since the roof truss elements were each one individual part, their beam section orientation had to be assigned individually. To find individual vectors which correspond well to each element was considered too cumbersome, and hence the approximate n1-vector was set to the global y-direction (0,1,0) for all roof truss elements. This choice was more accurate for truss beams located closer to the mid-span and less accurate for those located closer to the ends of the bridge, due to the longitudinal path of the curved roof. This is visualized in Figure 6.9.

Figure 6.9 *Roof truss elements closer to the mid-span (to the left) and roof truss elements closer to the end of the bridge (to the right).*

The edge beams and the cross beams in the deck were all assigned an approximate n1-vector in the global y-direction, since the curvature of their paths was rather small.

Both the deck and the roof surface shells were given a thickness of 10 mm and a stiffness of 1 Pa, since the entry of 0 Pa was not allowed.

6.2.4 Assembly module

In the assembly module all the parts were imported as independent instances. With the "render beam profile" option, the bridge structure with actual dimensions of the elements can be visualized. This is a good method of visually making sure that the materials, sections and beam section orientations are assigned correctly. A view of the bridge with unrendered and rendered beam profiles is shown in Figure 6.10.

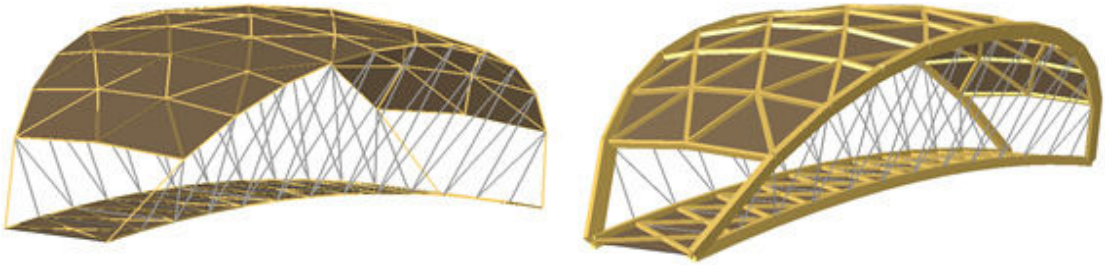

Figure 6.10 *Unrendered beam profiles (to the left) and rendered beam profiles (to the right).*

6.2.5 Step module

For the initial analysis where element stresses and displacements were to be extracted, a static, general step was chosen. No account was taken for initial imperfections due to the short length of the elements. A static, linear perturbation would have been suitable for this project, since this type of step allows for loads to be combined in the load case manager, but the "no compression" option for the cables was unfortunately found not to be supported in this step.

In the step module also the field and history output were specified. Field output, such as stresses and displacements, can be visualized by deformed shape, contour or symbol plots in the visualization module after an analysis has been run. Only stresses (S), displacements (U, which included both translations and rotations) and forces (SF, which included both section forces and moments) were requested. The directions of forces and moments are shown in Figure 6.11, where SF1 is the axial force, SF2 is the shear force in local 2-direction, SF3 is the shear force in local 1-direction, SM1 is the moment about local 1-axis, i.e. in the weak direction, SM2 is the moment about local 2-axis, i.e. in the strong direction and SM3 is the twisting moment.

It was sufficient to request data for the whole model at the last increment of the step. History output can be used for extracting output at specific points in the model and can be visualized as X-Y plots in the visualization module after an analysis has been run. Unfortunately the history output for node sets showed to give no results. Therefore no history output was used. In order to facilitate the extraction of values, after the analysis had been run, element sets were created for the elements contained in the connections chosen for design.

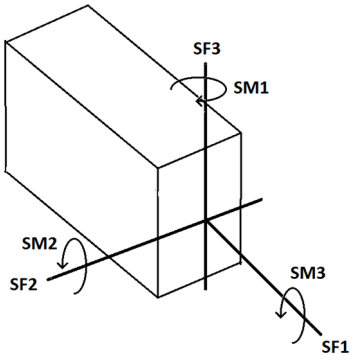

Figure 6.11 Directions of sectional forces and moments.

6.2.6 Interaction module

In order to connect the so far unconnected members, a number of connectors had to be applied to the bridge structure. To enable connection of the deck cross beams to each other, nodes at the intersections of these elements were needed and hence datum points were created in each intersection and the elements were then partitioned.

There are a few different methods for building connections between elements. The coincident builder is a convenient tool to use when only two points are to be connected, but in cases where three points are to be connected, this tool is not useful, since only two of the points will be connected. When having four point which are to be connected

to each other, the coincident builder connects the points pairwise, but does not connect the pairs to each other.

In cases where the coincident builder is considered not useful, wire section can be used. This tool is similar to the coincident builder, except that it enables toggling between the vertices located at the same node. It prompts the user to select the first node, which serves as the master node, and then select the second node, which serves as slave nodes. The tool creates pairs of the nodes just like the coincident builder, but with the difference that for a node with multiple elements, the master node can be selected multiple times in order to connect to one other node each time, representing the slave nodes.

Wire sections was considered a suitable approach for building connections in this project. First the wire sections, representing the connection paths in each connection, had to be created by pairwise linking elements to one another. A hierarchic order was chosen for the elements to decide which element should be the master and which should be the slaves. The order was chosen to be; arch > curved beams > roof truss elements for the connections in the roof and edge beams > deck truss elements for the connections in the deck. In connections containing the cables, these were always considered to be slaves. All groups of connections are listed in Table 6.7.

Table 6.7 Groups of connections.

Pinned connection	Fixed connections
Arch to arch at mid-span (incl. cables)	Deck truss beams to deck truss beams
Edge beam to edge beam at mid-span	Deck truss beams to edge beams
Edge beam to arch ends	Roof truss beams to curved beams
Cables to arch and edge beams	Curved beams to arch (incl. truss beams)

After that, two different connector sections of type basic were created, one for pinned connections and one for fixed connections. The connector section for the fixed connections was chosen such that translations of the connected nodes were constrained to be equal, translational type “join”, but the rotations were individually free, rotational type “rotation”, see Figure 6.12. This type of rotation allowed for spring-like behaviour options to be applied to all rotational degrees of freedom.

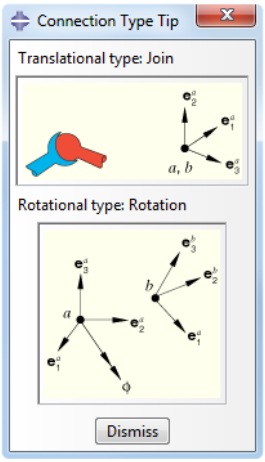

Figure 6.12 Connection section choices.

For the initial analysis, where all connections were assumed to be perfectly fixed or perfectly pinned, the spring-like behaviour option “rigid” was chosen, to simulate a fixed connection. In the final analysis, where the influence of rotational spring stiffness was investigated, a linear behaviour was chosen for all rotational degrees of freedom. The connector section for the pinned connections was assigned the translational type “join” and rotational type “none”, since no rotational spring stiffness was to be applied to these connections in any of the analyses. Finally the connector sections were assigned to the wire sections in order to complete the connections.

In order to be able to apply fixed connections between the deck and roof shells and the supporting beams below, geometry sets were created including the edges of the shells. Corresponding geometry sets had to be created for the supporting beams as well. The shells and the beams were then connected with tie constraints, choosing the supporting beam geometry set as the master and the shell edge geometry set as the slaves.

6.2.7 Load module

Boundary conditions were applied in the initial step to the vertices of the arches which represent the supports. The nodes had to be selected with care, to make sure the boundary conditions were assigned to the arch members only and not to any other members sharing the same node. Pinned boundary conditions were assigned to one side of the bridge, preventing the displacements in the U1, U2 and U3 directions while allowing for the rotations UR1, UR2, and UR3. The direction of the translations and rotations are shown in Figure 6.13. On the other side of the bridge, roller boundary conditions were assigned, preventing displacements in the U2 and U3 directions while allowing the displacement in U1 direction and the rotations UR1, UR2 and UR3. Additionally, the outermost deck surfaces were assigned boundary conditions along their outer edge, representing continuous supports of the ground, which prevent the translation in the U2 direction of these elements. It was desired to model these boundary conditions such that only translation in the negative global y-direction would be prevented, but no options for defining boundary conditions in only one direction was found.

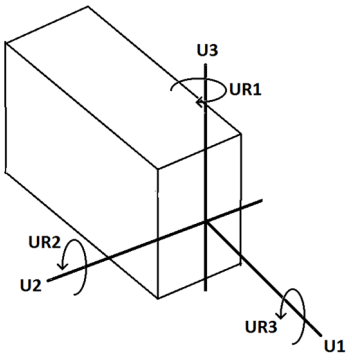

Figure 6.13 Directions of translation and rotations.

The model was loaded with self-weight, snow load, wind load, live load and a load representing a service vehicle. The self-weight of the structural components was modelled by a gravity load applied to the whole model with a magnitude of -9.807 m/s^2 in the global y-direction.

The snow load was applied to the roof as a surface traction which acts vertically in the global y-direction, and not as a pressure load, which would act in the normal of the roof, and hence would point towards the centre of the bridge due to the curvature of the roof. The differences can be seen by comparing Figure 6.14 and Figure 6.15.

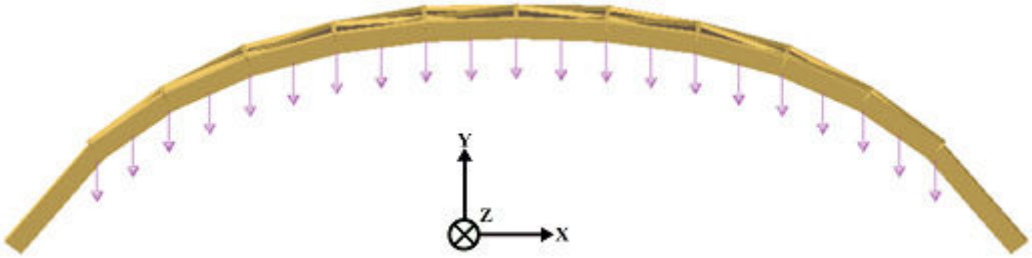

Figure 6.14 Load applied as traction acting vertically.

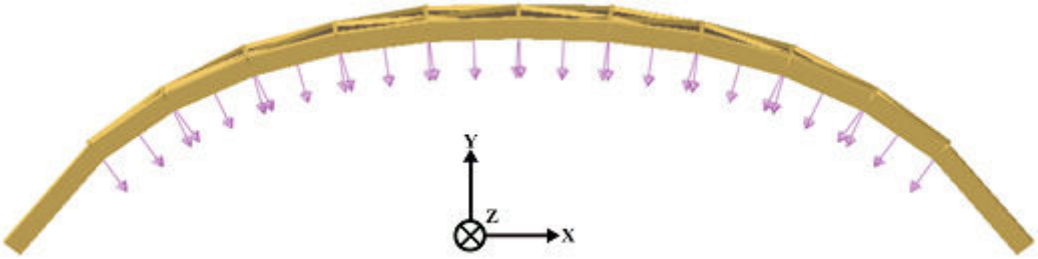

Figure 6.15 Load applied as pressure acting in the normal direction of the surface.

The wind load was divided into different components of vertical and horizontal loads, such as vertical downwind and horizontal wind acting in the longitudinal and transverse direction of the bridge. The wind loads were considered to act one at a time. The vertical downwind acts in the same way as the snow load, see Figure 6.14 above. In the horizontal plane there is transverse and longitudinal wind. Their applications are visualized in Figure 6.16 and Figure 6.17. According to Bro 2004 (Trafikverket, 2004), the surface live load and the vertical load from the service vehicle do not have to be combined and according to EN 1990:2002 A2.2.3(3) also the snow load does not have to be combined with traffic load of gr1, which is the vertical load from the service vehicle. The horizontal load from the service vehicle must still be included.

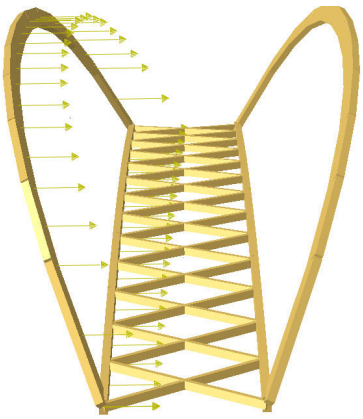

Figure 6.16 Wind load acting horizontally across the bridge.

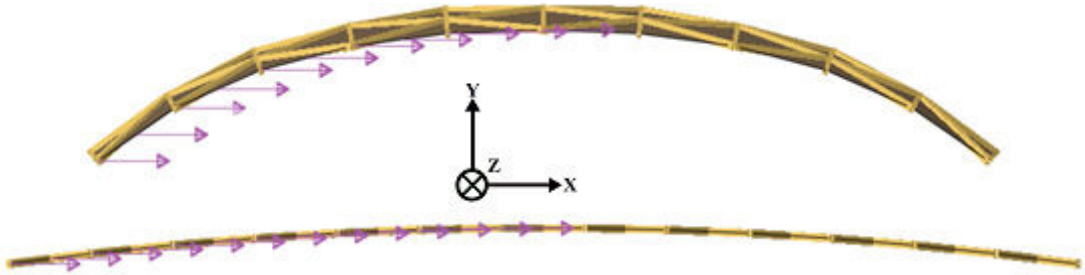

Figure 6.17 Wind load acting horizontally along the bridge.

The live load, which allows for people gatherings, was applied to the deck as a surface traction acting vertically in the global y-direction. The load of the service vehicle consists of two axle-loads of 40 kN and 80 kN respectively, with a distance of 3 m, which in turn consist of two point loads of 20 kN and 40 kN respectively with a distance of 1.6 m, see Figure 5.1 in Section 5.1.2. Since the bridge has only one span, it was assumed that the worst case occurs when the service vehicle is positioned close to the mid-span. The two axle-loads loads of 40 and 80 kN respectively were converted to two equivalent point loads placed as concentrated forces on the deck shells at the intersection of the deck cross-beams closest to the mid-span, see Figure 6.18 (the deck shells have been suppressed in the figure).

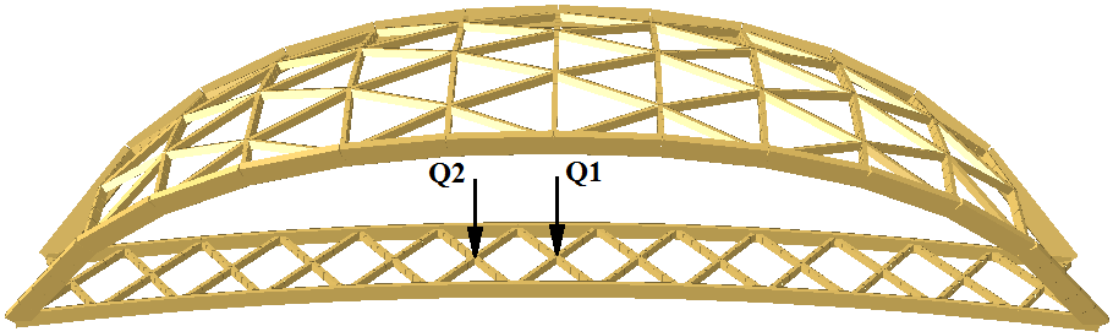

Figure 6.18 Live load of service vehicle applied as two point loads.

The magnitudes of these loads, which are placed 2.3 m apart, were calculated according to Equation (6.2) and (6.3), respectively. These loads create a moment about an axis located in the middle of the loads, which is equivalent to a moment created by the loads with magnitudes of 40 kN and 80 kN, positioned 3 m apart.

$$40\ kN \cdot \frac{3\ m}{2} = Q_1 \cdot \frac{2.3\ m}{2} \tag{6.2}$$

$$Q_1 = 52.174\ kN$$

$$80\ kN \cdot \frac{3\ m}{2} = Q_2 \cdot \frac{2.3\ m}{2} \tag{6.3}$$

$$Q_2 = 104.248\ kN$$

The bridge was also subjected to a horizontal force, which was placed in the same node as the higher value of the vertical service vehicle load, representing the acceleration or retardation of a vehicle with rear-wheel drive. Its value was taken as the greatest of 10% of the surface live load and 60% of the service vehicle load, according to Equation (6.4) and (6.5) (EN 1991-2:2003(E) 5.4(2)).

$$0.1 \cdot 5 \frac{kN}{m^2} \cdot 30\ m \cdot 4\ m = 60\ kN \tag{6.4}$$

$$0.6 \cdot 120\ kN = 72\ kN \tag{6.5}$$

Since the Static, General step does not allow for load cases to be created in the load case manager, the final model was copied multiple times (after all modules are treated), and the magnitude of the loads were then multiplied by the corresponding reduction factors manually for the respective load cases. Having four different loads (snow, live, wind and service vehicle), which in turns will act as main load, and wind occurring in one of three directions (vertically, axially and transversely), a total of 18 load cases were established, for SLS and ULS respectively, shown in Table 6.8 and Table 6.9. Taking uplift into account is of importance when considering the upwards deflections and the withdrawal capacity of fasteners of the boards on the roof and the deck. These were not considered in this project. Only the downwards deflections and the difference between upwards and downwards deflections were considered, and therefore uplift was omitted.

Table 6.8 Loads included in load case 1-9.

	Gravity	Live load (traffic)	Snow load	Wind load (downward)	Wind load (transversal)	Wind load (longitudinal)	Service vehicle (vertical)	Service vehicle (horizontal)
LC1	Yes	Main	Yes	Yes	No	No	No	Yes
LC2	Yes	Yes	Main	Yes	No	No	No	Yes
LC3	Yes	Yes	Yes	Main	No	No	No	Yes
LC4	Yes	Yes	Yes	Yes	No	No	No	Main
LC5	Yes	Main	Yes	No	Yes	No	No	Yes
LC6	Yes	Yes	Main	No	Yes	No	No	Yes
LC7	Yes	Yes	Yes	No	Main	No	No	Yes
LC8	Yes	Yes	Yes	No	Yes	No	No	Main
LC9	Yes	Main	Yes	No	No	Yes	No	Yes

Table 6.9 Loads included in load case 10-18.

	Gravity	Live load (traffic)	Snow load	Wind load (downward)	Wind load (transversal)	Wind load (longitudinal)	Service vehicle (vertical)	Service vehicle (horizontal)
LC10	Yes	Yes	Main	No	No	Yes	No	Yes
LC11	Yes	Yes	Yes	No	No	Main	No	Yes
LC12	Yes	Yes	Yes	No	No	Yes	No	Main
LC13	Yes	No	No	Yes	No	No	Main	Main
LC14	Yes	No	No	No	Yes	No	Main	Main
LC15	Yes	No	No	No	No	Yes	Main	Main
LC16	Yes	No	No	Main	No	No	Yes	Yes
LC17	Yes	No	No	No	Main	No	Yes	Yes
LC18	Yes	No	No	No	No	Main	Yes	Yes

6.2.8 Mesh module

In the mesh module, where the structure was meshed, the elements were assigned mesh element types and edge seeds. These are presented in Table 6.10. In order to facilitate the selection of elements, geometry and surface sets were created for the beam and truss elements and the shell elements, respectively. A convergence study was performed in order to verify the chosen number of edge seeds, and it is described in more detail in Chapter 6.2.11.

The mesh element type B31 is a two-node linear beam element in space which is shear-flexible (Timoshenko beam). The T3D2 element is a two-node linear truss element in space. They only require one seed per edge since they take only pure tension and compression, and no bending. The S3 element is a three-node triangular general-purpose shell element, with finite membrane strains. This type of element was chosen due to the triangular shape that the roof and deck truss elements create.

Table 6.10 Mesh element types and edge seeds for the different elements.

	Beams	Cables	Deck / roof
Mesh element type	B31	T3D2	S3
Edge seeds	5	1	5

The deck and roof shells were additionally given a mesh element shape. The deck and roof surfaces were given a triangular mesh element shape, instead of a quadratic, due to the same reasons discussed above. Figure 6.19 shows the meshing of the deck and roof surfaces.

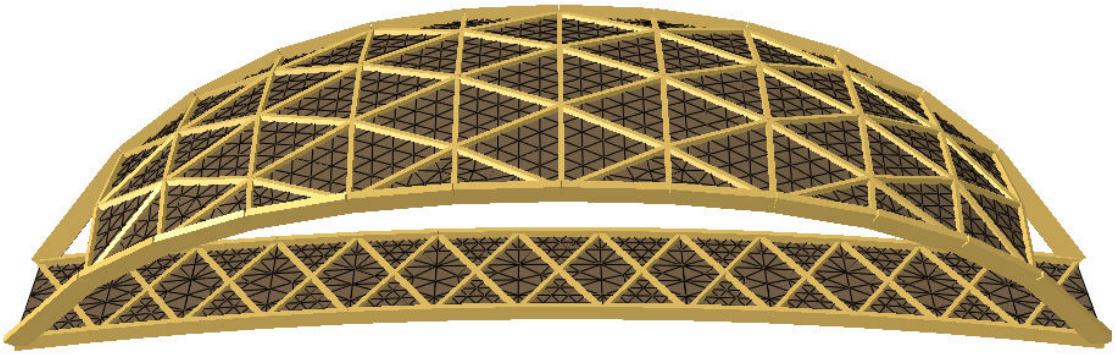

Figure 6.19 Meshing of the deck and roof surfaces.

6.2.9 Job module

In the job module, suitable names for the jobs were chosen and the default settings were accepted. The jobs were submitted and when completed, any errors or warnings that might have appeared were checked in the job monitor.

6.2.10 Visualization module

In the visualization module the results can be shown as a deformed shape with or without a contour plot. To quickly check which elements are in tension and which are in compression, to ensure a realistic structural behaviour, the max principal (abs) output was displayed and the legend was modified to show only two colours, red for tension and blue for compression. Figure 6.20 shows the tensioned (red) and compressed (blue) element in load case 1. Also the maximum and minimum values and the location of these values were requested to be shown.

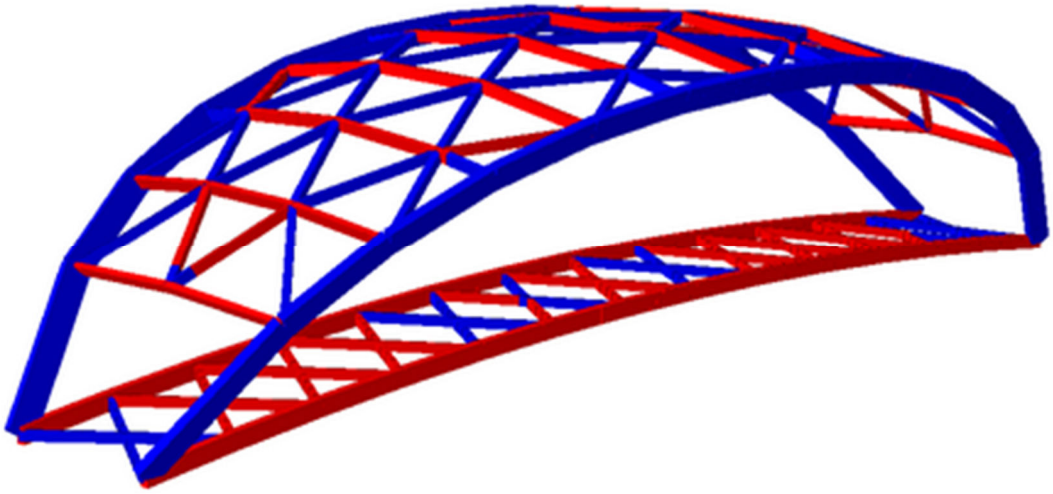

Figure 6.20 Parts subjected to tensile forces (red) and compressive forces (blue) in load case 1.

For the SLS analyses, the maximum and minimum deflections were checked. They are presented in Table 7.2 and Table 7.3. Especially the minimum deflection was of interest, since the minimum value is the lowest negative value, indicating a deflection

in the negative y-direction, i.e. downwards, whereas the maximum value is the highest positive value, indicating a deflection in the positive y-direction, i.e. upwards. If the deflections would show to be too large, the dimensions of the elements would be altered until a satisfactory maximum downward deflection is reached.

After a satisfactory maximum downward deflection was reached in SLS, all ULS load cases were analysed. First the maximum and minimum sectional forces and moments and the axial stress were checked for all beam and truss elements (the cables), respectively, and the utilization ratios of the most loaded elements of each type were calculated. No method of plotting the utilization ratio of the elements was found in *Abaqus*, therefore the utilization ratios were calculated according to Equation (6.6) and (6.7), where F and M are the extracted sectional forces and moments, σ is the capacity, A is the cross sectional area and W is the sectional modulus of the individual element types. The capacities of the individual element types are calculated in Appendix. A. The utilization ratios are presented in Table 7.4.

$$\frac{F}{\sigma_i \cdot A_i} \tag{6.6}$$

$$\frac{M}{\sigma_i \cdot W_i} \tag{6.7}$$

In order to be able to design the connections, the maximum and minimum sectional forces and moments for all beam elements contained in the chosen connection type were extracted, see Figure 6.21.

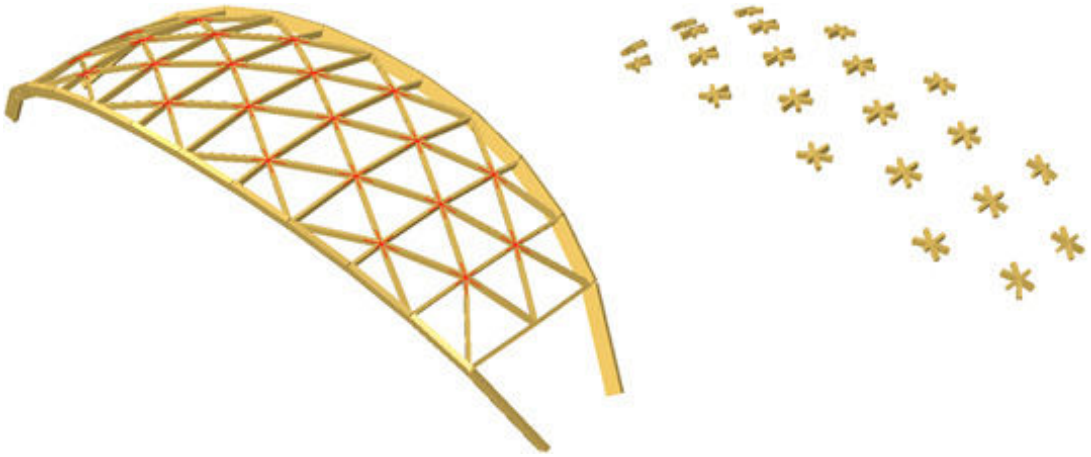

Figure 6.21 The location of the chosen connection type, the star connections (to the left) and rendered star connection elements (to the right).

The choice of connection type is described in Chapter 8. To check the exact magnitude of forces, moments or stresses in an element, or displacement of a node, the query tool can be used. Unfortunately it is not possible to find output on nodes which contain connections using the query tool. These values were instead extracted using reports of XY-data. The XY-data was created from ODB Field Output and the output requested for unique nodal points were SF1, SF2, SF3, SM1, SM2 and SM3.

6.2.11 Convergence study

A mesh convergence study of the bridge model was performed to verify the accuracy of the results. This was accomplished by first creating a mesh density consisting of very few mesh elements and then analysing the model. Thereafter a denser element distribution was created and the model was re-analysed, and its results were compared to the results from the previous mesh analysis. This procedure was repeated until convergence satisfactory was reached. In Figure 6.22, the density of the mesh and its associated axial force in one element is presented.

In this convergence study, the number of elements for the truss elements, i.e. the hangers and the cables in the deck, was kept constant at a value of one. However, the number of elements for the beams and shells was increased by the same amount each time, i.e. if the number of elements for beams was changed from 5 to 6, then this was applied for the shells as well. In the graph below, it can be seen that a mesh of density of 4 elements will not result in an accurate solution, but a mesh density of 5 elements or more indicates a satisfactory result. Further, analysing the difference of the axial force between the maximum and minimum value results in 0,014% deviation, which is very low. Therefore, for the analysis of this bridge model, the number of elements that has been used is 5 for both shells and beams.

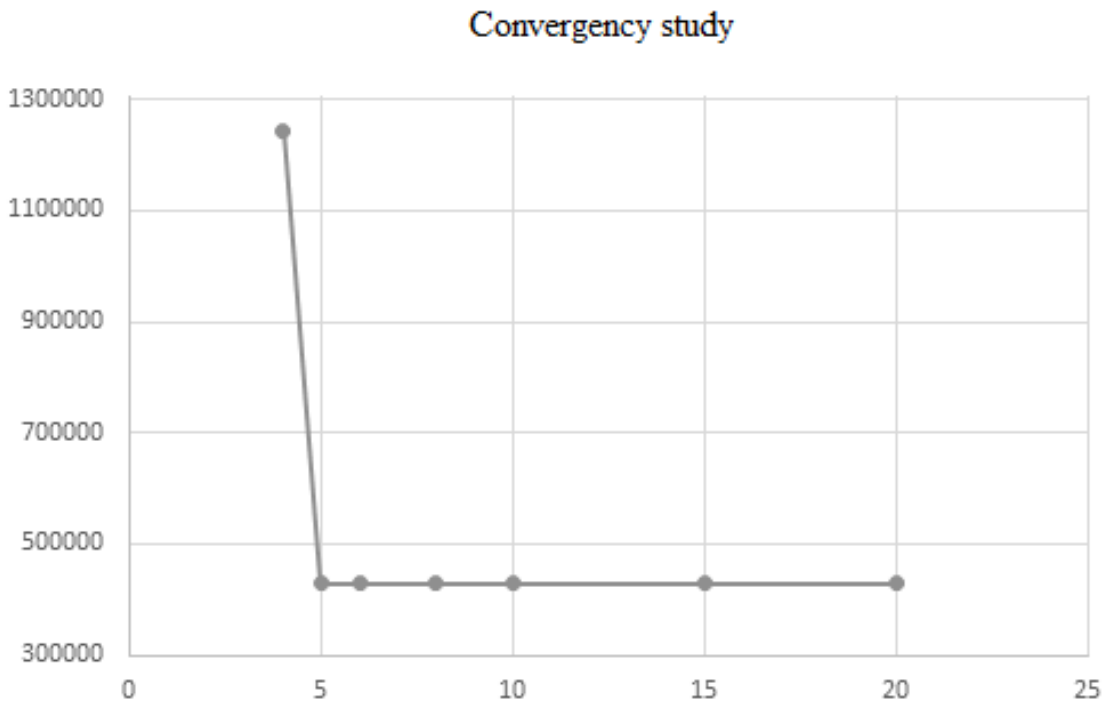

Figure 6.22 Mesh density (x-axis) and associated axial force [N] in one element (y-axis).

6.2.12 Application of rotational spring stiffness

When the design of the connections was finished, their rotational spring stiffness could be calculated according to Equations (6.8) and (6.9).

$$K_{ser} = \frac{\rho_m^{1.5} \cdot d \cdot n}{23} \tag{6.8}$$

$$K_{\theta} = K_{ser} \cdot I_p \tag{6.9}$$

An investigation of the influence of the magnitude of the rotational spring stiffness was made on all load cases. The rotational spring stiffness was assigned to the connections by the behaviour described in Section 6.2.6 ranging from 1 Nm/rad to 10^{10} Nm/rad. For the case with the loosest connections, the value 1 Nm/rad had to be chosen, since entering a value of 0 Nm/rad was not allowed in *Abaqus*. For rigid behaviour, *Abaqus* assigns the stiffness to be 10 times larger than the average stiffness of the surrounding elements to which the connector element attaches (Dassault Systèmes, 2013).

7 Results of numerical analysis

The final element dimensions, the results from the SLS and ULS analyses and the evaluation of the influence of applied rotational spring stiffness on the deflections are presented in the following sections.

7.1 Final element dimensions

The dimensions of the elements were altered until the SLS limit for deflection was reached. The final dimensions are presented in Table 7.1.

Table 7.1 Old dimensions and new dimensions, altered to satisfy SLS limit.

Component	Old dimensions	New dimensions
Arches	405 x 215 mm	630 x 215 mm
Roof curved beams	245 x 140 mm	270 x 140 mm
Roof truss beams	225 x 140 mm	225 x 170 mm
Edge beams	180 x 90 mm	405 x 215 mm
Deck truss beams	180 x 90 mm	225 x 140 mm
Cables	Ø 19mm	Ø 30 mm

7.2 Deflections in serviceability limit state

The resulting downwards deflections of the deck from all load cases for the final element dimensions are presented in Table 7.2 and Table 7.3.

Table 7.2 Deflection in the deck [$x10^{-2}$ mm] for load case 1-9.

LC1	LC2	LC3	LC4	LC5	LC6	LC7	LC8	LC9
7.53	6.77	7.65	5.92	6.83	6.02	5.18	5.22	6.81

Table 7.3 Deflection in the deck [$x10^{-2}$ mm] for load case 10-18.

LC10	LC11	LC12	LC13	LC14	LC15	LC16	LC17	LC18
5.99	5.11	5.20	7.79	7.15	7.39	5.28	3.25	3.45

The limit of deflections for straight beams, according to Equation (5.1) was 75 mm. The self-weight of the bridge alone gives an initial deflection when the bridge is just standing on its own, which will always be present. The difference of the total deflection and the deflection due to only the self-weight is the deflection that will be experienced on the bridge after it has been assembled, subjected to its own self-weight and the loads thereafter are been applied or altered. Due to this reasoning and the fact that the deck is not straight but curved, i.e. having an initial upward deflection, the largest final downwards deflection of 77.9 mm was considered to be acceptable.

7.3 Utilization rations in ultimate limit state

The utilization ratios of the most loaded elements of each type are presented in Table 7.4. The maximum and minimum sectional forces and moments were extracted from *Abaqus* and were then compared to equivalent capacity forces and moments. These were calculated by multiplying the different force and moment capacities by the cross sectional areas and sectional moduli, respectively, see Equations (6.6) and (6.7). Because of negative values, utilization ratios for both the maximum and the minimum values were calculated.

Table 7.4 Utilization ratios for the most loaded element of each type. Shaded cells indicate a utilization ratio above 100%.

	Arch	Curved	Truss	Edge	Cross	Cable
SF1 min	65.2%	2.7%	53.1%	33.8%	9.9%	
SF1 max	12.8%	37.6%	9.0%	49.4%	11.5%	
SF2 min	2.2%	4.3%	3.9%	2.3%	44.7%	
SF2 max	2.2%	4.3%	3.8%	2.3%	2.3%	
SF3 min	15.3%	13.0%	17.0%	9.2%	47.8%	
SF3 max	16.1%	24.5%	12.9%	14.2%	53.3%	
SM1 min	19.6%	11.6%	20.6%	6.6%	8.9%	
SM1 max	19.6%	11.6%	20.6%	6.6%	9.0%	
SM2 min	67.2%	94.6%	49.6%	54.5%	89.8%	
SM2 max	70.4%	94.6%	27.0%	33.7%	189.1%	
SM3 min	1065.2%	583.9%	839.0%	1395.6%	854.1%	
SM3 max	1065.2%	590.6%	838.6%	1389.1%	857.7%	
Force						49.6%

The utilization ratio of most elements is fairly low but the twisting moment (SM3) is very high because no consideration to the stiffness of the deck and roof boards were taken. These will prevent the rotation of the beams to some degree if secured properly, and hence these high values were not considered unlikely to occur and was therefore not included in the hand calculations. The high value of SM2 in deck cross beam is due to the application of the service vehicle.

7.3.1 Force extraction for design of connections

The overall maximum stress in the roof was the stress due to the moment about the local 1-axis in a truss element, which is located in a star connection very close to the entrance of the bridge. The connection to design was determined by the most stressed element with regard to sectional forces only, which was the truss element 21 located at node 37. For the all members contained in the connection at node 37, sectional forces and moments were extracted, see Table 7.5.

Table 7.5 Sectional forces [N] and moments [Nm] for elements contained in the connection at node 37.

	Curved-136/145	Truss-15	Truss-18	Truss-21	Truss-24
SF1	9.10E+04	-1.46E+05	-2.15E+05	-2.95E+05	-6.92E+04
SF2	-6.67E+02	-1.81E+02	2.90E+02	2.68E+02	-4.34E+02
SF3	-8.29E+03	5.06E+03	6.71E+03	5.72E+03	8.26E+03
SM1	3.46E+03	-1.36E+03	3.89E+03	3.60E+03	-7.53E+02
SM2	-1.30E+02	-7.54E+02	2.98E+02	4.10E+02	-5.81E+02
SM2	8.73E+02	-1.41E+03	-6.12E+02	1.28E+03	-1.33E+03

7.4 Influence of rotational stiffness

The resulting deflections in the deck for varying rotational spring stiffness for all load cases are presented in the figures below. The load cases are divided into groups depending on in which direction the wind load is acting. The results for the load cases having vertical wind load are presented in Figure 7.1, whereas Figure 7.2 and Figure 7.3 show the results for the load cases having horizontal wind load in the transverse and longitudinal directions respectively. There is also a separate group for load cases where the vertical load of the service vehicle is present. The results of these load cases are presented in Figure 7.4. The diamond markers indicate the resulting deflections for the calculated rotational spring stiffness from the connection design. As can be seen in the figures, joints having this rotational stiffness can be considered semi-rigid as they lie on the inclined part of the curves.

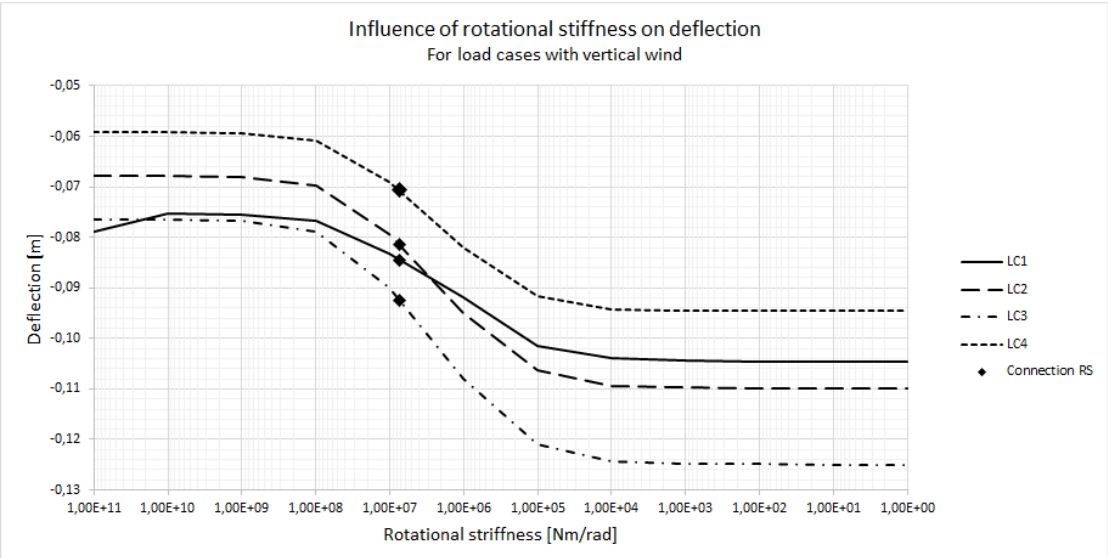

Figure 7.1 Deflection due to applied rotational stiffness for load cases with vertical wind load.

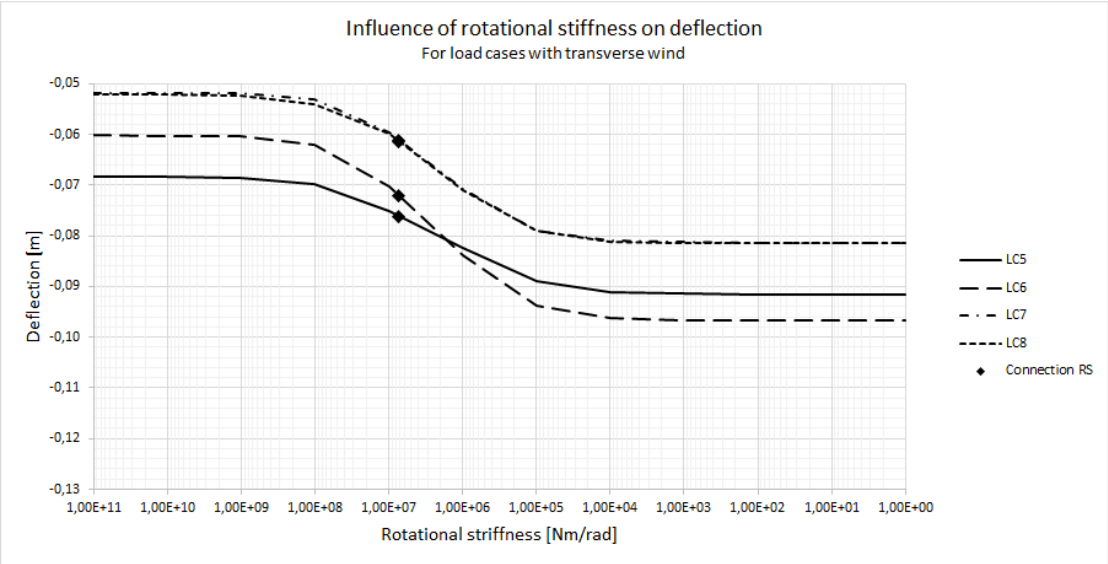

Figure 7.2 Deflection due to applied rotational stiffness for load cases with transverse wind load.

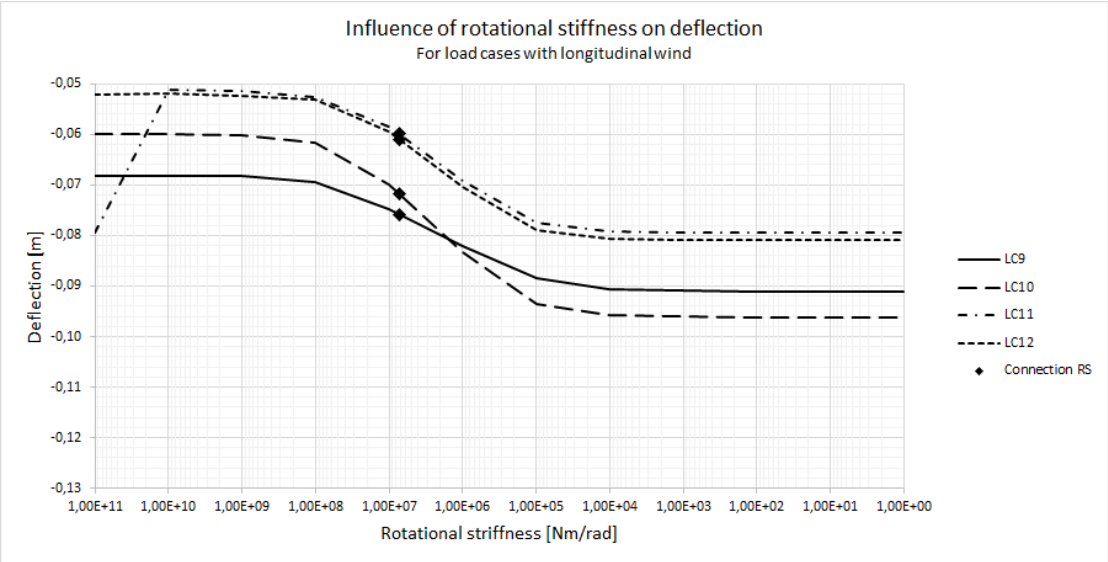

Figure 7.3 Deflection due to applied rotational stiffness for load cases with longitudinal wind load.

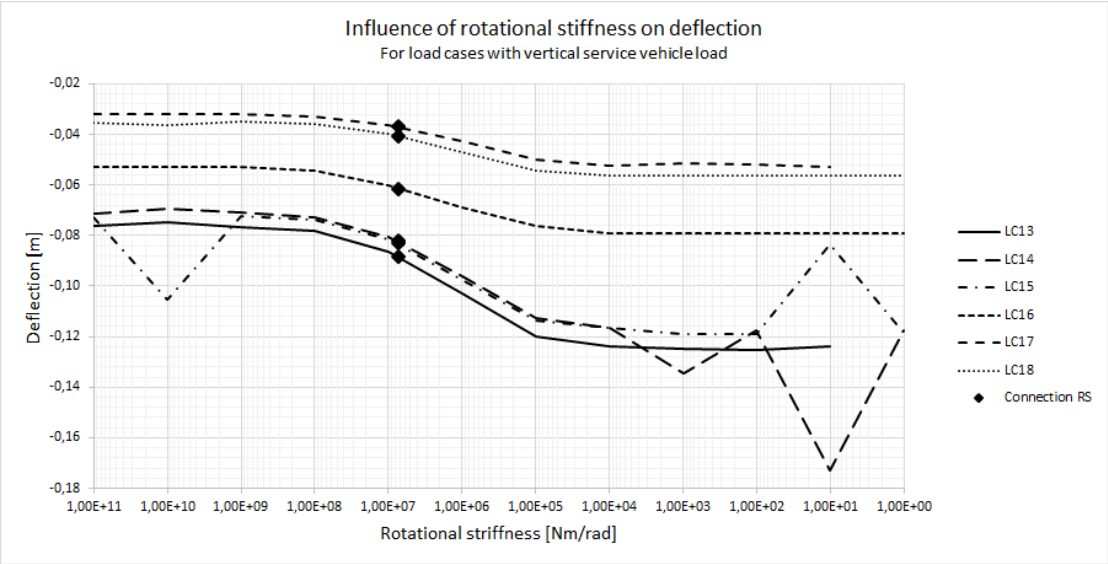

Figure 7.4 *Deflection due to applied rotational stiffness for load cases with vertical service vehicle load.*

8 Development of connection design

The connection chosen to be designed was the connection including the overall most stressed element in the roof structure. This connection will further be referred to as the star connection, due to its shape which resembles a star, see Figure 8.1. The truss elements have been given the names according to Figure 8.2.

Figure 8.1 Star connection.

8.1 Design proposals

The connection consists of steel plates and bolts. The plates connecting the truss elements to the curved beam are slotted in in the truss and secured by bolts. These slotted-in plates are further welded to the plates that are attached to the curved beam by bolts. In Figure 8.2, the construction of the connection is shown.

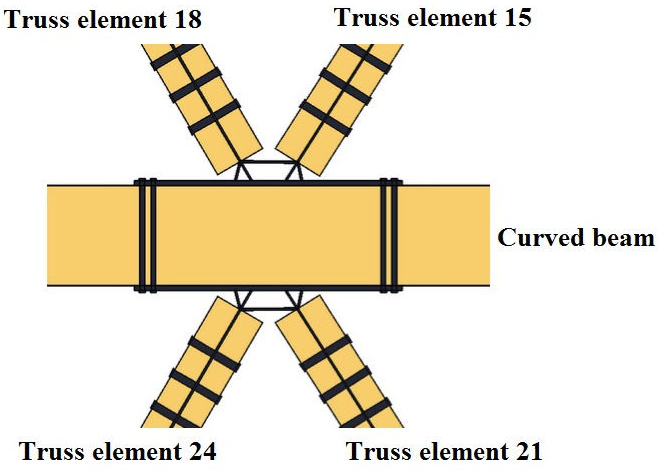

Figure 8.2 The star connection.

8.2 Hand calculations

In this chapter, the equations that were used to calculate different capacities of the connection and the controls that were taken into consideration are presented. These equations and controls are taken from SS-EN 1995-1 for timber connections and from SS-EN 1993-1 for steel connections.

8.2.1 Geometry and dimensions

The dimensions of the structural elements in the bridge are presented in Table 8.1, Table 8.2 and Table 8.3. For all wooden elements, the geometry is rectangular.

Table 8.1 Dimensions of the wooden elements [mm].

Element	Thickness	Height	Diameter
Main arch	215	630	-
Curved beam	140	270	-
Roof truss	170	225	-
Deck crosses	140	225	-
Edge beam	215	405	-
Cable	-	-	30

Table 8.2 Dimensions of the bolts [mm].

Bolts	Diameter	Length	Diameter hole
Roof truss bolts	20	170	23
Curved beam bolts	12	140	13

Table 8.3 Dimensions of the plates [mm].

Plates	Thickness
Roof truss plates [slotted-in steel plates]	20
Curved beam plates	12

8.2.2 Partial factors

In the next coming sections, some certain controls that must be fulfilled in order for the design to be considered as suitable are taken into account. In these controls, some partial and modification factors are included, which are further presented in Table 8.4, Table 8.5 and Table 8.6.

Table 8.4 Values of the partial factors.

Partial factors	Value
$\gamma_{M.cap}$	1,25
$\gamma_{\mathrm{M.2}}$	1,25
$\gamma_{\mathrm{R.cable}}$	1,0
k_{mod}	0,9
$k_{c.90}$	1,5
$k_{c.90.curved}$	1,0

$\gamma_{M.cap}$ = Partial factor for material property of timber in capacity calculations

$\gamma_{M.2}$ = Partial factor for material property of steel

$\gamma_{R.cable}$ = Partial factor for material property of steel cables

k_{mod} = Modification factor that considers load duration and moisture content

$k_{c.90}$ = Modification factor that considers load configuration, possibility of splitting and degree of compressive deformation

For rectangular sections of glued laminated timber, the characteristic value for bending and tension strength capacity should be multiplied by the factor, k_h, see Equation (8.1), if the height and the depth considering bending respective tension is below 600 mm.

$$k_h = \min\begin{cases}\left(\frac{600}{h}\right)^{0.1} \\ 1.1\end{cases} \tag{8.1}$$

where:

h = depth for bending members or width for tensile members

In Table 8.5, the values of the factor k_h for both bending and tension strength are presented for two cases. In the first case, see Table 8.5, bending is assumed to act in the strong direction while in the second case the bending is in the weak direction, see Table 8.6.

Table 8.5 Factors for bending and tension capacities in case of bending in the strong direction.

Element	$k_{h.i.h}$	$k_{h.i.t}$
Main arch	-	1,1
Curved beam	1,083	1,1
Roof truss	1,1	1,1
Deck crosses	1,1	1,1
Edge beam	1,04	1,1

Table 8.6 Factors for bending and tension capacities in case of bending in the weak direction.

Element	$k_{h.i.h}$	$k_{h.i.t}$
Main arch	1,1	-
Curved beam	1,1	1,083
Roof truss	1,1	1,1
Deck crosses	1,1	1,1
Edge beam	1,1	1,04

8.2.3 Material properties

In this Section, the stiffness, for both capacity analysis and deformation calculation, of the materials along with the characteristic and design values of different material properties are presented. For values of stiffness, see Table 8.7. The characteristic and design values for timber are shown in

Table 8.8, for steel cables in Table 8.9 and for bolts and plates in Table 8.10. The tensile strength of the bolts in different elements is presented in Table 8.11.

Table 8.7 Stiffness value for capacity analysis and deformation calculations.

Stiffness value	Capacity analysis [MPa]	Deformation calculations [MPa]
$E_{g.0.mean..GL}$	10800	13000
$G_{g.0.mean..GL}$	540	650
E_{cable}	150000	-
E_{steel}	210000	-

To obtain the design values of the material properties of timber, Equation (8.2) is used.

$$X_d = k_{\mathrm{mod}} \cdot \frac{X_k}{\gamma_M} \tag{8.2}$$

Additionally, Equation (8.2) is multiplied by the factor k_h, for bending and tension, since all the heights of the elements are below 600 mm. In Table 8.8 the characteristic and design values for different material properties of the wood are presented. As can be seen in the Table 8.9, the design value for bending is calculated around both the strong and the weak axis.

Table 8.8 Characteristic and design value for material properties of the timber elements.

Property	Characteristic value [MPa]	Design value [MPa]
$f_{m.g}$	30	See Table 8.9
$f_{t.0.g}$	19,5	15,44
$f_{t.90.g}$	0,5	0,35
$f_{c.0.g}$	24,5	17,64
$f_{c.90.g}$	2,5	1,8
$f_{v.g}$	3,5	2,52
$f_{r.g}$	1,2	0,864

$f_{m.g}$ = Bending parallel to the grain

$f_{t.0.g}$ = Tension parallel to the grain

$f_{t.90.g}$ = Tension perpendicular to the grain

$f_{c.0.g}$ = Compression parallel to the grain

$f_{c.90.g}$ = Compression perpendicular to the grain

$f_{v.g}$ = Shear strength

$f_{r.g}$ = Rolling shear strength

Table 8.9 Values of bending parallel to the grain around the weak and strong axis.

Element	$f_{m.g.1}$ [MPa]	$f_{m.g.2}$ [MPa]
Main arch	23,76	-
Curved beam	23,76	23,40
Roof truss	23,76	23,76
Deck crosses	23,76	23,76
Edge beam	23,76	23,47

$f_{m.g.1}$ = Bending around the weak axis

$f_{m.g.2}$ = Bending around the strong axis

As for the steel cable, the tension resistance of the cable should be calculated according to Equation (8.3). In Table 8.10 the characteristic and design value of the strength of the cables are presented.

$$F_{t.Rd.cable} = \min\left(\frac{F_{u.k}}{1.5 \cdot \gamma_{R.cable}}, \frac{F_k}{\gamma_{R.cable}}\right) \tag{8.3}$$

where:

$F_{u.k} = F_{\min} \cdot k_e$

$F_{\min} = K \cdot d^2 \cdot R_r$

$F_{u.k}$ = *Characteristic value of breaking strength*

k_e = *Loss factor*

K = *Minimum breaking force factor taking the spinning loss into account*

d = *Nominal diameter of the rope*

R = *Rope grade*

F_k = *Characteristic value of the proof strength*

Table 8.10 Characteristic and design values of the tension strength of the cables.

Element	$F_{u.k}$ [kN]	F_k [kN]	$F_{t.Rd}$ [kN]
Steel cable	731,2	531,5	487,5

Table 8.11 Tensile strength of the bolts.

Bolt/plate	$F_{u.k}$ [N/mm^2]
Curved beam bolt	400
Truss element bolt	1000
Steel plate	430

8.2.4 Bolted connection

In EN 1995-1-1:2004 (E), the minimum spacing between bolts, edge and end distance for timber, see Figure 8.3, is given, as shown in Table 8.12. These values were calculated with consideration of the dimension of the bolts and the angle between the horizontal coordinate axis and the resultant force acting on the material. Furthermore, the minimum and maximum spacing and edge/end distance regarding steel plates were calculated according to equations in Table 8.13. Determination of the final spacing and edge/end distance were based on the comparison of the different values for the different elements. Table 8.14 shows in which range each distance should be and in Table 8.15 the values that were chosen are presented.

Table 8.12 Spacing and end/edge distances for the bolts.

Spacing, end/edge distance	Angle	Minimum spacing or distance
a_1 (Parallel to grain)	$0^\circ \le \alpha \le 360^\circ$	$(4 + \lvert\cos\alpha\rvert)\cdot d$
a_2 (Perpendicular to grain)	$0^\circ \le \alpha \le 360^\circ$	$4 \cdot d$
$a_{3.t}$ (Loaded end)	$-90^\circ \le \alpha \le 90^\circ$	$\max(7 \cdot d, 80mm)$
$a_{3.c}$ (Unloaded end)	$-90^\circ \le \alpha \le 150^\circ$ $150^\circ < \alpha \le 210^\circ$ $210^\circ < \alpha \le 270^\circ$	$\max((1 + 6 \cdot \sin\alpha)\cdot d, 4 \cdot d)$ $4d$ $\max((1 + 6 \cdot \sin\alpha)\cdot d, 4 \cdot d)$
$a_{4.t}$ (Loaded end)	$0^\circ \le \alpha \le 180^\circ$	$\max((2 + 2 \cdot \sin\alpha)\cdot d, 3 \cdot d)$
$a_{4.c}$ (Unloaded end)	$180^\circ \le \alpha \le 360^\circ$	$3 \cdot d$

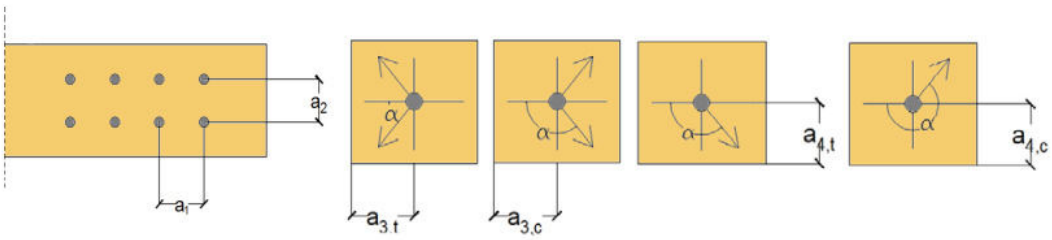

Figure 8.3 The spacing and end/edge distance depending on the resultant force acting on the element.

Table 8.13 Maximum and minimum values for the steel plates.

Spacing and end/edge distance	Minimum	Maximum
a_1 (Parallel to grain)	$2.2 \cdot d$	$\min(14 \cdot t, 200mm)$
a_2 (Perpendicular to grain)	$2.4 \cdot d$	$\min(14 \cdot t, 200mm)$
$a_{3.t}$ (Loaded end)	$1.2 \cdot d$	$40mm + 4 \cdot t$
$a_{3.c}$ (Unloaded end)	$1.2 \cdot d$	$40mm + 4 \cdot t$
$a_{4.t}$ (Loaded end)	$1.2 \cdot d$	$40mm + 4 \cdot t$
$a_{4.c}$ (Unloaded end)	$1.2 \cdot d$	$40mm + 4 \cdot t$

Table 8.14 The range of which the spacing and distance should be between [mm].

Element	a_1-range	a_2-range	a_3-range	a_4-range
Curved beam	$29 \le a_1 \le 168$	$48 \le a_2 \le 168$	$16 \le a_3 \le 88$	$16 \le a_4 \le 88$
Truss element	$100 \le a_1 \le 200$	$80 \le a_2 \le 168$	$80 \le a_3 \le 120$	$60 \le a_4 \le 88$

Table 8.15 Chosen values of the spacing, end and edge distance [mm].

Element	a_1	a_2	a_3	a_4
Curved beam	30	50	20	40
Truss element	100	85	80	70

8.2.5 Shear resistance of connection

The load carrying capacity of the connection for one row of bolts, oriented along the grain direction was checked against the shear force that is acting in the elements. From EN 1995-1-1:2004(E) the equations, which identified the failure modes in the connection and also calculates the value of the characteristic load carrying capacity for one bolt per shear plane were calculated, see Equations (8.4) and (8.5).

For the truss elements, where the connection is made out of slotted-in steel plates, three different failure mode can occur, see Figure 8.4. The first failure mode, f, indicates that the embedding strength of the wood is exceeded while the failure mode g describes that one elastic hinge can occur on each side of the slotted-in steel plates which eventually will result in exceeding of the embedding strength of the wood. The last failure mode, h, shows that plastic hinges can take place at both sides of the connector and in the material itself.

$$F_{v.Rk.slotted-in} = \min\begin{cases} f_{h.1.k} \cdot t_1 \cdot d \\ f_{h.1.k} \cdot t_1 \cdot d \cdot \left(\sqrt{2 + \dfrac{4 \cdot M_{y.Rk}}{f_{h.1.k} \cdot d \cdot {t_1}^2}} - 1 \right) \\ 2.3 \cdot \sqrt{M_{y.Rk} \cdot f_{h.1.k} \cdot d} \end{cases} \quad (8.4)$$

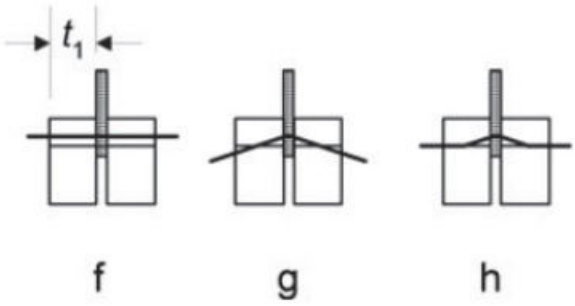

Figure 8.4 Failure modes for the slotted-in plate in the truss elements.

For the curved beam, where the steel plate are placed at the edges, the following three failure modes, see Figure 8.5, are likely to occur, see Equation (8.5). The first of these three failure modes, j/l, indicates that the failure occurs because exceeded embedding strength of the wood. The second failure mode shows that four plastic hinges develop, two just next to the plates and two in the wood itself.

$$F_{v.Rk.slotted-in} = \min\begin{cases} 0.5 \cdot f_{h.1.k} \cdot t_2 \cdot d \\ 1.15 \cdot \sqrt{M_{y.Rk} \cdot f_{h.2.k} \cdot d} \\ 2.3 \cdot \sqrt{M_{y.Rk} \cdot f_{h.2.k} \cdot d} \end{cases} \tag{8.5}$$

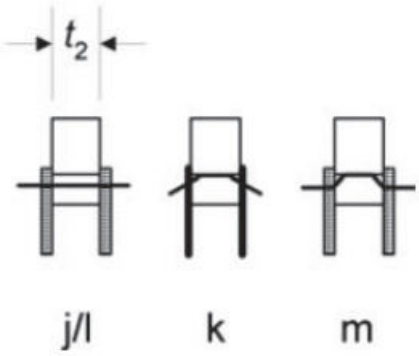

Figure 8.5 Failure modes for the plated attached to the curved beam.

The load carrying capacity of the connection was checked in both the longitudinal and transversal direction according to the following control, see Equation (8.6). The results obtained are presented in Table 8.16 and Table 8.17.

$$F_{v.ef.Rk} \geq F_{v.Ed} \tag{8.6}$$

where:

$$F_{v.ef.Rk} = F_{v.Rk} \cdot n_{bolts.ef} \cdot n_{shearplanes} \cdot n_{rows}$$

$$n_{bolts.ef} = \min\left(n_{bolts.row}, n_{bolts.row}^{0.9} \cdot \sqrt{\frac{a_1}{13 \cdot d}} \right)$$

$F_{v.ef.Rk}$ = *Effective load carrying capacity*

$n_{bolts.ef}$ = *Effective number of bolts per row*

$n_{shearplanes}$ = *Total number of shear planes*

n_{rows} = *Number of rows*

$n_{bolts.row}$ = *Actual number of bolts per row*

a_1 = *Spacing between bolts in the grain direction*

d = *Diameter of the bolt*

Table 8.16 Shear resistance control of the connection in the longitudinal direction.

Element	$F_{v.ef.Rk}$ [kN]	$F_{v.Ed}$ [kN]	Utilization ratio [%]	Control
Curved beam	183,4	96,4	52,6	Ok!
Truss element 15	434,8	137,3	31,6	Ok!
Truss element 18	434,8	233,5	53,7	Ok!
Truss element 21	434,8	312,8	72	Ok!
Truss element 24	434,8	58,8	13,5	Ok!

Table 8.17 Shear resistance control of the connection in the transversal direction.

Element	$F_{v.ef.Rk}$ [kN]	$F_{v.Ed}$ [kN]	Utilization ratio [%]	Control
Curved beam	208,3	10,8	5,2	Ok!
Truss element 15	417,5	6,3	1,50	Ok!
Truss element 18	417,5	6,2	1,49	Ok!
Truss element 21	417,5	6	1,43	Ok!
Truss element 24	417,5	13,6	3,27	Ok!

8.2.6 Shear resistance of bolts

The shear resistance of the most loaded bolt was checked according to Equation (8.7). See Appendix. A for the determination of the most loaded bolt.

$$\tau_{Rk.bolt} \geq \tau_{Ed.bolt} \tag{8.7}$$

where:

$$\tau_{Rd.bolt} = \frac{f_{u.k.bolt}}{\sqrt{3}}$$

$$\tau_{Ed.bolt} = \frac{F_{v.Ed.bolt}}{A_{bolt}}$$

$\tau_{Rk.bolt}$ = *Shear resistance capacity of one bolt*

$f_{u.k.bolt}$ = *Characteristic tensile strength of the bolt*

$\tau_{Ed.bolt}$ = *Shear stress in the most loaded bolt*

$F_{v.Ed.bolt}$ = *Shear force in the most loaded bolt*

A_{bolt} = *Cross-sectional area of the bolt*

Table 8.18 below presents the shear resistance and shear force that is acting on the most loaded bolt in both the curved beam and the truss elements.

Table 8.18 Shear resistance control of the bolts.

Bolt	$\tau_{Rk.bolt}$ [MPa]	$\tau_{Ed.bolt}$ [MPa]	Utilization ratio [%]	Control
Curved beam	230,1	134,5	58,2	Ok!
Truss element 15	577,4	27,8	4,8	Ok!
Truss element 18	577,4	47,2	8,2	Ok!
Truss element 21	577,4	62,7	10,9	Ok!
Truss element 24	577,4	16,7	2,9	Ok!

8.2.7 Embedment strength of plates

Even though the control of the shear capacity of bolts in the curved beam and the truss elements was satisfied, the material around the hole of these bolts needs to be checked so that no failure occurs. In the following controls, see Equation (8.8), consideration has been taken to the embedding strength of the steel plate, where two main failure modes are likely to occur, which are failure between the hole and end of the plate or failure between holes. Furthermore, the controls were established and the values are presented in Table 8.19.

$$F_{b.Rd.plate} \geq F_{v.Ed.hole} \tag{8.8}$$

where:

$F_{b.Rd.plate} = \min\left(F_{b.Rd.end}, F_{b.Rd.hole}\right)$

$F_{b.Rd.plate}$ = *Minimum capacity of the steel plate*

$F_{b.Rd.end}$ = *Capacity of the steel plate for failure between hole and end of plate*

$F_{b.Rd.hole}$ = *Capacity of the steel plate in case of failure between holes*

$F_{v.Ed.bolt}$ = *Shear force in the most loaded bolt*

Table 8.19 Shear resistance control for the plate for the most critical failure mode in longitudinal direction.

Plate	$F_{b,Rd,plate}$ [kN]	$F_{v,Ed,hole}$[kN]	Utilization ratio [%]	Control
Curved beam	64,3	15,2	23,7	Ok!
Truss element 15	344	8,7	2,5	Ok!
Truss element 18	344	14,85	4,3	Ok!
Truss element 21	344	19,7	5,7	Ok!
Truss element 24	344	5,2	1,5	Ok!

8.2.8 Withdrawal of bolts

The withdrawal capacity for the most loaded bolt was checked according to the Equation (8.9). In Table 8.20 the control for each element is presented.

$$F_{t.Rd} \geq F_{t.Ed} \tag{8.9}$$

where:

$$F_{t.Rd} = \frac{k_h \cdot f_{u.k} \cdot A_s}{\gamma_{M2}}$$

$F_{t.Rd}$ = *Tensile capacity of one bolt*

$F_{t.Ed}$ = *Tensile load effect on the most loaded bolt*

Table 8.20 The characteristic a design values of the strength capacity of one bolt in each element.

Plate	$F_{t.Rd}$ [kN]	$F_{t.Ed}$ [kN]	Utilization ratio [%]	Control
Curved beam	24,2	9,0	37,3	Ok!
Truss element 15	226,2	0,01	0,0056	Ok!
Truss element 18	226,2	0,01	0,0058	Ok!
Truss element 21	226,2	0,01	0,0047	Ok!
Truss element 24	226,1	0,03	0,013	Ok!

8.2.9 Combination of axial and shear load in bolts

The most loaded bolt in the connection is subjected to both axial and shear load, which means that combination of these two loads, should be taken into consideration. Equation (8.10) below, shows the combination of the axial and shear load and in Table 8.21, the controls for the most loaded in each element are presented.

$$\frac{F_{v.Ed.bolt}}{F_{v.Rd.bolt}} + \frac{F_{t.Ed.bolt}}{1.4 \cdot F_{t.Rd.bolt}} \leq 1 \tag{8.10}$$

where:

$F_{v.Ed.bolt}$ = *Shear force in the most loaded bolt*

$F_{v.Rd.bolt}$ = *Shear capacity of one bolt*

$F_{t.Ed.bolt}$ = *Tensile load effect on the most loaded bolt*

$F_{t.Rd.bolt}$ = *Tensile capacity of one bolt*

Table 8.21 Combination of axial and shear load in the most loaded bolt in each element.

Plate	$\frac{F_{v.Ed.bolt}}{F_{v.Rd.bolt}} + \frac{F_{t.Ed.bolt}}{1.4 \cdot F_{t.Rd.bolt}} \leq 1$	Utilization ratio [%]	Control
Curved beam	$0.701 + 0.226 \leq 1$	96,7	Ok!
Truss element 15	$0.058 + 4.017 \cdot 10^{-5} \leq 1$	5,8	Ok!
Truss element 18	$0.098 + 4.147 \cdot 10^{-5} \leq 1$	9,8	Ok!
Truss element 21	$0.131 + 3.35 \cdot 10^{-5} \leq 1$	13,1	Ok!
Truss element 24	$0.035 + 9.11 \cdot 10^{-5} \leq 1$	3,5	Ok!

8.2.10 Compression perpendicular to grain

The compression load acting in the perpendicular direction to the grain must be checked for timber elements. Since this kind of loading only occurs in the curved beam in this connection, it is only this element that has been controlled so that Equation (8.11) is satisfied. In Table 8.22, the result obtained is presented.

$$k_{c.90} \cdot f_{c.90.d} \geq \sigma_{c.90.c} \tag{8.11}$$

where:

$f_{c.90.d}$ = *Design compression capacity perpendicular to the grain*

$\sigma_{c.90.d}$ = *Stress perpendicular to the grain*

Table 8.22 Control of the compression load perpendicular to the grain for the curved beam.

Element	$\sigma_{c.90.d}$ [MPa]	$k_{c.90} \cdot f_{c.90.d}$ [MPa]	Utilization ratio [%]	Control
Curved beam	0,55	1,8	30,5	Ok!

8.2.11 Block and plug shear failure – truss elements

The block and plug shear failure were only calculated and controlled for the truss elements since the risk of this kind of failure was only likely to occur in these elements. The control was based on Equation (8.12) and the results are presented in Table 8.23.

$$F_{bs.Rk} \geq F_s \tag{8.12}$$

where:

$F_{bs.Rk}$ = *Characteristic block or plug shear capacity*

F_s = *Shear force acting on the element*

Table 8.23 Control of block and plug shear failure for the truss elements.

Element	$F_{bs.Rk}$ [kN]	F_s [kN]	Utilization ratio [%]	Control
Truss element 15	477,6	137,3	28,7	Ok!
Truss element 18	477,6	233.5	48,9	Ok!
Truss element 21	477,6	312.8	65,5	Ok!
Truss elements 24	477,6	58.8	12,3	Ok!

8.2.12 Welds

The capacity of the welds were controlled according to Equations (8.13) and (8.14), in which the equivalent stress parallel and perpendicular to the welds are considered, in both the horizontal and vertical direction. Because of the requirements that needed to be fulfilled, the thickness of the slotted-in plate hade to be 48 mm. The results are presented in Table 8.24 and Table 8.25.

$$\frac{f_u}{\beta_w \cdot \gamma_{M2}} \geq \sigma_{eq} \tag{8.13}$$

$$\frac{0.9 \cdot f_u}{\gamma_{M2}} \geq \sigma_{\perp eq} \tag{8.14}$$

Table 8.24 Control of the equivalent stress parallel to the welds in both horizontal and vertical direction.

Weld	$\frac{f_u}{\beta_w \cdot \gamma_{M2}}$	σ_{eq}	Utilization ratio [%]
Horizontal	344	342,8	99,6
Vertical	344	88,2	25,6

Table 8.25 Control of the equivalent stress perpendicular to the welds in both horizontal and vertical direction.

Weld	$\frac{0.9 \cdot f_u}{\gamma_{M2}}$	$\sigma_{\perp eq}$	Utilization ratio [%]
Horizontal	309,6	15,3	4,9
Vertical	309,6	26,9	8,7

8.2.13 Translational and Rotational stiffness

The translational and rotational spring stiffness was calculated and the values are presented in Table 8.26.

Table 8.26 Translational and rotational stiffness for curved beam and truss elements.

Element	Translational stiffness [N/mm]	Rotational stiffness [N/rad]
Curved beam	$9{,}304 \cdot 10^3$	$1{,}576 \cdot 10^{10}$
Truss element	$1{,}551 \cdot 10^4$	$1{,}347 \cdot 10^{10}$

9 Discussion

9.1 3D-modelling

In this Master's Thesis project the software *Abaqus* was used to model a covered pedestrian and bicycle timber bridge in 3D. The 3D-modelling was considered rather difficult and time consuming due to limited experience and lack of instructions on how to model both 3D-structures and connections as interactions between elements in *Abaqus*. More easily accessible information and a greater variety of tutorials would have reduced the time consumed for the modelling process.

9.2 Improvement of the *Leaf Bridge* concept

The work to improve the original *Leaf bridge* concept included consideration of more load cases, especially the addition of service vehicle load and wind load, not only in the vertical but also in the transversal and longitudinal directions. Additionally, the connections between cables, arches and the deck were, unlike all other connections, not considered to be fully fixed, but pinned. Also the degree of rotational fixation was included in the analysis of the model. These improvements resulted in a need for larger element dimensions in order to be able to satisfy SLS limits. The increase of element dimensions resulted in a decrease of utilization ratios of these elements. As can be seen in Table 7.4 the utilization ratios of the different capacities vary widely, indicating that many of the elements are over-dimensioned. The over-dimensioning could be reduced by aiming at further optimizing the element dimension such that the increase of capacity due to stiffness is higher than the increase of the load due to self-weight.

9.3 Connections in timber structures

Designing connections in timber structures can be complicated, especially in structures subjected to high loads, due to the low strength of timber compared to other materials, e.g. steel and concrete. The desire is to create a connection with a ductile behaviour, in which the failure occurs in the fasteners and not in the timber itself, since the failure of timber is brittle. To achieve this, the fasteners have to be weak enough to fail before the timber does. At the same time, a connection has to be strong enough to be able to carry the loads to which it is subjected. Increasing the number of fasteners will increase the strength of the whole connection, but will in turn lead to an increase in its size, which is not always desirable. It is generally the size of the connections that is decisive for the dimensions of the elements. A need for increasing of the size of the elements in order to accommodate the connections results in over-dimensioning of the elements. With the use of more efficient connections, the over-dimensioning can be reduced.

The connections which were designed in this project were initially designed for the sectional forces and moments originating from the case where rigid connections were assumed. Thereafter the design was also checked for the sectional forces and moments from the case with applied rotational spring stiffness. The resulting design fulfilled the considered requirements, but might not be completely realistic, due to the amount of fastener and the space they require in comparison to the length of the elements. Further improvements could be to increase the height of the truss beams in order to allow for more rows of fasteners. Without changing the total number of fasteners in the connection, the number of fasteners per row can be reduced, which in turn reduces the

group effect along the grain. This leads to a lower capacity of each row, but an increase of the capacity of the whole connection due to the addition of more rows.

Also the connection between the slotted-in plates from the truss beams and the steel plate attached to the curved beam is a critical area. Due to the moments which are to be transferred, the required length of the horizontal welds is excessive, with regard to the assumption of a solid cross section of the slotted-in plate. A solution to this problem could be to add stiffeners as shown in Figure 8.2, which would enable a reduction of the length of the horizontal weld and hence also the thickness of the slotted-in plate.

9.4 Influence of rotational stiffness

As can be seen in the graphs in Section 7.4 the influence of rotational spring stiffness is rather similar for all load cases except for the ones including the service vehicle as the main load and horizontal wind loads. One reason for these deviations could be that the elements are loaded to such an extent that they start to lose stiffness. When assigning rigid connections, the magnitude of the rotational spring stiffness is set to ten times the average stiffness of the connecting members, hence different types of connection will have different stiffnesses depending on which elements are included in that connection. Therefore, when assigning a specific magnitude, the chosen magnitude might be higher than that of the rigid one, which could have decreased due to the loss of stiffness in the elements.

It can also be seen that, for this structure, the connections with a rotational stiffness which is lower than 10 kN/rad can be considered to be completely pinned, and those with a rotational stiffness which is greater than 100 MN/rad can be considered to be completely fixed. Everything in between can be considered to be semi-rigid. The deflections due to the rotational stiffness from the connection design lie within the semi-rigid part of the curve. To increase the rotational stiffness of the connections further, in order to reduce the increasing deflections, the total polar moment needs to be increased, see Equation (6.9). This can be done either by increasing the distance to each fastener or by adding more fasteners. Both of these actions increases the space required to accommodate the connections, which in turn could increase the over-dimensioning.

Often connections are assumed to be completely pinned, which is an assumption on the safe side since the peak moment in the elements is larger than for a fully fixed element. To always consider choices to be on the safe side can result in excessive over-dimensioning, which is why taking semi-rigidity of connections in consideration is of value in order to make them more structurally and economically efficient.

10 Conclusions

- More information and tutorials regarding complex 3D-modelling in *Abaqus* are needed in order to facilitate and to streamline the 3D-modelling process.

- The size of the connection can be decisive for the dimension of the elements.

- For a constant rotational spring stiffness, the joint stiffness varies due to the stiffness of the connected elements.

- In order to increase the competitivity of timber as structural material in bridges, more efficient connections need to be developed, which reduce the over-dimensioning of the elements and hence save material, costs and environmental impacts.

Further studies should include:

- Proposal and analysis of other types of connection design.

- Dynamic analyses of the bridge with semi-rigid connections.

11 References

Al-Emrani et al. (2011): *Bärande konstruktioner, del 2*. Department of Civil and Environmental Engineering, Chalmers University of Technology, Publication no. 2011:1, Göteborg, Sweden.

American Institute of Timber Construction. (2012): *Timber Construction Manual, 6th Edition*. American Institute of Timber Construction. Somerset, NJ, USA.

Autodesk Inc. (2015): *AutoCAD 2015* [Computer program].

CADCAM-Services Franz Reiter. (2014): *gCAD3D* [Computer program] Available at http://gcad3d.org/ [Accessed 24, February 2015].

Connecticut history. (2015): *Town Patents the Lattice Truss Bridge.* Available at: http://connecticuthistory.org/twon-patents-the-lattice-truss-bridge-today-in-history/ [Accessed March 20, 2015].

Connections in timber structures. (2006): *Connections in timber structures.* Available at: http://www.scribd.com/doc/214611862/Connections#scribd [Accessed March 5, 2015].

Crocetti et al. (2011): *Design of timber structures.* Swedish Wood. Stockholm, Sweden.

Dassault Systèmes. (2015): *Abaqus/CAE* (Version 6.13-3) [Computer program].

Dassault Systèmes. (2013): *Abaqus Analysis User's Guide*. Dassault Systèmes. Available at: http://129.97.46.200:2080/v6.13/books/usb/default.htm [Accessed March 10, 2015].

Dahlbom, O., Olsson, K-G. (2010): *Strukturmekanik*. Studentlitteratur. Lund, Sweden.

Engström, D. (1993): *Förbandens inverkan på konkurrenskraften hos träkonstruktioner.* Department of Civil and Environmental Engineering, Chalmers University of Technology, Publication no. 1993:5, Göteborg, Sweden.

Engström, D. (1994): *Konstruktionsvirke och förband: anpassning och förbättring.* Department of Civil and Environmental Engineering, Chalmers University of Technology, Publication no. 1994:8, Göteborg, Sweden.

Engström, D. (1995): *Limits for semi-rigidity of timber joints.* Department of Civil and Environmental Engineering, Chalmers University of Technology, Publication no. 1995:9, Göteborg, Sweden.

Engström, D. (1997): *Connections for timber-framed structures: assembly properties and structural behaviour*. Department of Civil and Environmental Engineering, Chalmers University of Technology, Publication no. 1997:2, Göteborg, Sweden.

Federal Highway Administration. (2005): *Covered Bridge Manual*. U.S. Department of Transportation, Publication no. FHAW-HRT-04-098. McLean, VA, USA.

Farreyre, A., Journot, J. (2005): *Timber trussed arch for long span*. Department of Civil and Environmental Engineering, Chalmers University of Technology, Publication no. 2005:103, Göteborg, Sweden.

Madsen, B. (1998): *Reliable timber connections*. Department of Civil Engineering, University of British Columbia, Vancouver, Canada.

Martinsons. (2015): *Framtidens naturliga sätt att bygga broar*. Skellefteå, Sweden.

McGuire, J. (1995): *Notes on semi-rigid connections*. NASA. Available at: https://femci.gsfc.nasa.gov/semirigid/ [Accessed March 10, 2015].

Pousette A. (2008): *Träbroar: konstruktion och dimensionering*. Science Partner. SP Rapport 2008:50. Sweden.

Roth, M. (1981): *An Inventory of Historic Engineering and Industrial Sites*. Washington, D.C. United States.

Svenskt trä. (2003): *Träbroar – historisk återblick*. TräGuiden. Available at: http://www.traguiden.se/konstruktion/konstruktionsexempel/trabroar/trabroar--historisk-aterblick/trabroar--historisk-aterblick/ [Accessed March 2, 2015].

Svenskt trä. (2014): *Balkbro för gång- och cykeltrafik*. TräGuiden. Available at: http://www.traguiden.se/konstruktion/dimensionering/berakningsexempel/trabroar/balkbro-for-gang--och-cykeltrafik/ [Accessed March 5, 2015].

Svenskt trä. (2015): *Olika typer av förband*. TräGuiden. Available at: http://www.traguiden.se/TGtemplates/popup1spalt.aspx?id=803&contextPage=182 [Accessed March 5, 2015].

Teike, A. (2013): *Study of a multiple kingpost truss bridge with framed joints*. Department of Civil and Environmental Engineering, Chalmers University of Technology, Publication no. 2013:20, Göteborg, Sweden.

Trafikverket. (2004): *Bro 2004*. Trafikverket. Publ 2004:56. Sweden.

Trafikverket. (2011): *TRVK Bro 11*. Trafikverket. Publ 2011:085. Sweden.

Tredgold, T., Hurst, J. T. (1871): *Elementary principles of carpentry*. London, E. & F.N. Spon.

Wood Information Sheet. (2003): *Adhesively-bonded timber connections*. Wood Information Sheet 2/3-35. Available at: http://www.trada.co.uk/images/onlinebooks/B6EB545F-B4D8-4AF2-AB64-2065F11877D1/index.html [Accessed March 13, 2015].

Appendix A Calculations

Table of content

1. Geometry of the bridge

Length of bridge $L := 30m$

Width of bridge deck $w := 4m$

Maximum roof width $w_r := 10m$

1.1 Angles between elements

Since the node in which the connection is located contains several elements with their own local coordinate systems, a common local coordinate system of the connection was defined. It was defined as a coordinate system located in the middle of the two local coordinate systems of the attaching curved beam elements. The angles between axes and sectional forces in the local coordinate system of the individual elements and the local coordinate system of the connection node are extracted below.

Truss 15 to local coordinate system of connection node:

$\alpha_{t.15.c.c.x} := 32°$ $\alpha_{t.15.c.c.y} := 98°$ $\alpha_{t.15.c.c.z} := 121°$

Truss 18 to local coordinate system of connection node:

$\alpha_{t.18.c.c.x} := 32°$ $\alpha_{t.18.c.c.y} := 99°$ $\alpha_{t.18.c.c.z} := 60°$

Truss 21 to local coordinate system of connection node:

$\alpha_{t.21.c.c.x} := 148°$ $\alpha_{t.21.c.c.y} := 89°$ $\alpha_{t.21.c.c.z} := 122°$

$\alpha_{SF1.t.21.x} := 32°$ $\alpha_{SF1.t.21.y} := 91°$ $\alpha_{SF1.t.21.z} := 58°$

$\alpha_{SF2.t.21.x} := 121°$ $\alpha_{SF2.t.21.y} := 83°$ $\alpha_{SF2.t.21.z} := 32°$

$\alpha_{SF3.t.21.x} := 85°$ $\alpha_{SF3.t.21.y} := 7°$ $\alpha_{SF3.t.21.z} := 95°$

Truss 24 to local coordinate system of connection node:

$\alpha_{t.24.c.c.x} := 148°$ $\alpha_{t.24.c.c.y} := 90°$ $\alpha_{t.24.c.c.z} := 58°$

Curved beam element 136/145 to local coordinate system of connection node:

$\alpha_{c.136.c.c.x} := 90.5°$ $\alpha_{c.136.c.c.y} := 94°$ $\alpha_{c.136.c.c.z} := 176°$

$\alpha_{SF1.c.136.x} := 90°$ $\alpha_{SF1.c.136.y} := 94°$ $\alpha_{SF1.c.136.z} := 176°$

$\alpha_{SF2.c.136.x} := 180°$ $\alpha_{SF2.c.136.y} := 90°$ $\alpha_{SF2.c.136.z} := 90°$

$\alpha_{SF3.c.136.x} := 90°$ $\alpha_{SF3.c.136.y} := 176°$ $\alpha_{SF3.c.136.z} := 86°$

1.2 Dimensions

1.2.1 Structural elements

Height and thickness of

Arches	$h_{arch} := 630mm$	$t_{arch} := 215mm$
Curved beams	$h_{curved} := 270mm$	$t_{curved} := 140mm$
Roof trusses	$h_{rooftruss} := 225mm$	$t_{rooftruss} := 170mm$
Deck crosses	$h_{deck} := 225mm$	$t_{deck} := 140mm$
Edge beam	$h_{edgebeam} := 405mm$	$t_{edgebeam} := 215mm$

Diameter of the cables $\phi_{cable} := 30mm$

1.2.2 Cross sectional constants

The expression for polar moment of inertia used below is valid for circular sections and therefore the smallest of the rectangular cross sectional measurements is used.

Arches

Sectional modulus $W_{arch.1} := \frac{h_{arch} \cdot t_{arch}^{2}}{6} = 4.854 \times 10^{-3} \cdot m^{3}$

Sectional modulus $W_{arch.2} := \frac{t_{arch} \cdot h_{arch}^{2}}{6} = 0.014 \cdot m^{3}$

Polar moment of inertia $I_{p.arch} := \frac{\pi \cdot \left(\frac{t_{arch}}{2} \right)^{4}}{2} = 2.098 \times 10^{-4} \cdot m^{4}$

Curved beams

Sectional modulus $W_{curved.1} := \frac{h_{curved} \cdot t_{curved}^{2}}{6} = 8.82 \times 10^{-4} \cdot m^{3}$

Sectional modulus $W_{curved.2} := \frac{t_{curved} \cdot h_{curved}^{2}}{6} = 1.701 \times 10^{-3} \cdot m^{3}$

Polar moment of inertia $I_{p.curved} := \frac{\pi \cdot \left(\frac{t_{curved}}{2} \right)^{4}}{2} = 3.771 \times 10^{-5} \cdot m^{4}$

Roof trusses

Sectional modulus $W_{rooftruss.1} := \frac{h_{rooftruss} \cdot t_{rooftruss}^{2}}{6} = 1.084 \times 10^{-3} \cdot m^{3}$

Sectional modulus $W_{rooftruss.2} := \frac{t_{rooftruss} \cdot h_{rooftruss}^{2}}{6} = 1.434 \times 10^{-3} \cdot m^{3}$

Polar moment of inertia $I_{p.rooftruss} := \frac{\pi \cdot \left(\frac{t_{rooftruss}}{2} \right)^{4}}{2} = 8.2 \times 10^{-5} \cdot m^{4}$

Deck crosses

Sectional modulus $W_{deck.1} := \frac{h_{deck} \cdot t_{deck}^{2}}{6} = 7.35 \times 10^{-4} \cdot m^{3}$

Sectional modulus $W_{deck.2} := \frac{t_{deck} \cdot h_{deck}^{2}}{6} = 1.181 \times 10^{-3} \cdot m^{3}$

Polar moment of inertia $I_{p.deck} := \frac{\pi \cdot \left(\frac{t_{deck}}{2} \right)^{4}}{2} = 3.771 \times 10^{-5} \cdot m^{4}$

Edge beam

Sectional modulus $W_{edgebeam.1} := \frac{h_{edgebeam} \cdot t_{edgebeam}^{2}}{6} = 3.12 \times 10^{-3} \cdot m^{3}$

Sectional modulus $W_{edgebeam.2} := \frac{t_{edgebeam} \cdot h_{edgebeam}^{2}}{6} = 5.878 \times 10^{-3} \cdot m^{3}$

Polar moment of inertia $I_{p.edgebeam} := \frac{\pi \cdot \left(\frac{t_{edgebeam}}{2} \right)^{4}}{2} = 2.098 \times 10^{-4} \cdot m^{4}$

1.2.3 Fasteners

1.2.3.1 Bolts in truss connection

Diameter of bolts $d_{bolt.truss} := 20mm$

Diameter of hole

$$d_{0.hole.truss} := \begin{cases} d_{bolt.truss} & \text{if } d_{bolt.truss} \le 10mm \\ (d_{bolt.truss} + 1mm) & \text{if } 12mm \le d_{bolt.truss} \le 14mm \\ (d_{bolt.truss} + 2mm) & \text{if } 16mm \le d_{bolt.truss} \le 24mm \\ (d_{bolt.truss} + 3mm) & \text{if } d_{bolt.truss} \ge 27mm \end{cases} = 22 \cdot mm$$

1.2.3.2 Bolts in curved connection

Diameter of bolts $d_{bolt.curved} := 12mm$

Diameter of hole

$$d_{0.hole.curved} := \begin{cases} d_{bolt.curved} & \text{if } d_{bolt.curved} \le 10mm \\ (d_{bolt.curved} + 1mm) & \text{if } 12mm \le d_{bolt.curved} \le 14mm \\ (d_{bolt.curved} + 2mm) & \text{if } 16mm \le d_{bolt.curved} \le 24mm \\ (d_{bolt.curved} + 3mm) & \text{if } d_{bolt.curved} \ge 27mm \end{cases} = 13 \cdot mm$$

1.2.4 Plates

1.2.4.1 Slotted-in plate in truss elements

Thickness $t_{slot.plate} := 20mm$

The plates are considered thin or thick according to the following:

$$platethickness_{slot} := \begin{cases} \text{"thin"} & \text{if } t_{slot.plate} \le 0.5 \cdot d_{bolt.truss} = \text{"thick"} \\ \text{"thick"} & \text{if } t_{slot.plate} \ge d_{bolt.truss} \\ \text{"linear interpolation"} & \text{otherwise} \end{cases}$$

1.2.4.2 Plates at curved beams

Thickness $t_{curved.plate} := 12mm$

Height $h_{plate} := h_{curved} = 270 \cdot mm$

Length $l_{plate} := 780mm$

The plates are considered thin or thick according to the following:

$$platethickness_{curved} := \begin{cases} \text{"thin"} & \text{if } t_{curved.plate} \le 0.5 \cdot d_{bolt.curved} = \text{"thick"} \\ \text{"thick"} & \text{if } t_{curved.plate} \ge d_{bolt.curved} \\ \text{"linear interpolation"} & \text{otherwise} \end{cases}$$

2. Factors and coefficients

Partial factor for timber in capacity calculations $\gamma_{M.cap} := 1.25$

Partial factor for steel $\gamma_{M2} := 1.25$

Partial factor for welds $\beta_w := 1$

Partial factor for steel cables $\gamma_{R.cable} := 1.0$

Modification factor for duration of load and moisture content $k_{mod} := 0.90$

Factor taking into account the load configuration, the possibility of splitting and the degree of compressive deformation $k_{c.90} := 1.0$

Depth factor for elements smaller than 600mm

Arches $k_{h.arch.t} := \min\left[1.1, \left(\frac{600mm}{t_{arch}}\right)^{0.1}\right] = 1.1$

Curved beams $k_{h.curved.h} := \min\left[1.1, \left(\frac{600mm}{h_{curved}}\right)^{0.1}\right] = 1.083$

$k_{h.curved.t} := \min\left[1.1, \left(\frac{600mm}{t_{curved}}\right)^{0.1}\right] = 1.1$

Roof trusses $k_{h.rooftruss.h} := \min\left[1.1, \left(\frac{600mm}{h_{rooftruss}}\right)^{0.1}\right] = 1.1$

$k_{h.rooftruss.t} := \min\left[1.1, \left(\frac{600mm}{t_{rooftruss}}\right)^{0.1}\right] = 1.1$

Deck crosses $k_{h.deck.h} := \min\left[1.1, \left(\frac{600mm}{h_{deck}}\right)^{0.1}\right] = 1.1$

$k_{h.deck.t} := \min\left[1.1, \left(\frac{600mm}{t_{deck}}\right)^{0.1}\right] = 1.1$

Edge beam $k_{h.edgebeam.h} := \min\left[1.1, \left(\frac{600mm}{h_{edgebeam}}\right)^{0.1}\right] = 1.04$

$k_{h.edgebeam.t} := \min\left[1.1, \left(\frac{600mm}{t_{edgebeam}}\right)^{0.1}\right] = 1.1$

3. Material properties

3.1 Glulam GL30c

3.1.1 Characteristic values

	Capacity analysis	Deformation analysis
Bending parallel to grain	$f_{m.g.k} := 30MPa$	
Tension parallel to grain	$f_{t.0.g.k} := 19.5MPa$	
Tension perpendicular to grain	$f_{t.90.g.k} := 0.5MPa$	
Compression parallel to grain	$f_{c.0.g.k} := 24.5MPa$	
Compression perpendicular to grain	$f_{c.90.g.k} := 2.5MPa$	
Shear strenght	$f_{v.g.k} := 3.5MPa$	
Rolling shear strength	$f_{r.g.k.} := 1.2MPa$	
Elastic modulus	$E_{0.g.mean.cap} := 10800MPa$	$E_{0.g.mean.def} := 13000MPa$
Shear modulus	$G_{0.g.mean.cap} := 540MPa$	$G_{0.g.mean.def} := 650MPa$
Density	$\rho_{g.mean} := 430 \frac{kg}{m^3}$	
Species	$species := "softwood"$	

3.1.2 Design values

Bending strength about weak axis (1) and strong axis (2)

Arches

$$f_{m.d.arch.1} := \frac{k_{h.arch.t} \cdot k_{mod} \cdot f_{m.g.k}}{\gamma_{M.cap}} = 23.76 \cdot MPa$$

$$f_{m.d.arch.2} := \frac{k_{mod} \cdot f_{m.g.k}}{\gamma_{M.cap}} = 21.6 \cdot MPa$$

Curved beams

$$f_{m.d.curved.1} := \frac{k_{h.curved.t} \cdot k_{mod} \cdot f_{m.g.k}}{\gamma_{M.cap}} = 23.76 \cdot MPa$$

$$f_{m.d.curved.2} := \frac{k_{h.curved.h} \cdot k_{mod} \cdot f_{m.g.k}}{\gamma_{M.cap}} = 23.396 \cdot MPa$$

Roof trusses

$$f_{m.d.rooftruss.1} := \frac{k_{h.rooftruss.t} \cdot k_{mod} \cdot f_{m.g.k}}{\gamma_{M.cap}} = 23.76 \cdot MPa$$

$$f_{m.d.rooftruss.2} := \frac{k_{h.rooftruss.h} \cdot k_{mod} \cdot f_{m.g.k}}{\gamma_{M.cap}} = 23.76 \cdot MPa$$

Deck cross

$$f_{m.d.deck.1} := \frac{k_{h.deck.t} \cdot k_{mod} \cdot f_{m.g.k}}{\gamma_{M.cap}} = 23.76 \cdot MPa$$

$$f_{m.d.deck.2} := \frac{k_{h.deck.h} \cdot k_{mod} \cdot f_{m.g.k}}{\gamma_{M.cap}} = 23.76 \cdot MPa$$

Edge beams

$$f_{m.d.edgebeam.1} := \frac{k_{h.edgebeam.t} \cdot k_{mod} \cdot f_{m.g.k}}{\gamma_{M.cap}} = 23.76 \cdot MPa$$

$$f_{m.d.edgebeam.2} := \frac{k_{h.edgebeam.h} \cdot k_{mod} \cdot f_{m.g.k}}{\gamma_{M.cap}} = 22.466 \cdot MPa$$

Tension strength along the grain

Arches $f_{t.0.d.arch} := \frac{k_{h.arch.t} \cdot k_{mod} \cdot f_{t.0.g.k}}{\gamma_{M.cap}} = 15.444 \cdot MPa$

Curved beams $f_{t.0.d.curved} := \frac{k_{h.curved.t} \cdot k_{mod} \cdot f_{t.0.g.k}}{\gamma_{M.cap}} = 15.444 \cdot MPa$

Roof trusses $f_{t.0.d.rooftruss} := \frac{k_{h.rooftruss.t} \cdot k_{mod} \cdot f_{t.0.g.k}}{\gamma_{M.cap}} = 15.444 \cdot MPa$

Deck cross $f_{t.0.d.deck} := \frac{k_{h.deck.t} \cdot k_{mod} \cdot f_{t.0.g.k}}{\gamma_{M.cap}} = 15.444 \cdot MPa$

Edge beams $f_{t.0.d.edgebeam} := \frac{k_{h.edgebeam.t} \cdot k_{mod} \cdot f_{t.0.g.k}}{\gamma_{M.cap}} = 15.444 \cdot MPa$

Tension strength perpendicular to the grain

All glulam members $f_{t.90.d} := \frac{k_{mod} \cdot f_{t.90.g.k}}{\gamma_{M.cap}} = 0.36 \cdot MPa$

Compression strength along the grain

All glulam members $f_{c.0.d} := \frac{k_{mod} \cdot f_{c.0.g.k}}{\gamma_{M.cap}} = 17.64 \cdot MPa$

Compression strength perpendicular to the grain

All glulam members $f_{c.90.d} := \frac{k_{mod} \cdot f_{c.90.g.k}}{\gamma_{M.cap}} = 1.8 \cdot MPa$

Shear strength

All glulam members $f_{v.g.d} := \frac{k_{mod} \cdot f_{v.g.k}}{\gamma_{M.cap}} = 2.52 \cdot MPa$

Twisting strength

All glulam members $f_{r.g.d} := \frac{k_{mod} \cdot f_{r.g.k.}}{\gamma_{M.cap}} = 0.864 \cdot MPa$

3.2 Steel

3.2.1 Plate

Steel S275

Ultimate strength $f_{u.plate} := 430MPa$

3.2.2 Cables

Spiral strand rope

No catenary effects are considered, since the hangers are almost verical. It could be considered for the cables in the deck, but this is excluded. Many aspects of the cables have not been considered, hence factors are taken to be on the safest side.

Young's modulus $E_{steel.cable} := 150GPa$

Minimum breaking force factor $K_{cable} := 0.51$

Rope grade $R_{r.cable} := 1770MPa$

Loss factor $k_{e.cable} := 0.9$

$$F_{min.cable} := K_{cable} \cdot \phi_{cable}^{2} \cdot R_{r.cable}$$

Characteristic value of breaking strength $F_{u.k.cable} := F_{min.cable} \cdot k_{e.cable}$

Characteristic value of proof strength $F_{k.cable} := 531.5kN$

Design value of tension resistance $F_{t.Rd.cable} := \min\left(\frac{F_{u.k.cable}}{1.5 \cdot \gamma_{R.cable}}, \frac{F_{k.cable}}{\gamma_{R.cable}}\right) = 487.458 \cdot kN$

3.3 Fasteners

Young's molulus $E_{bolt} := 210GPa$

3.3.1 Bolts in truss connection

Characteristic tensile strength $f_{u.k.bolt.truss} := 1000 \frac{N}{mm^2}$

Characteristic yield moment

$$M_{y.Rk.bolt.truss} := 0.3 \cdot \frac{f_{u.k.bolt.truss}}{\frac{N}{mm^2}} \cdot \left(\frac{d_{bolt.truss}}{mm} \right)^{2.6} \cdot N \cdot mm = 0.724 \cdot MN \cdot mm$$

Shear strenght $\tau_{s.Rk.bolt.truss} := \frac{f_{u.k.bolt.truss}}{\sqrt{3}} = 577.35 \cdot MPa$

3.3.2 Bolts in curved connection

Characteristic tensile strength $f_{u.k.bolt.curved} := 400 \frac{N}{mm^2}$

Characteristic yield moment

$$M_{y.Rk.bolt.curved} := 0.3 \cdot \frac{f_{u.k.bolt.curved}}{\frac{N}{mm^2}} \cdot \left(\frac{d_{bolt.curved}}{mm} \right)^{2.6} \cdot N \cdot mm = 0.077 \cdot MN \cdot mm$$

Shear strenght $\tau_{s.Rk.bolt.curved} := \frac{f_{u.k.bolt.curved}}{\sqrt{3}} = 230.94 \cdot MPa$

3.4 Embedding strength of timber

3.4.1 Truss connection

For timber in bolted connections

$$k_{90.truss} := \begin{cases} \left(1.35 + 0.015 \cdot \frac{d_{bolt.truss}}{mm}\right) & \text{if species = "softwood"} \\ \left(1.30 + 0.015 \cdot \frac{d_{bolt.truss}}{mm}\right) & \text{if species = "LVL"} \\ \left(0.90 + 0.015 \cdot \frac{d_{bolt.truss}}{mm}\right) & \text{if species = "hardwood"} \end{cases} = 1.65$$

Characteristic embeddment strength parallel to grain

$$f_{h.0.k.truss} := 0.082\left(1 - 0.01 \cdot \frac{d_{bolt.truss}}{mm}\right)\rho_{g.mean} \cdot \frac{N \cdot m^3}{mm^2 \cdot kg} = 28.208 \cdot MPa$$

Angle between bolt and fibre direction

$$\alpha_{truss} := 90°$$

$$f_{h.90.k.truss} := \frac{f_{h.0.k.truss}}{k_{90.truss} \cdot \sin(\alpha_{truss})^2 + \cos(\alpha_{truss})^2} = 17.096 \cdot MPa$$

3.4.2 Curved connection

For timber in bolted connections

$$k_{90.curved} := \begin{cases} \left(1.35 + 0.015 \cdot \frac{d_{bolt.curved}}{mm}\right) & \text{if species = "softwood"} \\ \left(1.30 + 0.015 \cdot \frac{d_{bolt.curved}}{mm}\right) & \text{if species = "LVL"} \\ \left(0.90 + 0.015 \cdot \frac{d_{bolt.curved}}{mm}\right) & \text{if species = "hardwood"} \end{cases} = 1.53$$

Characteristic embeddment strength parallel to grain

$$f_{h.0.k.curved} := 0.082\left(1 - 0.01 \cdot \frac{d_{bolt.curved}}{mm}\right)\rho_{g.mean} \cdot \frac{N \cdot m^3}{mm^2 \cdot kg} = 31.029 \cdot MPa$$

Angle between bolt and fibre direction

$$\alpha_{curved} := 90°$$

$$f_{h.90.k.curved} := \frac{f_{h.0.k.curved}}{k_{90.curved} \cdot \sin(\alpha_{curved})^2 + \cos(\alpha_{curved})^2} = 20.28 \cdot MPa$$

4. Loads

4.1 Imposed loads

Pedestrians and bicyles on the deck $q_{k.pb} := 5\,\frac{kN}{m^2}$

$q_{k.pb.h} := 0.10 \cdot q_{k.pb} \cdot (L \cdot w) = 60 \cdot kN$

Service load

Vertical $P_{s.V1} := 80kN$

Vertical $P_{s.V2} := 40kN$

Horizontal $P_{s.H} := 0.60 \cdot (80 + 40)kN = 72 \cdot kN$

4.2 Snow load

Snow zone $s_k := 2.5\,\frac{kN}{m^2}$

Shape factor for roof angle less than 30 degree $\mu_1 := 0.8$

Characteristic snow load: $S_k := \mu_1 \cdot s_k = 2 \cdot \frac{kN}{m^2}$

4.3 Wind load

According to SS-EN 1991-1-4:2005 wind load action should be calculated in all direction. This will be done for the roof and the deck. The wind load acting in y-direction, along the bridge span, is calculated as 50% of the wind force in the x-direction.

Terrain type Terrain III

Air density $\rho_{air} := 1.25\,\frac{kg}{m^3}$

Basic wind speed $v_b := 25\,\frac{m}{s}$

Height of the deck and vehicle $d_{tot.d} := 4 + 0.250 = 4.25$

4.3.1 Wind load on deck

Coefficients, inclination of 7 degrees

Exposure coefficient $c_{e.d} := 1.3$

Drag Coefficient in x-direction $c_{f.d.x} := 2.35$

Drag coefficient in z-direction for $c_{f.d.z} := 0.9$

Uplift net pressure coefficient for deck part A $c_{p.net.d.U.A} := -0.97$

Uplift net pressure coefficient for deck part B $c_{p.net.d.U.B} := -1.72$

Uplift net pressure coefficient for deck part C $c_{p.net.d.U.C} := -1.6$

Uplift net pressure coefficient for deck part D $c_{p.net.d.U.D} := -1.42$

Down wind net pressure coefficient for deck part A $c_{p.net.d.D.A} := 0.64$

Downwind net pressure coefficient for deck part B $c_{p.net.d.D.B} := 1.8$

Downwind net pressure coefficient for deck part C $c_{p.net.d.D.C} := 1.34$

Downwind net pressure coefficient for deck part D $c_{p.net.d.D.D} := 0.4$

Wind forces

Wind load in x-direction $Q_{w.d.x} := \left(\frac{\rho_{air}}{2} \cdot v_b^{\,2} \cdot c_{e.d} \cdot c_{f.d.x} \right) = 1.193 \cdot \frac{kN}{m^2}$

Wind load in y-direction $Q_{w.d.y} := 0.5 \cdot Q_{w.d.x} = 0.597 \cdot \frac{kN}{m^2}$

Wind load in x-direction tranformed into a line load, kN/m $Q_{w.d.x.l} := \left(\frac{\rho_{air}}{2} \cdot v_b^{\,2} \cdot c_{e.d} \cdot c_{f.d.x} \right) 0.18m = 0.215 \cdot \frac{kN}{m}$

Uplift wind forces

Part A $Q_{w.d.U.A} := \frac{\rho_{air}}{2} \cdot v_b^{\,2} \cdot c_{e.d} \cdot c_{p.net.d.U.A} = -0.493 \cdot \frac{kN}{m^2}$

Part B $Q_{w.d.U.B} := \frac{\rho_{air}}{2} \cdot v_b^{\,2} \cdot c_{e.d} \cdot c_{p.net.d.U.B} = -0.873 \cdot \frac{kN}{m^2}$

Part C $Q_{w.d.U.C} := \frac{\rho_{air}}{2} \cdot v_b^2 \cdot c_{e.d} \cdot c_{p.net.d.U.C} = -0.813 \cdot \frac{kN}{m^2}$

Part D $Q_{w.d.U.D} := \frac{\rho_{air}}{2} \cdot v_b^2 \cdot c_{e.d} \cdot c_{p.net.d.U.D} = -0.721 \cdot \frac{kN}{m^2}$

Downward wind forces

Part A $Q_{w.d.D.A} := \frac{\rho_{air}}{2} \cdot v_b^2 \cdot c_{e.d} \cdot c_{p.net.d.D.A} = 0.325 \cdot \frac{kN}{m^2}$

Part B $Q_{w.d.D.B} := \frac{\rho_{air}}{2} \cdot v_b^2 \cdot c_{e.d} \cdot c_{p.net.d.D.B} = 0.914 \cdot \frac{kN}{m^2}$

Part C $Q_{w.d.D.C} := \frac{\rho_{air}}{2} \cdot v_b^2 \cdot c_{e.d} \cdot c_{p.net.d.D.C} = 0.68 \cdot \frac{kN}{m^2}$

Part D $Q_{w.d.D.D} := \frac{\rho_{air}}{2} \cdot v_b^2 \cdot c_{e.d} \cdot c_{p.net.d.D.D} = 0.203 \cdot \frac{kN}{m^2}$

4.3.2 Wind load on roof

Coefficients, inclination of 30 degrees

Exposure coeffiecient for the roof	$c_{e.r} := 1.9$
Drag Coefficient in x-direction for the roof	$c_{f.r.x} := 1.0$
Drag Coefficient in x-direction for the roof	$c_{f.r.z} := 0.9$
Uplift net pressure coefficient for roof part A	$c_{p.net.r.U.A} := -1.4$
Uplift net pressure coefficient for roof part B	$c_{p.net.r.U.B} := -1.85$
Uplift net pressure coefficient for roof part C	$c_{p.net.r.U.C} := -1.4$
Uplift net pressure coefficient for roof part D	$c_{p.net.r.U.D} := -2.0$
Downrind net pressure coefficient for roof part A	$c_{p.net.r.D.A} := 1.3$
Downwind net pressure coefficient for roof part B	$c_{p.net.r.D.B} := 1.9$
Downwind net pressure coefficient for roof part C	$c_{p.net.r.D.C} := 1.6$
Downwind net pressure coefficient for roof part D	$c_{p.net.r.D.D} := 0.7$

Wind forces

Wind load in x-direction

$$Q_{w.r.x} := \left(\frac{\rho_{air}}{2} \cdot v_b^{\,2} \cdot c_{e.r} \cdot c_{f.r.x} \right) \cdot 0.405\text{m} = 0.301 \cdot \frac{\text{kN}}{\text{m}}$$

Wind load in y-direction

$$Q_{w.r.y} := 0.5 \cdot Q_{w.r.x} = 0.15\,\text{m} \cdot \frac{\text{kN}}{\text{m}^2}$$

Wind load in x-direction tranformed into a line load, kN/m

$$Q_{w.r.x.l} := \left(\frac{\rho_{air}}{2} \cdot v_b^{\,2} \cdot c_{e.r} \cdot c_{f.r.x} \right) \cdot 0.405\text{m} = 0.301 \cdot \frac{\text{kN}}{\text{m}}$$

Uplift wind forces

Part A

$$Q_{w.r.U.A} := \frac{\rho_{air}}{2} \cdot v_b^{\,2} \cdot c_{e.r} \cdot c_{p.net.r.U.A} = -1.039 \cdot \frac{\text{kN}}{\text{m}^2}$$

Part B

$$Q_{w.r.U.B} := \frac{\rho_{air}}{2} \cdot v_b^{\,2} \cdot c_{e.r} \cdot c_{p.net.r.U.B} = -1.373 \cdot \frac{\text{kN}}{\text{m}^2}$$

Part C

$$Q_{w.r.U.C} := \frac{\rho_{air}}{2} \cdot v_b^{\,2} \cdot c_{e.r} \cdot c_{p.net.r.U.C} = -1.039 \cdot \frac{\text{kN}}{\text{m}^2}$$

Part D

$$Q_{w.r.U.D} := \frac{\rho_{air}}{2} \cdot v_b^{\,2} \cdot c_{e.r} \cdot c_{p.net.r.U.D} = -1.484 \cdot \frac{\text{kN}}{\text{m}^2}$$

Downward wind forces

Part A

$$Q_{w.r.D.A} := \frac{\rho_{air}}{2} \cdot v_b^{\,2} \cdot c_{e.r} \cdot c_{p.net.r.D.A} = 0.965 \cdot \frac{\text{kN}}{\text{m}^2}$$

Part B

$$Q_{w.r.D.B} := \frac{\rho_{air}}{2} \cdot v_b^{\,2} \cdot c_{e.r} \cdot c_{p.net.r.D.B} = 1.41 \cdot \frac{\text{kN}}{\text{m}^2}$$

Part C

$$Q_{w.r.D.C} := \frac{\rho_{air}}{2} \cdot v_b^{\,2} \cdot c_{e.r} \cdot c_{p.net.r.D.C} = 1.188 \cdot \frac{\text{kN}}{\text{m}^2}$$

Part D

$$Q_{w.r.D.D} := \frac{\rho_{air}}{2} \cdot v_b^{\,2} \cdot c_{e.r} \cdot c_{p.net.r.D.D} = 0.52 \cdot \frac{\text{kN}}{\text{m}^2}$$

5. Design of connection

5.1 Sectional forces in connection node (node 37)

	Truss element 15	Truss element 18
Axial force	$SF1_{t.15} := -137273N$	$SF1_{t.18} := -233540N$
Shear forces	$SF2_{t.15} := -203.511N$	$SF2_{t.18} := 210.121N$
	$SF3_{t.15} := 6279.96N$	$SF3_{t.18} := 6225.43N$
Bending moments	$SM1_{t.15} := -2658.36N \cdot m$	$SM1_{t.18} := 3578.97N \cdot m$
	$SM2_{t.15} := -1004.58N \cdot m$	$SM2_{t.18} := 277.337N \cdot m$

	Truss element 21	Truss element 24
Axial force	$SF1_{t.21} := -312823N$	$SF1_{t.24} := -58830.1N$
Shear forces	$SF2_{t.21} := 169.745N$	$SF2_{t.24} := 461.622N$
	$SF3_{t.21} := 5987.7N$	$SF3_{t.24} := 13641.94N$
Bending moments	$SM1_{t.21} := 6270.38N \cdot m$	$SM1_{t.24} := -5259.11N \cdot m$
	$SM2_{t.21} := -412.018N \cdot m$	$SM2_{t.24} := 443.259N \cdot m$
Twisting moment	$SM3_{t.21} := 0N \cdot m$	

	Curved beams
Axial force	$SF1_{c.136.145} := 96312.8N$
Shear forces	$SF2_{c.136.145} := -927.539N$
	$SF3_{c.136.145} := -4088.02N$
Bending moments	$SM1_{c.136.145} := 5929.52N \cdot m$
	$SM2_{c.136.145} := -580.761N \cdot m$
Twisting moment	$SM3_{c.136.145} := 0N \cdot m$

5.2 Truss connection

5.2.1 Geometry

$$\alpha_{1.space} := 0°$$

Maximum angle between horizontal axis and resultant force on the bolt in the truss element 15

$$\alpha_{space.4.15} := \operatorname{atan}\left(\frac{\left|SF1_{t.15}\right|}{\left|SF3_{t.15}\right|}\right) + 90° = 177.381 \cdot °$$

Maximum angle between horizontal axel and resultant force on the bolt in the truss element 18

$$\alpha_{space.4.18} := \operatorname{atan}\left(\frac{\left|SF1_{t.18}\right|}{\left|SF3_{t.18}\right|}\right) + 90° = 178.473 \cdot °$$

Maximum angle between horizontal axel and resultant force on the bolt in the truss element 21

$$\alpha_{space.4.21} := \operatorname{atan}\left(\frac{\left|SF1_{t.21}\right|}{\left|SF3_{t.21}\right|}\right) + 90° = 178.903 \cdot °$$

Maximum angle between horizontal axel and resultant force on the bolt in the truss element 24

$$\alpha_{space.4.24} := \operatorname{atan}\left(\frac{\left|SF1_{t.24}\right|}{\left|SF3_{t.24}\right|}\right) + 90° = 166.945 \cdot °$$

Minimum spacing between bolts in the direction of the grain

$$a_{1.truss.min} := \left(4 + \left|\cos\left(\alpha_{1.space}\right)\right|\right) \cdot d_{bolt.truss} = 100 \cdot mm$$

$$a_{1.truss.steel.min} := 2.2 \cdot d_{0.hole.truss} = 48.4 \cdot mm$$

$$a_{1.min} := \max\left(a_{1.truss.min}, a_{1.truss.steel.min}\right) = 100 \cdot mm$$

Minimum spacing between bolts perpendicular to the grain

$$a_{2.truss.min} := 4 \cdot d_{bolt.truss} = 80 \cdot mm$$

$$a_{2.truss.steel.min} := 2.4 \cdot d_{0.hole.truss} = 52.8 \cdot mm$$

$$a_{2.min} := \max\left(a_{2.truss.min}, a_{2.truss.steel.min}\right) = 80 \cdot mm$$

Minimum loaded end distance.

$$a_{3.truss.min.l} := \max\left(7 \cdot d_{bolt.truss}, 80mm\right) = 140 \cdot mm$$

Minimum unloaded end distance

$$a_{3.truss.min.un} := \max\left[\left(1 + 6 \cdot \sin\left(\alpha_{space.4.15}\right)\right) \cdot d_{bolt.truss}, 4 \cdot d_{bolt.truss}\right] = 80 \cdot mm$$

$$a_{3.truss.steel.min} := 1.2 \cdot d_{0.hole.truss} = 26.4 \cdot mm$$

Minimum distance of unloaded and loaded end distances

$$a_{3.min} := \max\left(a_{3.truss.min.l}, a_{3.truss.min.un}, a_{3.truss.steel.min}\right) = 140\cdot mm$$

Minimum loaded edge distance

$$a_{4.min.l.15} := \max\left[\left(2 + 2\cdot\sin\left(\alpha_{space.4.15}\right)\right)\cdot d_{bolt.truss}, 3\cdot d_{bolt.truss}\right] = 60\cdot mm$$

$$a_{4.min.l.18} := \max\left[\left(2 + 2\cdot\sin\left(\alpha_{space.4.18}\right)\right)\cdot d_{bolt.truss}, 3\cdot d_{bolt.truss}\right] = 60\cdot mm$$

$$a_{4.min.l.21} := \max\left[\left(2 + 2\cdot\sin\left(\alpha_{space.4.21}\right)\right)\cdot d_{bolt.truss}, 3\cdot d_{bolt.truss}\right] = 60\cdot mm$$

$$a_{4.min.l.24} := \max\left[\left(2 + 2\cdot\sin\left(\alpha_{space.4.24}\right)\right)\cdot d_{bolt.truss}, 3\cdot d_{bolt.truss}\right] = 60\cdot mm$$

$$a_{4.min.l} := \max\left(a_{4.min.l.15}, a_{4.min.l.18}, a_{4.min.l.21}, a_{4.min.l.24}\right) = 60\cdot mm$$

Minimum unloaded edge distance

$$a_{4.min.un} := 3\cdot d_{bolt.truss} = 60\cdot mm$$

$$a_{4.truss.steel.min} := 1.2\cdot d_{0.hole.truss} = 26.4\cdot mm$$

Minimum distance of unloaded and loaded edge distances

$$a_{4.min} := \max\left(a_{4.min.l}, a_{4.min.un}, a_{4.truss.steel.min}\right) = 60\cdot mm$$

Chosen spacing and distance values

$$a_{1.truss} := 100mm$$

$$a_{2.truss} := 85mm$$

$$a_{3.truss} := 80mm$$

$$a_{4.truss} := 70mm$$

Number of fastners per row

$$n_{bolts.row} := 8$$

Number of rows

$$n_{rows.truss} := 2$$

Total number of fasteners

$$n_{bolt.truss} := n_{bolts.row}\cdot n_{rows.truss} = 16$$

Number of shear planes

$$n_{shearplanes} := 2$$

$$e_{ext} := 3.5\cdot a_{1.truss} + a_{3.truss} = 430\cdot mm$$

$$t_{top.plate} := 5mm$$

$$b_{top.plate} := 140mm$$

$$l_{top.plate} := 500mm$$

$$l_{top.plate.ef} := l_{top.plate} + 2\cdot 30mm = 0.56\,m$$

Distance from rotational center to each bolt

$$x_{truss} := \begin{bmatrix} 3.5\cdot(a_{1.truss}) \\ 2.5\cdot(a_{1.truss}) \\ 1.5\cdot(a_{1.truss}) \\ 0.5\cdot(a_{1.truss}) \\ 0.5\cdot(-a_{1.truss}) \\ 1.5\cdot(-a_{1.truss}) \\ 2.5\cdot(-a_{1.truss}) \\ 3.5\cdot(-a_{1.truss}) \\ 3.5\cdot(-a_{1.truss}) \\ 2.5\cdot(-a_{1.truss}) \\ 1.5\cdot(-a_{1.truss}) \\ 0.5\cdot(-a_{1.truss}) \\ 0.5\cdot(a_{1.truss}) \\ 1.5\cdot(a_{1.truss}) \\ 2.5\cdot(a_{1.truss}) \\ 3.5\cdot(a_{1.truss}) \end{bmatrix} = \begin{bmatrix} 350 \\ 250 \\ 150 \\ 50 \\ -50 \\ -150 \\ -250 \\ -350 \\ -350 \\ -250 \\ -150 \\ -50 \\ 50 \\ 150 \\ 250 \\ 350 \end{bmatrix} \cdot mm$$

$$y_{truss} := \begin{bmatrix} 0.5(-a_{2.truss}) \\ 0.5(-a_{2.truss}) \\ 0.5(-a_{2.truss}) \\ 0.5(-a_{2.truss}) \\ 0.5(-a_{2.truss}) \\ 0.5(-a_{2.truss}) \\ 0.5(-a_{2.truss}) \\ 0.5(-a_{2.truss}) \\ 0.5(a_{2.truss}) \\ 0.5(a_{2.truss}) \\ 0.5(a_{2.truss}) \\ 0.5(a_{2.truss}) \\ 0.5(a_{2.truss}) \\ 0.5(a_{2.truss}) \\ 0.5(a_{2.truss}) \\ 0.5(a_{2.truss}) \end{bmatrix} = \begin{bmatrix} -42.5 \\ -42.5 \\ -42.5 \\ -42.5 \\ -42.5 \\ -42.5 \\ -42.5 \\ -42.5 \\ 42.5 \\ 42.5 \\ 42.5 \\ 42.5 \\ 42.5 \\ 42.5 \\ 42.5 \\ 42.5 \end{bmatrix} \cdot mm$$

$$z_{truss} := \begin{pmatrix} 0 \\ 0 \\ 0 \\ 0 \\ 0 \\ 0 \\ 0 \\ 0 \\ 0 \\ 0 \\ 0 \\ 0 \\ 0 \\ 0 \\ 0 \\ 0 \end{pmatrix} = \begin{bmatrix} 0 \\ 0 \\ 0 \\ 0 \\ 0 \\ 0 \\ 0 \\ 0 \\ 0 \\ 0 \\ 0 \\ 0 \\ 0 \\ 0 \\ 0 \\ 0 \end{bmatrix} \cdot mm$$

Polar moment of inertia

$$I_{p.xy.truss} := \sum_{i=0}^{n_{bolt.truss}-1} \left[\left(x_{truss_i} \right)^2 + \left(y_{truss_i} \right)^2 \right] = 8.689 \times 10^5 \cdot mm^2$$

$$I_{p.xz.truss} := \sum_{i=0}^{n_{bolt.truss}-1} \left[\left(x_{truss_i} \right)^2 + \left(z_{truss_i} \right)^2 \right] = 8.4 \times 10^5 \cdot mm^2$$

5.2.2 Resultant forces

Resultat forces of truss 15 acting in local coordinate system of connection node

$$x_{t.15.c.c} := SF1_{t.15} \cdot \cos\left(\alpha_{t.15.c.c.x}\right) = -116.414 \cdot kN$$

$$y_{t.15.c.c} := SF1_{t.15} \cdot \cos\left(\alpha_{t.15.c.c.y}\right) = 19.105 \cdot kN$$

$$z_{t.15.c.c} := SF1_{t.15} \cdot \cos\left(\alpha_{t.15.c.c.z}\right) = 70.701 \cdot kN$$

Resultat forces of truss 18 acting in local coordinate system of connection node

$$x_{t.18.c.c} := SF1_{t.18} \cdot \cos\left(\alpha_{t.18.c.c.x}\right) = -198.053 \cdot kN$$

$$y_{t.18.c.c} := SF1_{t.18} \cdot \cos\left(\alpha_{t.18.c.c.y}\right) = 36.534 \cdot kN$$

$$z_{t.18.c.c} := SF1_{t.18} \cdot \cos\left(\alpha_{t.18.c.c.z}\right) = -116.77 \cdot kN$$

Resultat forces of truss 21 acting in local coordinate system of connection node

$$x_{t.21.c.c} := SF1_{t.21} \cdot \cos\left(\alpha_{t.21.c.c.x}\right) = 265.289 \cdot kN$$

$$y_{t.21.c.c} := SF1_{t.21} \cdot \cos\left(\alpha_{t.21.c.c.y}\right) = -5.46 \cdot kN$$

$$z_{t.21.c.c} := SF1_{t.21} \cdot \cos\left(\alpha_{t.21.c.c.z}\right) = 165.771 \cdot kN$$

Resultat forces of truss 24 in local coordinate system of connection node

$$x_{t.24.c.c} := SF1_{t.24} \cdot \cos\left(\alpha_{t.24.c.c.x}\right) = 49.891 \cdot kN$$

$$y_{t.24.c.c} := SF1_{t.24} \cdot \cos\left(\alpha_{t.24.c.c.y}\right) = -3.602 \times 10^{-15} \cdot kN$$

$$z_{t.24.c.c} := SF1_{t.24} \cdot \cos\left(\alpha_{t.24.c.c.z}\right) = -31.175 \cdot kN$$

Load effect on bolts

Truss element 15

$$F_{x.truss.15} := \left[\frac{SF1_{t.15}}{n_{bolt.truss}} + \frac{SM2_{t.15} \cdot y_{truss}}{I_{p.xy.truss}} + \frac{\left(SF3_{t.15} \cdot e_{ext}\right) \cdot y_{truss}}{I_{p.xy.truss}} \right]$$

$$F_{x.truss.15.sum} := \sum_{i=0}^{n_{bolt.truss}-1} F_{x.truss.15_i} = -137.273 \cdot kN$$

$$F_{y.truss.15} := \left[\frac{SF3_{t.15}}{n_{bolt.truss}} + \left(\frac{SM2_{t.15} \cdot x_{truss}}{I_{p.xy.truss}} \right) + \frac{\left(SF3_{t.15} \cdot e_{ext}\right) \cdot x_{truss}}{I_{p.xy.truss}} \right]$$

$$F_{y.truss.15.sum} := \sum_{i=0}^{n_{bolt.truss}-1} F_{y.truss.15_i} = 6.28 \cdot kN$$

$$F_{z.truss.15} := \frac{SF2_{t.15}}{n_{bolt.truss}} + \frac{SM1_{t.15} \cdot z_{truss}}{I_{p.xz.truss}}$$

$$F_{z.truss.15.sum} := \sum_{i=0}^{n_{bolt.truss}-1} F_{z.truss.15_i} = -0.204 \cdot kN$$

Truss element 18

$$F_{x.truss.18} := \frac{SF1_{t.18}}{n_{bolt.truss}} + \left(\frac{SM2_{t.18} \cdot y_{truss}}{I_{p.xy.truss}} \right) + \frac{\left(SF3_{t.18} \cdot e_{ext}\right) \cdot y_{truss}}{I_{p.xy.truss}}$$

$$F_{x.truss.18.sum} := \sum_{i=0}^{n_{bolt.truss}-1} F_{x.truss.18_i} = -233.54 \cdot kN$$

$$F_{y.truss.18} := \frac{SF3_{t.18}}{n_{bolt.truss}} + \left(\frac{SM2_{t.18} \cdot x_{truss}}{I_{p.xy.truss}} \right) + \left[\frac{\left(SF3_{t.18} \cdot e_{ext}\right) \cdot x_{truss}}{I_{p.xy.truss}} \right]$$

$$F_{y.truss.18.sum} := \sum_{i=0}^{n_{bolt.truss}-1} F_{y.truss.18_i} = 6.225 \cdot kN$$

$$F_{z.truss.18} := \frac{SF2_{t.18}}{n_{bolt.truss}} + \frac{SM1_{t.18} \cdot z_{truss}}{I_{p.xz.truss}}$$

$$F_{z.truss.18.sum} := \sum_{i=0}^{n_{bolt.truss}-1} F_{z.truss.18_i} = 0.21 \cdot kN$$

Truss element 21

$$F_{x.truss.21} := \left[\frac{SF1_{t.21}}{n_{bolt.truss}} + \frac{SM2_{t.21} \cdot y_{truss}}{I_{p.xy.truss}} + \left[\frac{\left(SF3_{t.21} \cdot e_{ext}\right) \cdot y_{truss}}{I_{p.xy.truss}} \right] \right]$$

$$F_{x.truss.21.sum} := \sum_{i=0}^{n_{bolt.truss}-1} F_{x.truss.21_i} = -312.823 \cdot kN$$

$$F_{y.truss.21} := \frac{SF3_{t.21}}{n_{bolt.truss}} + \left(\frac{SM2_{t.21} \cdot x_{truss}}{I_{p.xy.truss}} \right) + \frac{\left(SF3_{t.21} \cdot e_{ext}\right) \cdot x_{truss}}{I_{p.xy.truss}}$$

$$F_{y.truss.21.sum} := \sum_{i=0}^{n_{bolt.truss}-1} F_{y.truss.21_i} = 5.988 \cdot kN$$

$$F_{z.truss.21} := \frac{SF2_{t.21}}{n_{bolt.truss}} + \frac{SM1_{t.21} \cdot z_{truss}}{I_{p.xz.truss}}$$

$$F_{z.truss.21.sum} := \sum_{i=0}^{n_{bolt.truss}-1} F_{z.truss.21_i} = 0.17 \cdot kN$$

Truss element 24

$$F_{x.truss.24} := \left[\frac{SF1_{t.24}}{n_{bolt.truss}} + \left(\frac{SM2_{t.24} \cdot y_{truss}}{I_{p.xy.truss}} \right) + \left[\frac{\left(SF3_{t.24} \cdot e_{ext}\right) \cdot y_{truss}}{I_{p.xy.truss}} \right] \right]$$

$$F_{x.truss.24.sum} := \sum_{i=0}^{n_{bolt.truss}-1} F_{x.truss.24_i} = -58.83 \cdot kN$$

$$F_{y.truss.24} := \frac{SF3_{t.24}}{n_{bolt.truss}} + \left(\frac{SM2_{t.24} \cdot x_{truss}}{I_{p.xy.truss}} \right) + \frac{\left(SF3_{t.24} \cdot e_{ext}\right) \cdot x_{truss}}{I_{p.xy.truss}}$$

$$F_{y.truss.24.sum} := \sum_{i=0}^{n_{bolt.truss}-1} F_{y.truss.24_i} = 13.642 \cdot kN$$

$$F_{z.truss.24} := \frac{SF2_{t.24}}{n_{bolt.truss}} + \frac{SM1_{t.24} \cdot z_{truss}}{I_{p.xz.truss}}$$

$$F_{z.truss.24.sum} := \sum_{i=0}^{n_{bolt.truss}-1} F_{z.truss.24_i} = 0.462 \cdot kN$$

5.2.3 Shear resistance of connection

Thickness of wood on each side of plate

$$t_{1.truss} := \frac{t_{rooftruss} - \left(t_{slot.plate}\right)}{2} = 0.075\,m$$

Shear resistance per fastener per shear plane

$$F_{v.Rk.slot.1} := f_{h.90.k.truss} \cdot t_{1.truss} \cdot d_{bolt.truss} = 25.644 \cdot kN$$

$$F_{v.Rk.slot.2} := f_{h.90.k.truss} \cdot t_{1.truss} \cdot d_{bolt.truss} \cdot \left(\sqrt{2 + \frac{4 \cdot M_{y.Rk.bolt.truss}}{f_{h.90.k.truss} \cdot d_{bolt.truss} \cdot t_{1.truss}^{2}}} - 1 \right) = 22.372 \cdot kN$$

$$F_{v.Rk.slot.3} := 2.3 \cdot \sqrt{M_{y.Rk.bolt.truss} \cdot f_{h.90.k.truss} \cdot d_{bolt.truss}} = 36.19 \cdot kN$$

$$F_{v.Rk.slot.basic} := \min\left(F_{v.Rk.slot.1}, F_{v.Rk.slot.2}, F_{v.Rk.slot.3}\right) = 22.372 \cdot kN$$

$$failuremode_{truss} := \begin{cases} \text{"Mode f"} & \text{if } F_{v.Rk.slot.basic} = F_{v.Rk.slot.1} \\ \text{"Mode g"} & \text{if } F_{v.Rk.slot.basic} = F_{v.Rk.slot.2} \\ \text{"Mode h"} & \text{if } F_{v.Rk.slot.basic} = F_{v.Rk.slot.3} \end{cases} = \text{"Mode g"}$$

5.2.3.1 Longitudinally

Group effect for one row of fasteners

$$n_{ef.truss.l} := \min\left(n_{bolts.row}, n_{bolts.row}^{0.9} \cdot \sqrt[4]{\frac{a_{1.truss}}{13 \cdot d_{bolt.truss}}} \right) = 5.117$$

Total shear resistance of fasteners

$$F_{v.ef.Rk.l} := F_{v.Rk.slot.basic} \cdot n_{ef.truss.l} \cdot n_{rows.truss} \cdot n_{shearplanes} = 457.937 \cdot kN$$

Controll of shear capacity

$$\text{if}\left(F_{v.ef.Rk.l} > \left|F_{x.truss.15.sum}\right|, \text{"ok"}, \text{"not ok"}\right) = \text{"ok"}$$

$$\text{if}\left(F_{v.ef.Rk.l} > \left|F_{x.truss.18.sum}\right|, \text{"ok"}, \text{"not ok"}\right) = \text{"ok"}$$

$$\text{if}\left(F_{v.ef.Rk.l} > \left|F_{x.truss.21.sum}\right|, \text{"ok"}, \text{"not ok"}\right) = \text{"ok"}$$

$$\text{if}\left(F_{v.ef.Rk.l} > \left|F_{x.truss.24.sum}\right|, \text{"ok"}, \text{"not ok"}\right) = \text{"ok"}$$

Utilization ratios

$$\frac{F_{x.truss.15.sum}}{F_{v.ef.Rk.l}} = -0.3 \qquad \frac{F_{x.truss.18.sum}}{F_{v.ef.Rk.l}} = -0.51$$

$$\frac{F_{x.truss.21.sum}}{F_{v.ef.Rk.l}} = -0.683 \qquad \frac{F_{x.truss.24.sum}}{F_{v.ef.Rk.l}} = -0.128$$

5.2.3.2 Transversally

Group effect for one row of fasteners

$$n_{ef.truss.t} := \min\left(n_{bolts.row}, n_{bolts.row}^{0.9} \cdot \sqrt[4]{\frac{a_{2.truss}}{13 \cdot d_{bolt.truss}}}\right) = 4.914$$

Total shear resistance of fasteners

$$F_{v.ef.Rk.t} := F_{v.Rk.slot.basic} \cdot n_{ef.truss.t} \cdot n_{rows.truss} \cdot n_{shearplanes} = 439.704 \cdot kN$$

Controll of shear capacity

$$\text{if}\left(F_{v.ef.Rk.t} > \left|F_{y.truss.15.sum}\right|, \text{"ok"}, \text{"not ok"}\right) = \text{"ok"}$$

$$\text{if}\left(F_{v.ef.Rk.t} > \left|F_{y.truss.18.sum}\right|, \text{"ok"}, \text{"not ok"}\right) = \text{"ok"}$$

$$\text{if}\left(F_{v.ef.Rk.t} > \left|F_{y.truss.21.sum}\right|, \text{"ok"}, \text{"not ok"}\right) = \text{"ok"}$$

$$\text{if}\left(F_{v.ef.Rk.t} > \left|F_{y.truss.24.sum}\right|, \text{"ok"}, \text{"not ok"}\right) = \text{"ok"}$$

Utilization ratios

$$\frac{F_{y.truss.15.sum}}{F_{v.ef.Rk.t}} = 0.014 \qquad \frac{F_{y.truss.18.sum}}{F_{v.ef.Rk.t}} = 0.014$$

$$\frac{F_{y.truss.21.sum}}{F_{v.ef.Rk.t}} = 0.014 \qquad \frac{F_{y.truss.24.sum}}{F_{v.ef.Rk.t}} = 0.031$$

5.2.4 Shear resistance of bolt

Load at each bolt

$$R_{tot.xy.15} := \sqrt{\left(F_{x.truss.15}\right)^2 + \left(F_{y.truss.15}\right)^2}$$

$$R_{tot.xy.18} := \sqrt{\left(F_{x.truss.18}\right)^2 + \left(F_{y.truss.18}\right)^2}$$

$$R_{tot.xy.21} := \sqrt{\left(F_{x.truss.21}\right)^2 + \left(F_{y.truss.21}\right)^2}$$

$$R_{tot.xy.24} := \sqrt{\left(F_{x.truss.24}\right)^2 + \left(F_{y.truss.24}\right)^2}$$

$$R_{tot.z.15} := \sqrt{\left(F_{z.truss.15}\right)^2}$$

$$R_{tot.z.18} := \sqrt{\left(F_{z.truss.18}\right)^2}$$

$$R_{tot.z.21} := \sqrt{\left(F_{z.truss.21}\right)^2}$$

$$R_{tot.z.24} := \sqrt{\left(F_{z.truss.24}\right)^2}$$

$$F_{v.Ed.bolt.truss.15} := \max\left(R_{tot.xy.15}\right) = 8.729 \cdot kN$$

$$F_{v.Ed.bolt.truss.18} := \max\left(R_{tot.xy.18}\right) = 14.825 \cdot kN$$

$$F_{v.Ed.bolt.truss.21} := \max\left(R_{tot.xy.21}\right) = 19.697 \cdot kN$$

$$F_{v.Ed.bolt.truss.24} := \max\left(R_{tot.xy.24}\right) = 5.235 \cdot kN$$

$$F_{t.Ed.bolt.truss.15} := \max\left(R_{tot.z.15}\right) = 0.013 \cdot kN$$

$$F_{t.Ed.bolt.truss.18} := \max\left(R_{tot.z.18}\right) = 0.013 \cdot kN$$

$$F_{t.Ed.bolt.truss.21} := \max\left(R_{tot.z.21}\right) = 0.011 \cdot kN$$

$$F_{t.Ed.bolt.truss.24} := \max\left(R_{tot.z.24}\right) = 0.029 \cdot kN$$

Shear stress in most loaded bolt

$$\tau_{bolt.truss.15} := \frac{F_{v.Ed.bolt.truss.15} \cdot 4}{\pi \cdot d_{bolt.truss}^{2}} = 27.785 \cdot MPa$$

$$\tau_{bolt.truss.18} := \frac{F_{v.Ed.bolt.truss.18} \cdot 4}{\pi \cdot d_{bolt.truss}^{2}} = 47.19 \cdot MPa$$

$$\tau_{bolt.truss.21} := \frac{F_{v.Ed.bolt.truss.21} \cdot 4}{\pi \cdot d_{bolt.truss}^{2}} = 62.696 \cdot MPa$$

$$\tau_{bolt.truss.24} := \frac{F_{v.Ed.bolt.truss.24} \cdot 4}{\pi \cdot d_{bolt.truss}^{2}} = 16.663 \cdot MPa$$

Controll of shear stress

$$\text{if}\left(\tau_{bolt.truss.15} \le \tau_{s.Rk.bolt.truss}, \text{"ok"}, \text{"not ok"}\right) = \text{"ok"}$$

$$\text{if}\left(\tau_{bolt.truss.18} \le \tau_{s.Rk.bolt.truss}, \text{"ok"}, \text{"not ok"}\right) = \text{"ok"}$$

$$\text{if}\left(\tau_{bolt.truss.21} \le \tau_{s.Rk.bolt.truss}, \text{"ok"}, \text{"not ok"}\right) = \text{"ok"}$$

$$\text{if}\left(\tau_{bolt.truss.24} \le \tau_{s.Rk.bolt.truss}, \text{"ok"}, \text{"not ok"}\right) = \text{"ok"}$$

Utilization ratios

$$\frac{\tau_{bolt.truss.15}}{\tau_{s.Rk.bolt.truss}} = 0.048 \qquad \frac{\tau_{bolt.truss.18}}{\tau_{s.Rk.bolt.truss}} = 0.082$$

$$\frac{\tau_{bolt.truss.21}}{\tau_{s.Rk.bolt.truss}} = 0.109 \qquad \frac{\tau_{bolt.truss.24}}{\tau_{s.Rk.bolt.truss}} = 0.029$$

Shear failure in bolt

$$\alpha_{v.truss} := 0.6$$

$$F_{v.Rd.bolt.truss} := \frac{\alpha_{v.truss} \cdot f_{u.k.bolt.truss} \cdot \pi \left(\frac{d_{bolt.truss}}{2} \right)^2}{\gamma_{M.cap}} = 150.796 \cdot kN$$

Controll of shear force

$$if\left(F_{v.Ed.bolt.truss.15} \le F_{v.Rd.bolt.truss}, "ok", "not ok"\right) = "ok"$$

$$if\left(F_{v.Ed.bolt.truss.18} \le F_{v.Rd.bolt.truss}, "ok", "not ok"\right) = "ok"$$

$$if\left(F_{v.Ed.bolt.truss.21} \le F_{v.Rd.bolt.truss}, "ok", "not ok"\right) = "ok"$$

$$if\left(F_{v.Ed.bolt.truss.24} \le F_{v.Rd.bolt.truss}, "ok", "not ok"\right) = "ok"$$

Utilization ratios

$$\frac{F_{v.Ed.bolt.truss.15}}{F_{v.Rd.bolt.truss}} = 0.058 \qquad \frac{F_{v.Ed.bolt.truss.18}}{F_{v.Rd.bolt.truss}} = 0.098$$

$$\frac{F_{v.Ed.bolt.truss.21}}{F_{v.Rd.bolt.truss}} = 0.131 \qquad \frac{F_{v.Ed.bolt.truss.24}}{F_{v.Rd.bolt.truss}} = 0.035$$

5.2.5 Block and plug shear failure

Spacing and end distances

$$l_v := \begin{pmatrix} 140mm \\ 100mm \\ 100mm \\ 100mm \\ 100mm \\ 100mm \\ 100mm \\ 100mm \end{pmatrix} \qquad l_t := (85mm)$$

Total net length of the shear fracture area

Extracting position in vectors

$$pos_{lv} := rows\left(l_v\right) - 1 = 7$$

$$L_{net.v} := 2\left(\sum_{i=0}^{pos_{lv}} l_{v_i} \right) = 1.68\,m$$

Net width of the cross-section perpendicular to the grain

Extracting position in vectors

$$pos_{lt} := rows\left(l_t\right) - 1 = 0$$

$$L_{net.t} := \sum_{i=0}^{pos_{lt}} l_{t_i} = 0.085\,m$$

Effective depth depending of the failure mode of the fastener

$$t_{ef.thin} := \begin{cases} 0.4 \cdot t_{1.truss} & \text{if } failuremode_{truss} = \text{"Mode a"} \\ 1.4 \sqrt{\dfrac{M_{y.Rk.bolt.truss}}{f_{h.90.k.truss} \cdot d_{bolt.truss}}} & \text{if } failuremode_{truss} = \text{"Mode b"} \\ 0 & \text{otherwise} \end{cases} = 0$$

$$t_{ef.thick} := \begin{cases} 2 \sqrt{\dfrac{M_{y.Rk.bolt.truss}}{f_{h.90.k.truss} \cdot d_{bolt.truss}}} & \text{if } failuremode_{truss} = \text{"Mode d"} \\ 2 \sqrt{\dfrac{M_{y.Rk.bolt.truss}}{f_{h.90.k.truss} \cdot d_{bolt.truss}}} & \text{if } failuremode_{truss} = \text{"Mode h"} \\ t_{1.truss} \cdot \left(\sqrt{2 + \dfrac{M_{y.Rk.bolt.truss}}{f_{h.90.k.truss} \cdot d_{bolt.truss} \cdot t_{1.truss}^{2}}} - 1 \right) & \text{if } failuremode_{truss} = \text{"Mode c"} \\ t_{1.truss} \cdot \left(\sqrt{2 + \dfrac{M_{y.Rk.bolt.truss}}{f_{h.90.k.truss} \cdot d_{bolt.truss} \cdot t_{1.truss}^{2}}} - 1 \right) & \text{if } failuremode_{truss} = \text{"Mode g"} \\ 0 & \text{otherwise} \end{cases}$$

$t_{ef.thick} = 0.088\,\text{m}$

$$t_{ef} := \begin{cases} t_{ef.thin} & \text{if } platethickness_{slot} = \text{"thin"} \quad = 0.088 \\ t_{ef.thick} & \text{if } platethickness_{slot} = \text{"thick"} \\ \text{"linear interpolation"} & \text{otherwise} \end{cases}$$

Net cross-sectional area perpendicular to grain

$A_{net.t} := L_{net.t} \cdot t_{1.truss} = 6.375 \times 10^{-3}\,\text{m}^2$

$$A_{net.v} := \begin{cases} L_{net.v} \cdot t_{1.truss} & \text{if } failuremode_{truss} = \text{"Mode e"} \quad = 0.219 \\ L_{net.v} \cdot t_{1.truss} & \text{if } failuremode_{truss} = \text{"f"} \\ L_{net.v} \cdot t_{1.truss} & \text{if } failuremode_{truss} = \text{"j"} \\ L_{net.v} \cdot t_{1.truss} & \text{if } failuremode_{truss} = \text{"k"} \\ L_{net.v} \cdot t_{1.truss} & \text{if } failuremode_{truss} = \text{"m"} \\ \dfrac{L_{net.v}}{2} \cdot \left(L_{net.t} + 2 \cdot t_{ef} \right) & \text{otherwise} \end{cases}$$

Charachteristic block shear or plug shear capacity

$$F_{bs.Rk} := \max\left(1.5 \cdot A_{net.t} \cdot f_{t.0.g.k}, 0.7 \cdot A_{net.v} \cdot f_{v.g.k} \right) = 537.109 \cdot \text{kN}$$

Controll of block shear capacity

$$\text{if}\left(F_{bs.Rk} > \left|F_{x.truss.15.sum}\right|, \text{"ok"}, \text{"not ok"}\right) = \text{"ok"}$$

$$\text{if}\left(F_{bs.Rk} > \left|F_{x.truss.18.sum}\right|, \text{"ok"}, \text{"not ok"}\right) = \text{"ok"}$$

$$\text{if}\left(F_{bs.Rk} > \left|F_{x.truss.21.sum}\right|, \text{"ok"}, \text{"not ok"}\right) = \text{"ok"}$$

$$\text{if}\left(F_{bs.Rk} > \left|F_{x.truss.24.sum}\right|, \text{"ok"}, \text{"not ok"}\right) = \text{"ok"}$$

Utilization ratios

$$\frac{\left|F_{x.truss.15.sum}\right|}{F_{bs.Rk}} = 0.256 \qquad \frac{\left|F_{x.truss.18.sum}\right|}{F_{bs.Rk}} = 0.435$$

$$\frac{\left|F_{x.truss.21.sum}\right|}{F_{bs.Rk}} = 0.582 \qquad \frac{\left|F_{x.truss.24.sum}\right|}{F_{bs.Rk}} = 0.11$$

5.2.6 Embedding strength of plate

Capacity of steel plate

For failure between hole and end of plate

$$\alpha_{d.end.truss.SF1} := \frac{a_{3.truss}}{3 \cdot d_{0.hole.truss}} = 1.212$$

$$\alpha_{b.end.truss.SF1} := \min\left(\alpha_{d.end.truss.SF1}, \frac{f_{u.k.bolt.truss}}{f_{u.plate}}, 1\right) = 1$$

$$k_{1.end.truss.SF1} := \min\left(2.8 \cdot \frac{a_{4.truss}}{d_{0.hole.truss}} - 1.7, 2.5\right) = 2.5$$

$$F_{b.Rd.end.truss.SF1} := \frac{k_{1.end.truss.SF1} \cdot \alpha_{b.end.truss.SF1} \cdot f_{u.plate} \cdot d_{bolt.truss} \cdot t_{slot.plate}}{\gamma_{M.cap}} = 344 \cdot kN$$

For failure between two holes

$$\alpha_{d.hole.truss.SF1} := \frac{a_{1.truss}}{3 \cdot d_{0.hole.truss}} - \frac{1}{4} = 1.265$$

$$k_{1.hole.truss.SF1} := \min\left(1.4 \cdot \frac{a_{2.truss}}{d_{0.hole.truss}} - 1.7, 2.5\right) = 2.5$$

$$\alpha_{b.hole.truss.SF1} := \min\left(\alpha_{d.hole.truss.SF1}, \frac{f_{u.k.bolt.truss}}{f_{u.plate}}, 1\right) = 1$$

$$F_{b.Rd.hole.truss.SF1} := \frac{k_{1.hole.truss.SF1} \cdot \alpha_{b.hole.truss.SF1} \cdot f_{u.plate} \cdot d_{bolt.truss} \cdot t_{slot.plate}}{\gamma_{M.cap}} = 344 \cdot kN$$

Minimum capacity of steel plate

$$F_{b.Rd.plate.truss.SF1} := \min\left(F_{b.Rd.end.truss.SF1}, F_{b.Rd.hole.truss.SF1}\right) = 344 \cdot kN$$

Controll of plate capacity

$$\text{if}\left(F_{v.Ed.bolt.truss.15} \le F_{b.Rd.plate.truss.SF1}, \text{"ok"}, \text{"not ok"}\right) = \text{"ok"}$$

$$\text{if}\left(F_{v.Ed.bolt.truss.18} \le F_{b.Rd.plate.truss.SF1}, \text{"ok"}, \text{"not ok"}\right) = \text{"ok"}$$

$$\text{if}\left(F_{v.Ed.bolt.truss.21} \le F_{b.Rd.plate.truss.SF1}, \text{"ok"}, \text{"not ok"}\right) = \text{"ok"}$$

$$\text{if}\left(F_{v.Ed.bolt.truss.24} \le F_{b.Rd.plate.truss.SF1}, \text{"ok"}, \text{"not ok"}\right) = \text{"ok"}$$

Utilization ratios

$$\frac{F_{v.Ed.bolt.truss.15}}{F_{b.Rd.plate.truss.SF1}} = 0.025 \qquad \frac{F_{v.Ed.bolt.truss.18}}{F_{b.Rd.plate.truss.SF1}} = 0.043$$

$$\frac{F_{v.Ed.bolt.truss.21}}{F_{b.Rd.plate.truss.SF1}} = 0.057 \qquad \frac{F_{v.Ed.bolt.truss.24}}{F_{b.Rd.plate.truss.SF1}} = 0.015$$

5.2.7 Shear failure mode

$$F_{v.Rd.truss} := \min\left(F_{v.Rd.bolt.truss}, F_{b.Rd.plate.truss.SF1}\right) = 150.796 \cdot kN$$

$$\text{if}\left(F_{v.Rd.truss} = F_{v.Rd.bolt.truss}, \text{"Shear failure bolt"}, \text{"Embedding failure plate"}\right) = \text{"Shear failure bolt"}$$

5.2.8 Withdrawal of bolts

Tensile capacity of one bolt

Reduction factor considering bending

$$k_2 := 0.9$$

Stressed area of bolt

$$A_s := 1.28 \cdot \frac{\pi \cdot d_{bolt.truss}^2}{4} = 402.124 \cdot mm^2$$

Tensile capacity of one bolt

$$F_{t.Rd.bolt.truss} := \frac{k_2 \cdot f_{u.k.bolt.truss} \cdot A_s}{\gamma_{M.cap}} = 289.529 \cdot kN$$

Controll of withdrawal capacity

$$\text{if}\left(F_{t.Ed.bolt.truss.15} \le F_{t.Rd.bolt.truss}, \text{"ok"}, \text{"not ok"}\right) = \text{"ok"}$$

$$\text{if}\left(F_{t.Ed.bolt.truss.18} \le F_{t.Rd.bolt.truss}, \text{"ok"}, \text{"not ok"}\right) = \text{"ok"}$$

$$\text{if}\left(F_{t.Ed.bolt.truss.21} \le F_{t.Rd.bolt.truss}, \text{"ok"}, \text{"not ok"}\right) = \text{"ok"}$$

$$\text{if}\left(F_{t.Ed.bolt.truss.24} \le F_{t.Rd.bolt.truss}, \text{"ok"}, \text{"not ok"}\right) = \text{"ok"}$$

Utilization ratios

$$\frac{F_{t.Ed.bolt.truss.15}}{F_{t.Rd.bolt.truss}} = 4.393 \times 10^{-5} \qquad \frac{F_{t.Ed.bolt.truss.18}}{F_{t.Rd.bolt.truss}} = 4.536 \times 10^{-5}$$

$$\frac{F_{t.Ed.bolt.truss.21}}{F_{t.Rd.bolt.truss}} = 3.664 \times 10^{-5} \qquad \frac{F_{t.Ed.bolt.truss.24}}{F_{t.Rd.bolt.truss}} = 9.965 \times 10^{-5}$$

5.2.9 Combination of normal and shear force

Controll of combined axial and shear loading

$$\text{if}\left(\frac{F_{v.Ed.bolt.truss.15}}{F_{v.Rd.bolt.truss}} + \frac{F_{t.Ed.bolt.truss.15}}{1.4 \cdot F_{t.Rd.bolt.truss}} \le 1, \text{"ok"}, \text{"not ok"}\right) = \text{"ok"}$$

$$\text{if}\left(\frac{F_{v.Ed.bolt.truss.18}}{F_{v.Rd.bolt.truss}} + \frac{F_{t.Ed.bolt.truss.18}}{1.4 \cdot F_{t.Rd.bolt.truss}} \le 1, \text{"ok"}, \text{"not ok"}\right) = \text{"ok"}$$

$$\text{if}\left(\frac{F_{v.Ed.bolt.truss.21}}{F_{v.Rd.bolt.truss}} + \frac{F_{t.Ed.bolt.truss.21}}{1.4 \cdot F_{t.Rd.bolt.truss}} \le 1, \text{"ok"}, \text{"not ok"}\right) = \text{"ok"}$$

$$\text{if}\left(\frac{F_{v.Ed.bolt.truss.24}}{F_{v.Rd.bolt.truss}} + \frac{F_{t.Ed.bolt.truss.24}}{1.4 \cdot F_{t.Rd.bolt.truss}} \le 1, \text{"ok"}, \text{"not ok"}\right) = \text{"ok"}$$

Utilization ratio

$$\frac{F_{v.Ed.bolt.truss.15}}{F_{v.Rd.bolt.truss}} + \frac{F_{t.Ed.bolt.truss.15}}{1.4 \cdot F_{t.Rd.bolt.truss}} = 0.058$$

$$\frac{F_{v.Ed.bolt.truss.18}}{F_{v.Rd.bolt.truss}} + \frac{F_{t.Ed.bolt.truss.18}}{1.4 \cdot F_{t.Rd.bolt.truss}} = 0.098$$

$$\frac{F_{v.Ed.bolt.truss.21}}{F_{v.Rd.bolt.truss}} + \frac{F_{t.Ed.bolt.truss.21}}{1.4 \cdot F_{t.Rd.bolt.truss}} = 0.131$$

$$\frac{F_{v.Ed.bolt.truss.24}}{F_{v.Rd.bolt.truss}} + \frac{F_{t.Ed.bolt.truss.24}}{1.4 \cdot F_{t.Rd.bolt.truss}} = 0.035$$

5.2.10 Translational and rotational stiffness

The translational and rotational spring stiffnesses are calculated for SLS

Translational stiffness

$$K_{t.ser.truss} := \frac{\left(\frac{\rho_{g.mean}}{\frac{kg}{m^3}}\right)^{1.5} \cdot \frac{d_{bolt.truss}}{mm}}{23} \cdot n_{shearplanes} \cdot \frac{N}{mm} = 1.551 \times 10^{4} \cdot \frac{N}{mm}$$

Rotational stiffness

$$K_{\theta.ser.truss} := K_{t.ser.truss} \cdot I_{p.xy.truss} = 1.347 \times 10^{7} \cdot \frac{N \cdot m}{rad}$$

5.3 Curved connection

5.3.1 Geometry

Minumum spacing and edge and end distances for timber parts

Spacing between fasteners parallel to grain

$\alpha_{parallel} := 0°$

$a_{1.timber.min} := 4mm + \left|\cos\left(\alpha_{parallel}\right)\right| \cdot d_{bolt.curved} = 16 \cdot mm$

$a_{1.steel.min} := 2.2 \cdot d_{0.hole.curved} = 28.6 \cdot mm$

$a_{1.curved.min} := \max\left(a_{1.timber.min}, a_{1.steel.min}\right) = 28.6 \cdot mm$

Spacing between fastners perpendicular to grain

$a_{2.timber.min} := 4 \cdot d_{bolt.curved} = 48 \cdot mm$

$a_{2.steel.min} := 2.4 \cdot d_{0.hole.curved} = 31.2 \cdot mm$

$a_{2.curved.min} := \max\left(a_{2.timber.min}, a_{2.steel.min}\right) = 48 \cdot mm$

Distance to loaded end

$a_{3.t.curved.timber.min} := \max\left(7 \cdot d_{bolt.curved}, 80mm\right) = 84 \cdot mm$

Distance to unloaded end

$a_{3.c.curved.timber.min} := 4 \cdot d_{bolt.curved} = 48 \cdot mm$

For steel, distance to both unloaded and loaded end

$a_{3.curved.steel.min} := 1.2 \cdot d_{0.hole.curved} = 15.6 \cdot mm$

Distance to loaded edge

$\alpha_{edge.curved} := 180°$

$a_{4.t.curved.timber.min} := \max\left(2mm + 2 \cdot \sin\left(\alpha_{edge.curved}\right) \cdot d_{bolt.curved}, 3 \cdot d_{bolt.curved}\right) = 36 \cdot mm$

Distance to unloaded edge

$a_{4.c.curved.timber.min} := 3 \cdot d_{bolt.curved} = 36 \cdot mm$

For steel, distance to both unloaded and loaded edge

$a_{4.curved.steel.min} := 1.2 \cdot d_{0.hole.curved} = 15.6 \cdot mm$

Maximum spacing and edge and end distances for steel plates

Spacing between fasteners parallel to grain

$a_{1.curved.steel.max} := \min\left(14 \cdot t_{curved.plate}, 200mm\right) = 168 \cdot mm$

Spacing between fastners perpendicular to grain

$a_{2.curved.steel.max} := \min\left(14 \cdot t_{curved.plate}, 200mm\right) = 168 \cdot mm$

Distance to both unloaded and loaded end

$a_{3.curved.steel.max} := 40mm + 4 \cdot t_{curved.plate} = 88 \cdot mm$

Distance to both unloaded and loaded edge

$a_{4.curved.steel.max} := 40mm + 4 \cdot t_{curved.plate} = 88 \cdot mm$

Design of connection (chosen values)

Number of bolts per row $n_{bolts.curved.row} := 4$

Number of rows $n_{rows.curved} := 4$

Total number of fasteners $n_{bolts.curved.tot} := n_{bolts.curved.row} \cdot n_{rows.curved} = 16$

Number of shear planes $n_{shearplanes.curved} := 2$

Thickness of slotted-in plate $t_{slot.plate} = 20\,mm$

Minimmum distance between outer stiffeners $l_{plate.stiffeners} := 2 \cdot (260mm + t_{slot.plate}) = 560 \cdot mm$

Margin from stiffener to first bolt (assumed) $a_{margin} := 30mm$

Spacings and end/edge distances $a_{1.curved} := 30mm$ $a_{2.curved} := 50mm$

$a_{3.curved.steel} := 20mm$ $a_{4.curved.steel} := 40mm$

Length of plate

$$l_{plate.curved} := \begin{bmatrix} l_{plate.stiffeners} + 2a_{margin} \cdots \\ + a_{1.curved} \cdot (n_{bolts.curved.row} - 2) + 2a_{3.curved.steel} \end{bmatrix} = 720 \cdot mm$$

Length of shorter part of curved beam $l_{curved.short} := 1660mm$

Maximum length of plate $l_{plate.curved.max} := 2 \cdot \frac{l_{curved.short}}{2} = 1.66 \times 10^3 \cdot mm$

The plate must be larger than the following value in order to fit the slotted-in plate from the truss elements.

Height of plate

$$h_{plate.curved} := 2a_{4.curved.steel} + a_{2.curved} \cdot (n_{rows.curved} - 1) = 230 \cdot mm$$

The height of the plate is restricted to the following value due to the curvature of the curved beam. It is also dependant on the length of the plate.

Maximum height of plate $h_{plate.curved.max} := 266mm$

End distance for timber member $a_{3.curved.timber} := 830mm$

Edge distance for timber member

$$a_{4.curved.timber} := \frac{h_{curved} - a_{2.curved} \cdot (n_{rows.curved} - 1)}{2} = 60 \cdot mm$$

Checks of minimum and maximum spacing and end/edge distances

$$\text{if}\left(a_{1.curved.min} \le a_{1.curved} \le a_{1.curved.steel.max}, \text{"ok"}, \text{"not ok"}\right) = \text{"ok"}$$

$$\text{if}\left(a_{2.curved.min} \le a_{2.curved} \le a_{2.curved.steel.max}, \text{"ok"}, \text{"not ok"}\right) = \text{"ok"}$$

$$\text{if}\left(a_{3.curved.steel.min} \le a_{3.curved.steel} \le a_{3.curved.steel.max}, \text{"ok"}, \text{"not ok"}\right) = \text{"ok"}$$

$$\text{if}\left(\max\left(a_{3.t.curved.timber.min}, a_{3.c.curved.timber.min}\right) \le a_{3.curved.timber}, \text{"ok"}, \text{"not ok"}\right) = \text{"ok"}$$

$$\text{if}\left(a_{4.curved.steel.min} \le a_{4.curved.steel} \le a_{4.curved.steel.max}, \text{"ok"}, \text{"not ok"}\right) = \text{"ok"}$$

$$\text{if}\left(\max\left(a_{4.t.curved.timber.min}, a_{4.c.curved.timber.min}\right) \le a_{4.curved.timber}, \text{"ok"}, \text{"not ok"}\right) = \text{"ok"}$$

$$\text{if}\left[\left(h_{plate.curved} \le h_{plate.curved.max}\right), \text{"ok"}, \text{"not ok"}\right] = \text{"ok"}$$

$$\text{if}\left(l_{plate.curved} \le l_{plate.curved.max}, \text{"ok"}, \text{"not ok"}\right) = \text{"ok"}$$

Distance from rotational center to each bolt

$$z_{curved.first} := \frac{l_{plate.stiffeners}}{2} + a_{margin} = 310 \cdot mm$$

$$z_{curved.second} := z_{curved.first} + a_{1.curved} = 340 \cdot mm$$

$$z_{curved.third} := z_{curved.second} + a_{1.curved} = 370 \cdot mm$$

$$z_{curved.fourth} := z_{curved.third} + a_{1.curved} = 400 \cdot mm$$

$$y_{curved} := \begin{pmatrix} 1.5 \cdot a_{2.curved} \\ 0.5 \cdot a_{2.curved} \\ -0.5 \cdot a_{2.curved} \\ -1.5 \cdot a_{2.curved} \\ 1.5 \cdot a_{2.curved} \\ 0.5 \cdot a_{2.curved} \\ -0.5 \cdot a_{2.curved} \\ -1.5 \cdot a_{2.curved} \\ 1.5 \cdot a_{2.curved} \\ 0.5 \cdot a_{2.curved} \\ -0.5 \cdot a_{2.curved} \\ -1.5 \cdot a_{2.curved} \\ 1.5 \cdot a_{2.curved} \\ 0.5 \cdot a_{2.curved} \\ -0.5 \cdot a_{2.curved} \\ -1.5 \cdot a_{2.curved} \end{pmatrix} = \begin{pmatrix} 75 \\ 25 \\ -25 \\ -75 \\ 75 \\ 25 \\ -25 \\ -75 \\ 75 \\ 25 \\ -25 \\ -75 \\ 75 \\ 25 \\ -25 \\ -75 \end{pmatrix} \cdot mm \qquad z_{curved} := \begin{pmatrix} -z_{curved.first} \\ -z_{curved.first} \\ -z_{curved.first} \\ -z_{curved.first} \\ z_{curved.first} \\ z_{curved.first} \\ z_{curved.first} \\ z_{curved.first} \\ -z_{curved.second} \\ -z_{curved.second} \\ -z_{curved.second} \\ -z_{curved.second} \\ z_{curved.second} \\ z_{curved.second} \\ z_{curved.second} \\ z_{curved.second} \end{pmatrix} = \begin{pmatrix} -310 \\ -310 \\ -310 \\ -310 \\ 310 \\ 310 \\ 310 \\ 310 \\ -340 \\ -340 \\ -340 \\ -340 \\ 340 \\ 340 \\ 340 \\ 340 \end{pmatrix} \cdot mm$$

Polar moment of inertia

$$I_{p.curved.YZ} := \sum_{i=0}^{n_{bolts.curved.tot}-1} \left[\left(y_{curved_i} \right)^2 + \left(z_{curved_i} \right)^2 \right] = 1.744 \times 10^6 \cdot mm^2$$

5.3.2 Resultant forces

Resultant forces and moment rotated to act in the local coordinate system of the connection (cloc).

Forces

$$R_{x.curved.F.cloc.x} := \left| SF1_{c.136.145} \cdot \cos\left(\alpha_{SF1.c.136.x} \right) \right| = 5.897 \times 10^{-15} \cdot kN$$

$$R_{x.curved.F.cloc.y} := \left| SF1_{c.136.145} \cdot \cos\left(\alpha_{SF1.c.136.y} \right) \right| = 6.718 \cdot kN$$

$$R_{x.curved.F.cloc.z} := \left| SF1_{c.136.145} \cdot \cos\left(\alpha_{SF1.c.136.z} \right) \right| = 96.078 \cdot kN$$

$$R_{y.curved.F.cloc.x} := \left| SF3_{c.136.145} \cdot \cos\left(\alpha_{SF3.c.136.x} \right) \right| = 0 \cdot kN$$

$$R_{y.curved.F.cloc.y} := \left| SF3_{c.136.145} \cdot \cos\left(\alpha_{SF3.c.136.y} \right) \right| = 4.078 \cdot kN$$

$$R_{y.curved.F.cloc.z} := \left| SF3_{c.136.145} \cdot \cos\left(\alpha_{SF3.c.136.z} \right) \right| = 0.285 \cdot kN$$

$$R_{z.curved.F.cloc.x} := \left| SF2_{c.136.145} \cdot \cos\left(\alpha_{SF2.c.136.x} \right) \right| = 0.928 \cdot kN$$

$$R_{z.curved.F.cloc.y} := \left| SF2_{c.136.145} \cdot \cos\left(\alpha_{SF2.c.136.y} \right) \right| = 0 \cdot kN$$

$$R_{z.curved.F.cloc.z} := \left| SF2_{c.136.145} \cdot \cos\left(\alpha_{SF2.c.136.z} \right) \right| = 0 \cdot kN$$

Moments

$$R_{x.curved.M.cloc.x} := \left| SM1_{c.136.145} \cdot \cos\left(\alpha_{SF1.c.136.x} \right) \right| = 0 \cdot kN \cdot m$$

$$R_{x.curved.M.cloc.y} := \left| SM1_{c.136.145} \cdot \cos\left(\alpha_{SF1.c.136.y} \right) \right| = 0.414 \cdot kN \cdot m$$

$$R_{x.curved.M.cloc.z} := \left| SM1_{c.136.145} \cdot \cos\left(\alpha_{SF1.c.136.z} \right) \right| = 5.915 \cdot kN \cdot m$$

$$R_{y.curved.M.cloc.x} := \left| SM3_{c.136.145} \cdot \cos\left(\alpha_{SF3.c.136.x} \right) \right| = 0 \cdot kN \cdot m$$

$$R_{y.curved.M.cloc.y} := \left| SM3_{c.136.145} \cdot \cos\left(\alpha_{SF3.c.136.y} \right) \right| = 0 \cdot kN \cdot m$$

$$R_{y.curved.M.cloc.z} := \left| SM3_{c.136.145} \cdot \cos\left(\alpha_{SF3.c.136.z} \right) \right| = 0 \cdot kN \cdot m$$

$$R_{z.curved.M.cloc.x} := \left| SM2_{c.136.145} \cdot \cos\left(\alpha_{SF2.c.136.x} \right) \right| = 0.581 \cdot kN \cdot m$$

$$R_{z.curved.M.cloc.y} := \left| SM2_{c.136.145} \cdot \cos\left(\alpha_{SF2.c.136.y} \right) \right| = 0 \cdot kN \cdot m$$

$$R_{z.curved.M.cloc.z} := \left| SM2_{c.136.145} \cdot \cos\left(\alpha_{SF2.c.136.z} \right) \right| = 0 \cdot kN \cdot m$$

Sum of resultants acting in cloc

Forces

$$R_{curved.F.cloc.x} := R_{x.curved.F.cloc.x} + R_{y.curved.F.cloc.x} + R_{z.curved.F.cloc.x} = 0.928 \cdot kN$$

$$R_{curved.F.cloc.y} := R_{x.curved.F.cloc.y} + R_{y.curved.F.cloc.y} + R_{z.curved.F.cloc.y} = 10.797 \cdot kN$$

$$R_{curved.F.cloc.z} := R_{x.curved.F.cloc.z} + R_{y.curved.F.cloc.z} + R_{z.curved.F.cloc.z} = 96.363 \cdot kN$$

Moments

$$R_{curved.M.cloc.x} := R_{x.curved.M.cloc.x} + R_{x.curved.M.cloc.x} + R_{z.curved.M.cloc.x} = 0.581 \cdot kN \cdot m$$

$$R_{curved.M.cloc.y} := R_{x.curved.M.cloc.y} + R_{y.curved.M.cloc.y} + R_{z.curved.M.cloc.y} = 0.414 \cdot kN \cdot m$$

$$R_{curved.M.cloc.z} := R_{x.curved.M.cloc.z} + R_{y.curved.M.cloc.z} + R_{z.curved.M.cloc.z} = 5.915 \cdot kN \cdot m$$

5.3.3 Shear resistance of connection

Shear resistance per fastener per shear plane

$$F_{v.Rk.DS.1} := 0.5 \cdot f_{h.90.k.curved} \cdot t_{curved} \cdot d_{bolt.curved} = 17.035 \cdot kN$$

$$F_{v.Rk.DS.2} := 1.15 \cdot \sqrt{2 \cdot M_{y.Rk.bolt.curved} \cdot f_{h.90.k.curved} \cdot d_{bolt.curved}} = 7.029 \cdot kN$$

$$F_{v.Rk.DS.3} := 2.3 \cdot \sqrt{M_{y.Rk.bolt.curved} \cdot f_{h.90.k.curved} \cdot d_{bolt.curved}} = 9.94 \cdot kN$$

$$F_{v.Rk.DS.basic} := \begin{cases} \min\left(F_{v.Rk.DS.1}, F_{v.Rk.DS.2}\right) & \text{if } platethickness_{curved} = \text{"thin"} \\ \min\left(F_{v.Rk.DS.1}, F_{v.Rk.DS.3}\right) & \text{if } platethickness_{curved} = \text{"thick"} \\ \text{"linear interpolation"} & \text{otherwise} \end{cases} = 9.94 \cdot kN$$

Governing failure mode

$$failuremode_{curved} := \begin{cases} \text{"Mode j/l"} & \text{if } F_{v.Rk.DS.basic} = F_{v.Rk.DS.1} \\ \text{"Mode k"} & \text{if } F_{v.Rk.DS.basic} = F_{v.Rk.DS.2} \\ \text{"Mode m"} & \text{if } F_{v.Rk.DS.basic} = F_{v.Rk.DS.3} \end{cases} = \text{"Mode m"}$$

Failure mode j/l is not desireable, since the timber fails before the bolt. Aim for failure mode k or m. M is the most desirable. M can only occur for thick plates. A plate is thick if its thickness is equal or greater than the bolt diameter.

5.3.3.1 Longitudinally

Group effect for one row of fasteners

$$n_{ef.curved} := \min\left(n_{bolts.curved.row}, n_{bolts.curved.row}^{0.9} \cdot \sqrt[4]{\frac{a_{1.curved}}{13 \cdot d_{bolt.curved}}}\right) = 2.306$$

Total shear resistance of fasteners

$$F_{v.Rk.DS.total} := F_{v.Rk.DS.basic} \cdot n_{ef.curved} \cdot n_{rows.curved} \cdot n_{shearplanes.curved} = 183.368 \cdot kN$$

Load effects on bolts

$$i := 0 .. n_{bolts.curved.tot} - 1$$

Normal force per bolt

$$N_{curved} := \frac{R_{curved.F.cloc.z}}{n_{bolts.curved.tot}} = 6.023 \cdot kN$$

Shear force per bolt

$$V_{curved} := \frac{R_{curved.F.cloc.y}}{n_{bolts.curved.tot}} = 0.675 \cdot kN$$

Moment per bolt about strong axis

$$M_{curved_i} := R_{curved.M.cloc.x}$$

$$R_{curved.M.cloc.x} = 0.581 \cdot kN \cdot m$$

Moment around rotational center due to shear force

$$M_{v.curved_i} := V_{curved} \cdot \left(-z_{curved_i}\right)$$

Total shear force in each bolt, for the bolts not located in y=0

$$F_{v.curved_i} := N_{curved} + \frac{M_{curved_i} \cdot y_{curved_i}}{I_{p.curved.YZ}} + \frac{M_{v.curved_i}}{y_{curved_i}}$$

$$\frac{M_{v.curved_i}}{y_{curved_i}} = \begin{bmatrix} 2.789 \\ 8.367 \\ -8.367 \\ -2.789 \\ -2.789 \\ -8.367 \\ 8.367 \\ 2.789 \\ 3.059 \\ 9.177 \\ -9.177 \\ -3.059 \\ -3.059 \\ -9.177 \\ 9.177 \\ 3.059 \end{bmatrix} \cdot kN \qquad F_{v.curved} = \begin{bmatrix} 8.837 \\ 14.398 \\ -2.353 \\ 3.209 \\ 3.259 \\ -2.336 \\ 14.382 \\ 8.787 \\ 9.107 \\ 15.208 \\ -3.163 \\ 2.939 \\ 2.989 \\ -3.146 \\ 15.191 \\ 9.057 \end{bmatrix} \cdot kN$$

$$F_{v.curved.sum} := \sum_{i=0}^{n_{bolts.curved.tot}-1} F_{v.curved_i} = 96.363 \cdot kN$$

Controll of shear capacity

$$if\left(F_{v.Rk.DS.total} > \left|F_{v.curved.sum}\right|, "ok", "not ok"\right) = "ok"$$

Utilization ratio

$$\frac{\left|F_{v.curved.sum}\right|}{F_{v.Rk.DS.total}} = 0.526$$

5.3.3.2 Transversally

Group effect for one row of fasteners

$$n_{ef.curved.t} := \min\left(n_{rows.curved}, n_{rows.curved}^{0.9} \cdot \sqrt[4]{\frac{a_{2.curved}}{13 \cdot d_{bolt.curved}}}\right) = 2.62$$

Total shear resistance of fasteners

$$F_{v.Rk.DS.total.t} := F_{v.Rk.DS.basic} \cdot n_{ef.curved.t} \cdot n_{rows.curved} \cdot n_{shearplanes.curved} = 208.347 \cdot kN$$

Load effects on bolts

Normal force per bolt

$$N_{curved.t} := \frac{R_{curved.F.cloc.y}}{n_{bolts.curved.tot}} = 0.675 \cdot kN$$

Shear force per bolt

$$V_{curved.t} := \frac{R_{curved.F.cloc.z}}{n_{bolts.curved.tot}} = 6.023 \cdot kN$$

Moment per bolt about strong axis

$$M_{curved.t_i} := R_{curved.M.cloc.x}$$

$$R_{curved.M.cloc.x} = 0.581 \cdot kN \cdot m$$

Moment around rotational center due to shear force

$$M_{v.curved.t_i} := V_{curved.t} \cdot y_{curved_i}$$

Total shear force in each bolt

$$F_{v.curved.t_i} := N_{curved.t} + \frac{M_{curved.t_i} \cdot \left(-z_{curved_i}\right)}{I_{p.curved.YZ}} + \frac{M_{v.curved.t_i}}{z_{curved_i}}$$

$$\frac{M_{v.curved.t}}{z_{curved}} = \begin{bmatrix} -1.457 \\ -0.486 \\ 0.486 \\ 1.457 \\ 1.457 \\ 0.486 \\ -0.486 \\ -1.457 \\ -1.329 \\ -0.443 \\ 0.443 \\ 1.329 \\ 1.329 \\ 0.443 \\ -0.443 \\ -1.329 \end{bmatrix} \cdot kN \qquad F_{v.curved.t} = \begin{bmatrix} -0.679 \\ 0.292 \\ 1.264 \\ 2.235 \\ 2.029 \\ 1.057 \\ 0.086 \\ -0.886 \\ -0.541 \\ 0.345 \\ 1.231 \\ 2.117 \\ 1.89 \\ 1.004 \\ 0.119 \\ -0.767 \end{bmatrix} \cdot kN$$

$$F_{v.curved.sum.t} := \sum_{i=0}^{n_{bolts.curved.tot}-1} F_{v.curved.t_i} = 10.797 \cdot kN$$

Controll of shear capacity

$$\text{if}\left(F_{v.Rk.DS.total.t} > \left|F_{v.curved.sum.t}\right|, \text{"ok"}, \text{"not ok"}\right) = \text{"ok"}$$

Utilization ratio

$$\frac{\left|F_{v.curved.sum.t}\right|}{F_{v.Rk.DS.total.t}} = 0.052$$

5.3.4 Shear resistance of bolt

Load effect at each bolt

$$R_{z.curved_i} := F_{v.curved_i}$$

$$R_{y.curved_i} := F_{v.curved.t_i}$$

$$R_{v.curved_i} := \left|\sqrt{\left(R_{z.curved_i}\right)^2 + \left(R_{y.curved_i}\right)^2}\right|$$

$$R_{v.curved} = \begin{pmatrix} 8.863 \\ 14.401 \\ 2.671 \\ 3.91 \\ 3.838 \\ 2.564 \\ 14.382 \\ 8.831 \\ 9.123 \\ 15.212 \\ 3.394 \\ 3.622 \\ 3.536 \\ 3.302 \\ 15.192 \\ 9.089 \end{pmatrix} \cdot kN$$

$$F_{v.Ed.bolt.curved} := \max\left(R_{v.curved}\right) = 15.212 \cdot kN$$

Shear stress in most loaded bolt

$$\tau_{bolt.curved} := \frac{F_{v.Ed.bolt.curved} \cdot 4}{\pi \cdot d_{bolt.curved}^2} = 134.503 \cdot MPa$$

Controll of shear stress

$$\text{if}\left(\tau_{bolt.curved} \leq \tau_{s.Rk.bolt.curved}, \text{"ok"}, \text{"not ok"}\right) = \text{"ok"}$$

Utilization ratio

$$\frac{\tau_{bolt.curved}}{\tau_{s.Rk.bolt.curved}} = 0.582$$

Shear failure in bolt

Capacity of one bolt

$$\alpha_{v.curved} := 0.6$$

$$F_{v.Rd.bolt.curved} := \frac{\alpha_{v.curved} \cdot f_{u.k.bolt.curved} \cdot \pi \left(\frac{d_{bolt.curved}}{2} \right)^2}{\gamma_{M2}} = 21.715 \cdot kN$$

Controll of shear force

$$\text{if}\left(F_{v.Ed.bolt.curved} \le F_{v.Rd.bolt.curved}, \text{"ok"}, \text{"not ok"}\right) = \text{"ok"}$$

Utilization ratio

$$\frac{F_{v.Ed.bolt.curved}}{F_{v.Rd.bolt.curved}} = 0.701$$

5.3.5 Embedding strength of plate

Capacity of steel plate

For failure between hole and end of plate

$$\alpha_{d.end.curved} := \frac{a_{3.curved.steel}}{2 \cdot d_{0.hole.curved}} = 0.769$$

$$k_{1.end.curved} := \min\left(2.8 \cdot \frac{a_{4.curved.steel}}{d_{0.hole.curved}} - 1.7, 2.5\right) = 2.5$$

$$\alpha_{b.end.curved} := \min\left(\alpha_{d.end.curved}, \frac{f_{u.k.bolt.curved}}{f_{u.plate}}, 1\right) = 0.769$$

$$k\alpha_{end} := k_{1.end.curved} \cdot \alpha_{b.end.curved}$$

$$F_{b.Rd.end.curved} := \frac{k\alpha_{end} \cdot f_{u.plate} \cdot d_{bolt.curved} \cdot t_{curved.plate}}{\gamma_{M2}} = 95.262 \cdot kN$$

For failure between two holes

$$\alpha_{d.hole.curved} := \frac{a_{1.curved}}{3 \cdot d_{0.hole.curved}} - \frac{1}{4} = 0.519$$

$$k_{1.hole.curved} := \min\left(1.4 \cdot \frac{a_{2.curved}}{d_{0.hole.curved}} - 1.7, 2.5\right) = 2.5$$

$$\alpha_{b.hole.curved} := \min\left(\alpha_{d.hole.curved}, \frac{f_{u.k.bolt.curved}}{f_{u.plate}}, 1\right) = 0.519$$

$$k\alpha_{hole} := k_{1.hole.curved} \cdot \alpha_{b.hole.curved}$$

$$F_{b.Rd.hole.curved} := \frac{k\alpha_{hole} \cdot f_{u.plate} \cdot d_{bolt.curved} \cdot t_{curved.plate}}{\gamma_{M2}} = 64.302 \cdot kN$$

Minimum capacity of steel plate

$$F_{b.Rd.plate.curved} := \min\left(F_{b.Rd.end.curved}, F_{b.Rd.hole.curved}\right) = 64.302 \cdot kN$$

Controll of plate capacity

$$\text{if}\left(F_{v.Ed.bolt.curved} \le F_{b.Rd.plate.curved}, \text{"ok"}, \text{"not ok"}\right) = \text{"ok"}$$

Utilization ratio

$$\frac{F_{v.Ed.bolt.curved}}{F_{b.Rd.plate.curved}} = 0.237$$

5.3.6 Shear failure mode

$$F_{v.Rd.curved} := \min\left(F_{v.Rd.bolt.curved}, F_{b.Rd.plate.curved}\right) = 21.715 \cdot kN$$

$$\text{if}\left(F_{v.Rd.curved} = F_{v.Rd.bolt.curved}, \text{"Shear failure bolt"}, \text{"Embedding failure plate"}\right) = \text{"Shear failure bolt"}$$

5.3.7 Withdrawal of bolts

Tensile load on bolt

Transvers force $T_{x.curved.w} := R_{curved.F.cloc.x} = 0.928 \cdot kN$

Moment about y $M_{y.curved.w} := R_{curved.M.cloc.y} = 0.414 \cdot kN \cdot m$

Moment about z $M_{z.curved.w} := R_{curved.M.cloc.z} = 5.915 \cdot kN \cdot m$

Eccentricity of My and Mz to bolts

$$x_{curved} := \begin{pmatrix} 0 \\ 0 \\ 0 \\ 0 \\ 0 \\ 0 \\ 0 \\ 0 \\ 0 \\ 0 \\ 0 \\ 0 \\ 0 \\ 0 \\ 0 \end{pmatrix} mm \qquad y_{curved} = \begin{pmatrix} 75 \\ 25 \\ -25 \\ -75 \\ 75 \\ 25 \\ -25 \\ -75 \\ 75 \\ 25 \\ -25 \\ -75 \\ 75 \\ 25 \\ -25 \\ -75 \end{pmatrix} \cdot mm \qquad z_{curved} = \begin{pmatrix} -310 \\ -310 \\ -310 \\ -310 \\ 310 \\ 310 \\ 310 \\ 310 \\ -340 \\ -340 \\ -340 \\ -340 \\ 340 \\ 340 \\ 340 \\ 340 \end{pmatrix} \cdot mm$$

Polar moment of inertia

$$I_{p.curved.XY} := \sum_{i=0}^{n_{bolts.curved.tot}-1} \left[\left(x_{curved_i} \right)^2 + \left(y_{curved_i} \right)^2 \right] = 5 \times 10^4 \cdot mm^2$$

$$I_{p.curved.XZ} := \sum_{i=0}^{n_{bolts.curved.tot}-1} \left[\left(x_{curved_i} \right)^2 + \left(z_{curved_i} \right)^2 \right] = 1.694 \times 10^6 \cdot mm^2$$

Resultant forces at each bolt

$$R_{x.curved.w_i} := \left| \frac{T_{x.curved.w}}{n_{bolts.curved.tot}} + \frac{M_{y.curved.w} \cdot z_{curved_i}}{I_{p.curved.XZ}} + \frac{M_{z.curved.w} \cdot y_{curved_i}}{I_{p.curved.XY}} \right|$$

Most loaded bolt $F_{t.Ed.bolt.curved} := \max\left(R_{x.curved.w}\right) = 9.014 \cdot kN$

Tensile capacity of one bolt

Reduction factor considering bending $k_{2.curved} := 0.9$

Stressed area of bolt witd d=12mm $A_{s.curved} := 84mm^2$

Tensile capacity of one bolt

$$F_{t.Rd.bolt.curved} := \frac{k_{2.curved} \cdot f_{u.k.bolt.curved} \cdot A_{s.curved}}{\gamma_{M2}} = 24.192 \cdot kN$$

Controll of withdrawal capacity $\text{if}\left(F_{t.Ed.bolt.curved} \le F_{t.Rd.bolt.curved}, \text{"ok"}, \text{"not ok"}\right) = \text{"ok"}$

Utilization ratio $\frac{F_{t.Ed.bolt.curved}}{F_{t.Rd.bolt.curved}} = 0.373$

5.3.8 Combination of normal and shear force

Controll of combined axial and shear loading

$$\text{if}\left(\frac{F_{v.Ed.bolt.curved}}{F_{v.Rd.curved}} + \frac{F_{t.Ed.bolt.curved}}{1.4 \cdot F_{t.Rd.bolt.curved}} \le 1, \text{"ok"}, \text{"not ok"} \right) = \text{"ok"}$$

Utilization ratio $\frac{F_{v.Ed.bolt.curved}}{F_{v.Rd.curved}} + \frac{F_{t.Ed.bolt.curved}}{1.4 \cdot F_{t.Rd.bolt.curved}} = 0.967$

5.3.9 Compression prependicular to the grain

Sum of forces acting as pressure on the curved beam

$$F_{x.curved} := \sum_{i=0}^{n_{bolts.curved.tot}-1} R_{x.curved.w_i} = 94.641 \cdot kN$$

Area of plate

$$A_{plate.curved.ef} := h_{plate.curved} \cdot \left(l_{plate.curved} + 30mm\right) = 0.173\,m^2$$

Pressure

$$\sigma_{c.90.d.curved} := \frac{F_{x.curved}}{A_{plate.curved.ef}} = 0.549 \cdot MPa$$

Check of capacity

$$if\left(\sigma_{c.90.d.curved} \le k_{c.90} \cdot f_{c.90.d}, "ok", "not\ ok"\right) = "ok"$$

Utilization ratio

$$\frac{\sigma_{c.90.d.curved}}{\left(k_{c.90} \cdot f_{c.90.d}\right)} = 0.305$$

5.3.10 Translational and rotational stiffness

The translational and rotational spring stiffnesses are calculated for SLS

Translational stiffness

$$K_{t.ser.curved} := \frac{\left(\frac{\rho_{g.mean}}{\frac{kg}{m^3}}\right)^{1.5} \cdot \frac{d_{bolt.curved}}{mm}}{23} \cdot n_{shearplanes.curved} \cdot \frac{N}{mm} = 9.304 \times 10^3 \cdot \frac{N}{mm}$$

Rotational stiffness

$$K_{\theta.ser.curved} := K_{t.ser.curved} \cdot I_{p.curved.XZ} = 1.5758 \times 10^7 \cdot \frac{N \cdot m}{rad}$$

5.4 Rotational stiffness of whole connection

Springs in series

$$K_{tot} := \frac{1}{\left(\frac{1}{K_{\theta.ser.curved}} + \frac{1}{K_{\theta.ser.truss}}\right)} = 7.263 \times 10^6 \cdot \frac{N \cdot m}{rad}$$

5.5 Weld design

The welds between truss element 21 and the curved beam is the most loaded, and hence only this weld will be checked.

5.5.1 Geometry

"A-measurement" in weld

$$a_{weld.21.vert} := 13mm$$

$$a_{weld.21.hor} := 13mm$$

Iterated thickness of slotted-in plate due to weld capacity

$$t_{slot.plate.new} := t_{slot.plate}$$

Length of weld

$$L_{weld.21.vert} := h_{rooftruss} = 225 \cdot mm$$

$$L_{weld.21.hor} := t_{slot.plate.new} = 20 \cdot mm$$

Number of weld, both horizontal and longitudianl, adjacent to the plate of truss 21

$$n_{welds.21} := 2$$

Distances to center of gravity

$$y_{21} := \frac{L_{weld.21.vert}}{2} = 112.5 \cdot mm$$

$$z_{21} := \frac{L_{weld.21.hor}}{2} = 10 \cdot mm$$

Cross sectional constants of the welds

$$I_{21.vert} := 2\left[\frac{a_{weld.21.vert} \cdot \left(L_{weld.21.vert} - 2 \cdot a_{weld.21.hor}\right)^3}{12} \ldots + L_{weld.21.hor} \cdot a_{weld.21.hor} \cdot \left(y_{21}\right)^2\right] = 2.366 \times 10^7 \cdot mm^4$$

$$I_{21.hor} := 2\left[\frac{a_{weld.21.hor} \cdot L_{weld.21.hor}^3}{12} + L_{weld.21.vert} \cdot a_{weld.21.vert} \cdot \left(z_{21}\right)^2\right] = 6.023 \times 10^5 \cdot mm^4$$

Contribution of vertical and horizontal welds, respectively

$$share_{21.vert} := \frac{L_{weld.21.vert}}{L_{weld.21.vert} + L_{weld.21.hor}} = 0.918$$

$$share_{21.hor} := \frac{L_{weld.21.hor}}{L_{weld.21.vert} + L_{weld.21.hor}} = 0.082$$

5.5.2 Resultant forces

Resultant forces acting at truss beam node in local coordinate system of the truss (tloc)

$$R_{x.21.F.tloc} := \left|SF1_{t.21}\right| + \frac{SM2_{t.21}}{\frac{h_{rooftruss}}{2}} + \frac{SM1_{t.21}}{\frac{t_{slot.plate.new}}{2}} = 936.199 \cdot kN$$

$$R_{y.21.F.tloc} := SF3_{t.21} + \frac{SM3_{t.21}}{\frac{t_{slot.plate.new}}{2}} = 5.988 \cdot kN$$

$$R_{z.21.F.tloc} := SF2_{t.21} + \frac{SM3_{t.21}}{\frac{h_{rooftruss}}{2}} = 0.17 \cdot kN$$

Resultant forces and moment after translation to curved beam, still in local coordinate system of the truss section (tloc)

Length of lever arm

$$a_{lever} := 140mm$$

Forces

$$R_{x.21.c.F.tloc} := R_{x.21.F.tloc} = 936.199 \cdot kN$$

$$R_{y.21.c.F.tloc} := R_{y.21.F.tloc} = 5.988 \cdot kN$$

$$R_{z.21.c.F.tloc} := R_{z.21.F.tloc} = 0.17 \cdot kN$$

Moments

$$R_{y.21.c.M.tloc} := R_{z.21.F.tloc} \cdot a_{lever} = 0.024 \cdot kN \cdot m$$

$$R_{z.21.c.M.tloc} := R_{y.21.F.tloc} \cdot a_{lever} = 0.838 \cdot kN \cdot m$$

Resultant forces and moment rotated to act in the local coordinate system of the connection (cloc)

Forces

$$R_{x.21.F.cloc.x} := R_{x.21.c.F.tloc} \cdot \cos\left(\alpha_{SF1.t.21.x}\right) = 793.941 \cdot kN$$

$$R_{x.21.F.cloc.y} := R_{x.21.c.F.tloc} \cdot \cos\left(\alpha_{SF1.t.21.y}\right) = -16.339 \cdot kN$$

$$R_{x.21.F.cloc.z} := R_{x.21.c.F.tloc} \cdot \cos\left(\alpha_{SF1.t.21.z}\right) = 496.11 \cdot kN$$

$$R_{y.21.F.cloc.x} := R_{y.21.c.F.tloc} \cdot \cos\left(\alpha_{SF3.t.21.x}\right) = 0.522 \cdot kN$$

$$R_{y.21.F.cloc.y} := R_{y.21.c.F.tloc} \cdot \cos\left(\alpha_{SF3.t.21.y}\right) = 5.943 \cdot kN$$

$$R_{y.21.F.cloc.z} := R_{y.21.c.F.tloc} \cdot \cos\left(\alpha_{SF3.t.21.z}\right) = -0.522 \cdot kN$$

$$R_{z.21.F.cloc.x} := R_{z.21.c.F.tloc} \cdot \cos\left(\alpha_{SF2.t.21.x}\right) = -0.087 \cdot kN$$

$$R_{z.21.F.cloc.y} := R_{z.21.c.F.tloc} \cdot \cos\left(\alpha_{SF2.t.21.y}\right) = 0.021 \cdot kN$$

$$R_{z.21.F.cloc.z} := R_{z.21.c.F.tloc} \cdot \cos\left(\alpha_{SF2.t.21.z}\right) = 0.144 \cdot kN$$

Moments

$$R_{y.21.M.cloc.x} := R_{y.21.c.M.tloc} \cdot \cos\left(\alpha_{SF3.t.21.x}\right) = 2.071 \times 10^{-3} \cdot kN \cdot m$$

$$R_{y.21.M.cloc.y} := R_{y.21.c.M.tloc} \cdot \cos\left(\alpha_{SF3.t.21.y}\right) = 0.024 \cdot kN \cdot m$$

$$R_{y.21.M.cloc.z} := R_{y.21.c.M.tloc} \cdot \cos\left(\alpha_{SF3.t.21.z}\right) = -2.071 \times 10^{-3} \cdot kN \cdot m$$

$$R_{z.21.M.cloc.x} := R_{z.21.c.M.tloc} \cdot \cos\left(\alpha_{SF2.t.21.x}\right) = -0.432 \cdot kN \cdot m$$

$$R_{z.21.M.cloc.y} := R_{z.21.c.M.tloc} \cdot \cos\left(\alpha_{SF2.t.21.y}\right) = 0.102 \cdot kN \cdot m$$

$$R_{z.21.M.cloc.z} := R_{z.21.c.M.tloc} \cdot \cos\left(\alpha_{SF2.t.21.z}\right) = 0.711 \cdot kN \cdot m$$

Sum of resultants acting in cloc

Forces

$$R_{21.F.cloc.x} := R_{x.21.F.cloc.x} + R_{y.21.F.cloc.x} + R_{z.21.F.cloc.x} = 794.376 \cdot kN$$

$$R_{21.F.cloc.y} := R_{x.21.F.cloc.y} + R_{y.21.F.cloc.y} + R_{z.21.F.cloc.y} = -10.375 \cdot kN$$

$$R_{21.F.cloc.z} := R_{x.21.F.cloc.z} + R_{y.21.F.cloc.z} + R_{z.21.F.cloc.z} = 495.732 \cdot kN$$

Moments

$$R_{21.M.cloc.x} := R_{y.21.M.cloc.x} + R_{z.21.M.cloc.x} = -0.43 \cdot kN \cdot m$$

$$R_{21.M.cloc.y} := R_{y.21.M.cloc.y} + R_{z.21.M.cloc.y} = 0.126 \cdot kN \cdot m$$

$$R_{21.M.cloc.z} := R_{y.21.M.cloc.z} + R_{z.21.M.cloc.z} = 0.709 \cdot kN \cdot m$$

5.5.3 Stresses in welds

5.5.3.1 Vertical welds

Stress due to force

$$\sigma_{F.\perp.21.vert} := \frac{R_{21.F.cloc.x} \cdot share_{21.vert}}{n_{welds.21} \cdot a_{weld.21.vert} \cdot L_{weld.21.vert}} = 124.706 \cdot MPa$$

Stress due to moment

$$\sigma_{M.\perp.21.vert} := \frac{R_{21.M.cloc.x} \cdot y_{21}}{I_{21.vert}} + \frac{R_{21.M.cloc.y} \cdot z_{21}}{I_{21.hor}} + \frac{R_{21.M.cloc.z} \cdot y_{21}}{I_{21.vert}} = 3.415 \cdot MPa$$

Shear stress

$$\tau_{\parallel.21.vert} := \frac{R_{21.F.cloc.y}}{n_{welds.21} \cdot a_{weld.21.vert} \cdot L_{weld.21.vert}} = -1.774 \cdot MPa$$

Resultant stresses in one vertical weld section (the smaller one)

Angle to midpoint of weld section $\alpha_{weld.21.vert.small} := \frac{\alpha_{SF1.t.21.z}}{2} = 29.^\circ$

Normal stress perpendicular to weld

$$\sigma_{\perp.21.vert.small} := \left(\sigma_{F.\perp.21.vert} + \sigma_{M.\perp.21.vert}\right) \cdot \cos\left(\alpha_{weld.21.vert.small}\right) = 112.057 \cdot MPa$$

Shear stress perpendicular to weld

$$\tau_{\perp.21.vert.small} := \left(\sigma_{F.\perp.21.vert} + \sigma_{M.\perp.21.vert}\right) \cdot \sin\left(\alpha_{weld.21.vert.small}\right) = 62.114 \cdot MPa$$

Shear stress parallel to weld

$$\tau_{\parallel.21.vert.small} := \tau_{\parallel.21.vert} = -1.774 \cdot MPa$$

Equivalent stress

$$\sigma_{eq.21.vert.small} := \sqrt{\sigma_{\perp.21.vert.small}^{2} + 3\left(\tau_{\perp.21.vert.small}^{2} + \tau_{\parallel.21.vert.small}^{2}\right)} = 155.373 \cdot MPa$$

Controll of capacity of welds

$$Check_{1.vert.small} := \sigma_{eq.21.vert.small} \le \frac{f_{u.plate}}{\beta_w \cdot \gamma_{M2}}$$

$$Check_{2.vert.small} := \left|\sigma_{\perp.21.vert.small}\right| \le \frac{0.9 \cdot f_{u.plate}}{\gamma_{M2}}$$

$$if\left(Check_{1.vert.small} \wedge Check_{2.vert.small}, "ok", "not ok"\right) = "ok"$$

Utilization ratio

$$\frac{\sigma_{eq.21.vert.small}}{\frac{f_{u.plate}}{\beta_w \cdot \gamma_{M2}}} = 0.452 \qquad \frac{\left|\sigma_{\perp.21.vert.small}\right|}{\frac{0.9 \cdot f_{u.plate}}{\gamma_{M2}}} = 0.362$$

Resultant stresses in one vertical weld section (the larger one)

Angle to midpoint of weld section

$$\alpha_{weld.21.vert.large} := \frac{180° - \alpha_{SF1.t.21.z}}{2} = 61 \cdot °$$

Normal stress perpendicular to weld

$$\sigma_{\perp.21.vert.large} := \left(\sigma_{F.\perp.21.vert} + \sigma_{M.\perp.21.vert}\right) \cdot \cos\left(\alpha_{weld.21.vert.large}\right) = 62.114 \cdot MPa$$

Shear stress perpendicular to weld

$$\tau_{\perp.21.vert.large} := \left(\sigma_{F.\perp.21.vert} + \sigma_{M.\perp.21.vert}\right) \cdot \sin\left(\alpha_{weld.21.vert.large}\right) = 112.057 \cdot MPa$$

Shear stress parallel to weld

$$\tau_{\parallel.21.vert.large} := \tau_{\parallel.21.vert} = -1.774 \cdot MPa$$

Equivalent stress

$$\sigma_{eq.21.vert.large} := \sqrt{\sigma_{\perp.21.vert.large}^{2} + 3\left(\tau_{\perp.21.vert.large}^{2} + \tau_{\parallel.21.vert.large}^{2}\right)} = 203.809 \cdot MPa$$

Controll of capacity of welds

$$Check_{1.vert.large} := \sigma_{eq.21.vert.large} \le \frac{f_{u.plate}}{\beta_w \cdot \gamma_{M2}} = 1$$

$$Check_{2.vert.large} := \left|\sigma_{\perp.21.vert.large}\right| \le \frac{0.9 \cdot f_{u.plate}}{\gamma_{M2}} = 1$$

$$if\left(Check_{1.vert.large} \wedge Check_{2.vert.large}, "ok", "not ok"\right) = "ok"$$

Utilization ratio

$$\frac{\sigma_{eq.21.vert.large}}{\frac{f_{u.plate}}{\beta_w \cdot \gamma_{M2}}} = 0.592 \qquad \frac{\left|\sigma_{\perp.21.vert.large}\right|}{\frac{0.9 \cdot f_{u.plate}}{\gamma_{M2}}} = 0.201$$

5.5.3.2 Horizontal welds

Stress due to force

$$\sigma_{F.\perp.21.hor} := \frac{R_{21.F.cloc.x} \cdot share_{21.hor}}{n_{welds.21} \cdot a_{weld.21.hor} \cdot L_{weld.21.hor}} = 124.706 \cdot MPa$$

Stress due to moment

$$\sigma_{M.\perp.21.hor} := \frac{R_{21.M.cloc.x} \cdot y_{21}}{I_{21.vert}} + \frac{R_{21.M.cloc.y} \cdot z_{21}}{I_{21.hor}} + \frac{R_{21.M.cloc.z} \cdot y_{21}}{I_{21.vert}} = 3.415 \cdot MPa$$

Shear stress

$$\tau_{\parallel .21.hor} := \frac{R_{21.F.cloc.z}}{n_{welds.21} \cdot a_{weld.21.hor} \cdot L_{weld.21.hor}} = 953.33 \cdot MPa$$

Resultant stresses in one horizontal weld section (the smaller one)

Angle to midpoint of weld section $\alpha_{weld.21.hor.small} := \frac{\alpha_{SF1.t.21.x}}{2} = 16 \cdot °$

Normal stress perpendicular to weld

$$\sigma_{\perp.21.hor.small} := \left(\sigma_{F.\perp.21.hor} + \sigma_{M.\perp.21.hor}\right) \cdot \cos\left(\alpha_{weld.21.hor.small}\right) = 123.158 \cdot MPa$$

Shear stress perpendicular to weld

$$\tau_{\perp.21.hor.small} := \left(\sigma_{F.\perp.21.hor} + \sigma_{M.\perp.21.hor}\right) \cdot \sin\left(\alpha_{weld.21.hor.small}\right) = 35.315 \cdot MPa$$

Shear stress parallel to weld

$$\tau_{\parallel .21.hor.small} := \tau_{\parallel .21.hor} = 953.33 \cdot MPa$$

Equivalent stress

$$\sigma_{eq.21.hor.small} := \sqrt{\sigma_{\perp.21.hor.small}^{2} + 3\left(\tau_{\perp.21.hor.small}^{2} + \tau_{\parallel .21.hor.small}^{2}\right)} = 1.657 \times 10^{3} \cdot MPa$$

Controll of capacity of welds

$$Check_{1.hor.small} := \sigma_{eq.21.hor.small} \leq \frac{f_{u.plate}}{\beta_w \cdot \gamma_{M2}}$$

$$Check_{2.hor.small} := \left|\sigma_{\perp.21.hor.small}\right| \leq \frac{0.9 \cdot f_{u.plate}}{\gamma_{M2}}$$

$$if\left(Check_{1.hor.small} \wedge Check_{2.hor.small}, "ok", "not ok"\right) = "not ok"$$

Utilization ratio

$$\frac{\sigma_{eq.21.hor.small}}{\frac{f_{u.plate}}{\beta_w \cdot \gamma_{M2}}} = 4.817 \qquad \frac{\left|\sigma_{\perp.21.hor.small}\right|}{\frac{0.9 \cdot f_{u.plate}}{\gamma_{M2}}} = 0.398$$

Resultant stresses in one horizontal weld section (the larger one)

Angle to midpoint of weld section $\alpha_{weld.21.hor.large} := \frac{180° - \alpha_{SF1.t.21.x}}{2} = 74.°$

Normal stress perpendicular to weld

$\sigma_{\perp.21.hor.large} := \left(\sigma_{F.\perp.21.hor} + \sigma_{M.\perp.21.hor}\right) \cdot \cos\left(\alpha_{weld.21.hor.large}\right) = 35.315 \cdot MPa$

Shear stress perpendicular to weld

$\tau_{\perp.21.hor.large} := \left(\sigma_{F.\perp.21.hor} + \sigma_{M.\perp.21.hor}\right) \cdot \sin\left(\alpha_{weld.21.hor.large}\right) = 123.158 \cdot MPa$

Shear stress parallel to weld

$\tau_{\parallel.21.hor.large} := \tau_{\parallel.21.hor} = 953.33 \cdot MPa$

Equivalent stress

$\sigma_{eq.21.hor.large} := \sqrt{\sigma_{\perp.21.hor.large}^{2} + 3\left(\tau_{\perp.21.hor.large}^{2} + \tau_{\parallel.21.hor.large}^{2}\right)} = 1.665 \times 10^{3} \cdot MPa$

Controll of capacity of welds

$Check_{1.hor.large} := \sigma_{eq.21.hor.large} \leq \frac{f_{u.plate}}{\beta_w \cdot \gamma_{M2}}$

$Check_{2.hor.large} := \left|\sigma_{\perp.21.hor.large}\right| \leq \frac{0.9 \cdot f_{u.plate}}{\gamma_{M2}}$

$if\left(Check_{1.hor.large} \wedge Check_{2.hor.large}, "ok", "not ok"\right) = "not ok"$

Utilization ratio

$\frac{\sigma_{eq.21.hor.large}}{\frac{f_{u.plate}}{\beta_w \cdot \gamma_{M2}}} = 4.841$ $\frac{\left|\sigma_{\perp.21.hor.large}\right|}{\frac{0.9 \cdot f_{u.plate}}{\gamma_{M2}}} = 0.114$

The utilization ratio is so high that it is not possible to improve the behaviour with increasing measurements of plates or bolts or the material properties of the steel. Other actions will have to be taken in order to satisfy this condition.

A thickness of 57mm is needed for the slotted-in plate, which is welded to the curved connection in order to satisfy this condition. This is not realistic. Hence stiffeneres are needed.